IN VITRO STUDIES ON CYANIDIN PROTECTION AGAINST DOXORUBICIN CARDIOMYOCYTE CYTOTOXICITY AND ANTICANCER ACTIVITY

A Thesis Submitted to the
College of Graduate and Postdoctoral Studies.
in Partial Fulfillment of the Requirements
for the Degree of Doctor of Philosophy
in the College of Pharmacy and Nutrition
University of Saskatchewan
Saskatoon

By

MUATH HEKMAT HELAL

PERMISSION TO USE

In presenting this thesis/dissertation in partial fulfillment of the requirements for a Postgraduate degree from the University of Saskatchewan, I agree that the Libraries of this University may make it freely available for inspection. I further agree that permission for copying of this thesis/dissertation in any manner, in whole or in part, for scholarly purposes may be granted by the professor or professors who supervised my thesis/dissertation work or, in their absence, by the Head of the Department or the Dean of the College in which my thesis work was done. It is understood that any copying or publication or use of this thesis/dissertation or parts thereof for financial gain shall not be allowed without my written permission. It is also understood that due recognition shall be given to me and to the University of Saskatchewan in any scholarly use which may be made of any material in my thesis/dissertation.

Requests for permission to copy or to make other uses of materials in this thesis/dissertation in whole or part should be addressed to:

Dean of the College of Pharmacy and Nutrition

University of Saskatchewan

104 Clinic Place,

Saskatoon, SK S7N 2Z4

Canada

OR

Dean of the College of Graduate and Postdoctoral Studies
University of Saskatchewan
116 Thorvaldson Building, 110 Science Place
Saskatoon, SK S7N 5C9
Canada

ABSTRACT

Mitochondrial reactive oxygen species (ROS) are recognized for their role in several health related problems when produced at excessively high concentrations. Due to their potent antioxidant activity and potential mitochondriotropic behavior, the anthocyanidins may have potential to lower mitochondrial ROS levels. Nevertheless, the effect of anthocyanidins remains overlooked due to their presumed low stability and bioavailability. In addition, this instability has lead to a general belief that the phenolic degradation products, protocatechuic acid (PCA) and phloroglucinaldehye (PGA), exert the bioactivity rather than the parent compound.

In this work, doxorubicin-induced cytotoxicity in differentiated H9c2 cardiomyocytes was initially established as a model in which the mitochondrial antioxidant activity of the selected flavonoids would be examined. First, we delineated the mechanisms by which doxorubicin affected H9c2 cell survival and mitochondrial function. The results showed that early effects of doxorubicin on mitochondrial superoxide generation led to a delayed effect on cell survival. Using this model, we then revealed the protective ability of cyanidin against doxorubicin-induced cytological damage, showing protection to mitochondria. While cyanidin co-incubation with doxorubicin did not show protection when cell survival was assessed after 24 h, it gave delayed protection after a further 24 h drug-free period. Using the delayed protection model, we also showed that cyanidin had greater bioactivity over other flavonoids tested (quercetin, catechin and cyanidin-3-glucoside (C3G)). The protection by cyanidin also exceeded that of its degradation products (PCA and PGA), suggesting that the parent compound has additional bioactivity. The cytoprotective ability of the flavonoids was related to their ability to lower mitochondrial superoxide at early time points, with cyanidin being the most effective. Experiments on doxorubicin cytotoxicity to HepG2 (liver cancer) and K562 (erythroleukemia) cells showed no

protective effect with cyanidin. These results suggest cyanidin protects cardiomyocytes but does not interfere with the cytotoxic activity of doxorubicin in the cancer cell lines.

Investigations on the degradation of cyanidin in physiological media, UV-vis, HPLC and MS analytical techniques provided evidence that cyanidin does not degrade immediately to PCA and PGA. Instead, intermediate compounds (hemiketal and chalcone) survived for sufficient periods to exert putative bioactivity. Studies on the influence of different medium on the degradation of cyanidin showed that stability in human serum was significantly higher (t½ 43.2 min at room temperature, 22 ± 1°C) compared to phosphate buffered saline and Dulbecco's Modified Eagle's Medium with and without 10% fetal bovine serum (t½ 10.2-32.6 min).

In conclusion, using differentiated H9c2 cells, our results show an ability of cyanidin to survive long enough in cell culture media, and presumably intracellularly, to exert cytoprotection against doxorubicin which exceeded that of other flavonoids (quercetin, catechin, C3G) and its degradation products (PCA and PGA). The results present cyanidin as a possible antioxidant choice to use in clinical practice to protect the heart from the mitochondrial toxicity of doxorubicin and warrants investigation into this possible therapeutic application.

Acknowledgments

بسم الله الرحمن الرحيم

In the name of Allâh (God), the Most Gracious, The most Merciful

All my praises and thanks be to Allâh

I would like to express my appreciation and thankfulness to my supervisors, Dr. Brian Bandy and Dr. Jane Alcorn for their guidance, encouragement and mentorship.

I also thank my advisory committee members Dr. Nicholas Low, Dr. Jonathan Dimmock, Dr. Anas El-Aneed, and committee chair Dr. David Blackburn for their valuable input in this work.

I truly appreciate my friends and colleagues, Ahmed Almousa, Ziad Ghaith, Omar Abu Hussein for their help and support during times of difficulty. I also thank Ms. Deborah Michel for her great assistance and technical support in various stages of my work. I also appreciate the help provided by our office staff, Erin and Clair.

I express my acknowledgment to University of Saskatchewan and College of Pharmacy and Nutrition for funding me and providing the necessary environment and to conduct my research. I also thank the funding agency Saskatchewan Health Research Foundation (SHRF) for funding my research.

Dedicated to

Palestine, my beloved country where I was raised and learned my initial steps to success,

Mom and dad, who provided me with care, encouragement, support and prayers to pursue my ambitions,

My wife, Heba who gave me endless love, support and strength when greatly needed,

My daughter, Zeina, whom without knowing persuaded me to pursue my career for a better tomorrow,

My sister, Ayah, who was always there for me when challenges were extremely difficult,

My brothers, Mohammed, Hussein and Hamzah, who also gave me strength and encouragement throughout my life,

My Aunts, Rowayda and Jehan, who gave me all the support needed through out my elementary stages of my education.

Table of Contents

List of Figures:

List of abbreviations

can	Acetonitrile
ATP	Adenosine triphosphate
C3G	Cyanidin-3-glucoside
DCFH-DA	Dichlorodihydrofluorescein diacetate
DMEM	Dulbecco's modified eagles medium
DMSO	Dimethyl sulfoxide
DNA	Deoxyribonucleic acid
ECG	Electrocardiogram
ETC	Electron transport chain
FA	Formic acid
FMN	Flavin mononucleotide (oxidized)
$FMNH_2$	Flavin mononucleotide (reduced)
H9c2	Rat cardiomyoblast cell line
HEPES	(4-(2-hydroxyethyl)-1-piperazineethanesulfonic acid)
HPLC	High performance liquid chromatography
h	Hour(s)
IR	Infrared
IV	Intravenous
min	Minutes
MMP	Mitochondrial membrane potential
mPTP	Mitochondrial permeability transition pore
MS	Mass spectrometry
MTT	3-(4,5-dimethylthiazol-2-yl)-2,5-diphenyltetrazolium bromide
PBS	Phosphate buffered saline
PCA	Protocatechuic acid
PGA	2,4,6-Trihydroxybenzaldehyde (phloroglucinaldehyde)
ROS	Reactive oxygen species

SD	Standard deviation
SRB	Sulforhodamine B
TPP	Triphenylphosphine
UV-vis	Ultraviolet/visible

CHAPTER ONE: INTRODUCTION AND LITERATURE REVIEW

1.1. INTRODUCTION

Mitochondrial reactive oxygen species (ROS) have been implicated in aging, cancer and several mitochondrial diseases when found in excessively high concentrations. Lowering the concentrations of mitochondrial ROS, may then mitigate their health related problems. Flavonoids, including anthocyanidins, are known for their antioxidant behaviour and ability to decrease concentrations of ROS (Kahkonen and Heinonen, 2003). The enhanced mitochondriotropic characteristic of anthocyanidins over other flavonoids (Peng, 2012) potentially enables their enhanced protection against mitochondrial oxidative stress. Their favourable more positive charge in physiological conditions compared to other flavonoids (such as catechin and quercetin) and sufficient lipophilicity (compared to cyanidin-3-glucoside (C3G)) may be two crucial characteristics that enables their attraction towards the mitochondrial matrix side of the inner membrane. However, despite these favourable structural features, anthocyanidins are presumed to suffer from low stability and oral bioavailability. Given these characteristics, the health benefits of anthocyanins/anthocyanidins are generally believed to be mediated by their phenolic degradation products; protocatechuic acid (PCA) and phloroglucinaldehyde (PGA) (Kay *et al*, 2009). However, observations from the literature (Peng, 2012; Rodriguez-Mateos *et al*, 2014; Stevens and Maier, 2016) have challenged this claim and suggest that cyanidin itself or other compounds in the cyanidin degradation pathway act as potent bioactive agents.

The novelty of this work is to provide evidence that the mitochondriotropic property of cyanidin may provide better cytoprotective activity than other potent flavonoids (quercetin, catechin, C3G) and its degradation products (PCA, PGA) against a mitochondrial oxidative stress

inducer, such as doxorubicin. Also, despite the favourable protective activities of antioxidants, their ability to lower ROS may impede the cytotoxicity of cancer chemotherapies reducing the therapeutic benefit of chemotherapeutics against cancer cells. We therefore investigated the effect of cyanidin on doxorubicin cytotoxicity against hepatic cancer (HepG2) and leukemic (K562) cell lines.

1.2. LITERATURE REVIEW

1.2.1. Reactive oxygen species

ROS are strong oxidants formed intracellularly in mitochondria (Kirkinezos *et al*, 2001), endoplasmic reticulum (Zeeshan *et al*, 2016), and peroxisomes (Sandalio *et al*, 2013). They are also associated with plasma membrane NADPH oxidase activity (Panday *et al*, 2015). ROS include many molecules such as peroxides, superoxide, hydroxyl radical and singlet oxygen. At physiological levels, ROS have a crucial role in many physiological processes such as embryo development (Dennery *et al*, 2007), muscle exercise (Barbieri and Sestili, 2012; Steinbacher and Eckl, 2015) and macrophage function (Hsu and Wen, 2002). At the cellular level, ROS play a significant role in apoptosis, cell proliferation (Circu and Aw, 2010; Schieber and Chandel, 2014) and cell signaling (Thannickal and Fanburg, 2000). Despite these important roles, excessive ROS production leading to oxidative stress is implicated in a number of pathological conditions including cancer, aging, stroke, heart failure, and neurodegenerative diseases (Alvarez, *et al*, 2008; Armstrong, 2010; Belin *et al*, 2007; Davidson, 2010; de Moura *et al*, 2010; Fang *et al*, 2002; Gaweda-Walerych *et al*, 2013; Harman, 1972; Ladiges *et al*, 2010; Popa-Wagner *et al*, 2013; Popa-Freidovich, 1999; Schieber and Chandel, 2014; Witte *et al*, 2010; Zuo *et al*, 2015).

ROS cause cytotoxicity by reacting with important cellular macromolecules. Reactions with DNA, for example, can cause extensive damage to its structure leading to cell death (Gabbita *et al*, 1998; Lovell *et al*, 2007). In addition, ROS can attack the double bonds in unsaturated lipids causing the generation of highly reactive lipid peroxy radicals, which can further attack other unsaturated fatty acids in a chain reaction leading to extensive cellular damage (Berlett and Stadtman, 1997; Dalle-Donne *et al*, 2006). Moreover, these compounds can result in protein

modifications that can disrupt many functions and initiate apoptosis (Gella and Durary, 2009; Keller *et al*, 1997; Mattson *et al*, 2003).

To overcome oxidative stress, a condition caused by excessive production of ROS, many endogenous enzymes and exogenous antioxidants may react with ROS to suppress their reactivity. These agents have a common ability of scavenging ROS and minimizing their harmful effects (Birben *et al*, 2012; Grabacka *et al*, 2014). The widely variable exogenous antioxidants are divided into many classes and subclasses based on their chemical structure and characteristics.

1.2.2. Oxidative damage and mitochondrial ROS-related diseases

Mitochondrial oxidative stress and mitochondrial damage have been associated with the normal aging process and several different clinical implications including cancer, and certain neurological, muscular and cardiovascular diseases (Ballinger, 2005; Harman, 1956; Liou and Storz, 2010; Miquel *et al*, 1980; Terrill *et al*, 2013). For example, myocardial infarction, heart failure, and ischemia-reperfusion are conditions that involve elevated mitochondrial ROS (Gao *et al*, 2008; Tsutsui *et al*, 2006). Therefore, inhibition of mitochondrial ROS has been a reasonable approach to reduce the complications of these illnesses (Gao *et al*, 2008; Dhalla *et al*, 2000; Handy and Loscalzo, 2012; Madamanchi and Runge, 2007; Matsushima *et al*, 2006; Zhang and Gutterman, 2007).

1.2.3. ROS production in physiological conditions: involvement of the electron transport chain (ETC) and the fate of ROS once formed

Approximately 1-3% of mitochondrial oxygen consumption results in the production of ROS (Kirkinezos *et al*, 2001) making this organelle a major site of cellular ROS generation (Ott *et al*, 2007). Therefore, mechanisms of mitochondrial ROS production in physiological conditions have been widely investigated. The involvement of the electron transport chain (ETC) in the

production of ROS is well characterised. The widely accepted explanation to the production of ROS is the "leakage" of the electrons from the ETC, particularly from complexes I and III, and reduction of oxygen to form the superoxide free radical and other ROS (**Figure 1.1**). (Cadenas and Davies, 2000; Murphy, 2009; Turrens, 2003)

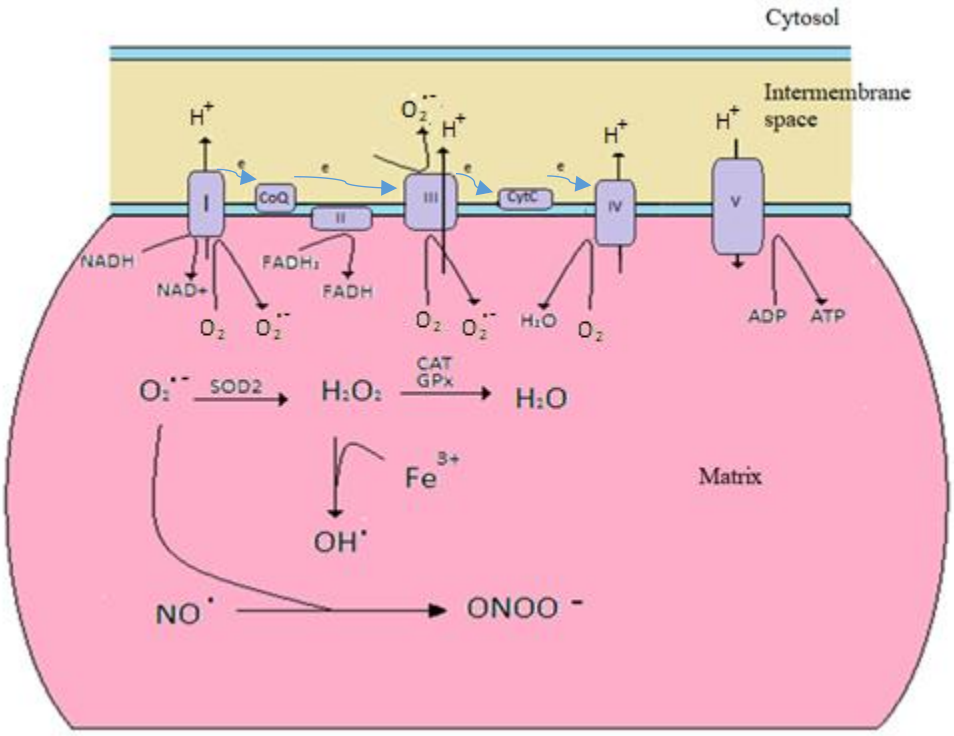

Figure 1.1: **Mitochondrial complexes and reactive oxygen species (ROS) production.** The electron transport chain (ETC) involves oxidation of electron carriers, NADH and $FADH_2$, and reduction of ubiquinone in mitochondrial complexes I and II. The energy released during the transport of the electrons is used by the complexes to pump protons from the mitochondrial matrix to the inter membrane space. The proton gradient formed across the membrane is utilized by ATP synthase (complex V) to generate ATP. The electrons are used to reduce oxygen to water at complex IV. ROS is released by the leakage of electrons from mainly complexes I and III to reduce oxygen and form a free-radical superoxide and other ROS. (Cadenas and Davies, 2000; Osellame *et al*, 2012; Turrens, 2003).

Several mechanisms exist to prevent the accumulation of ROS in cells. Once superoxide ($O_2^{\bullet -}$) molecules are formed, their half-life is short and several fates await them. They can form other oxygen derived reactive species such as peroxyl radical ($RO_2^{\bullet}$), hypochlorous acid (HOCl),

and alkoxyl radical ($RO^{\bullet}$). Alternatively, the negatively charged superoxide reacts rapidly with nitric oxide ($NO^{\bullet}$) to form the potent oxidant peroxynitrite ($ONOO^{-}$) and other reactive nitrogen species (RNS). Superoxide is also able to interact with some mitochondrial iron-sulfur containing proteins causing further damage to the mitochondria (Powers and Jackson, 2008). Cellular superoxide can also be rapidly dismutated to hydrogen peroxide (H_2O_2) spontaneously or *via* superoxide dismutase 1 (SOD1), 2 (SOD2) and 3 (SOD3) (Cadenas and Davies, 2000; Fridovich, 1986). H_2O_2 can penetrate membranes and oxidize thiol groups on cellular enzymes (Vranova *et al*, 2002). H_2O_2 can also react with Fe^{2+} to produce the highly reactive hydroxyl radical ($OH^{\bullet}$) by the Fenton reaction (Halliwell and Gutteridge, 1990). The $OH^{\bullet}$ is a very reactive molecule with strong oxidizing potential enabling it to interact with and damage any macromolecule in its proximity. Collectively, many mechanisms exist to prevent ROS from increasing to oxidative stress levels. Although highly efficient, these mechanisms may be overwhelmed by the many intrinsic and extrinsic factors that increase ROS levels. Examples of these extrinsic factors include ultraviolet (UV) irradiation, redox-cycling of quinones, medications, toxicants, metals and aging (Beal, 2005; Carvour *et al*, 2008; Kitazawa *et al*, 2002; 2001; Sheu *et al*, 2006).

1.2.4. ROS production as a side effect of medications and food

Medications and food consumption are associated with increases in ROS production. For example, high intakes of carbohydrates and fats are known to increase ROS production in muscles (Gregersen *et al*, 2012), liver and vascular system (Lozano *et al*, 2016). Food additives such as aspartame (Iyyaswamy and Rathinasamy, 2012) and food-borne toxins such as dioxins (Reichard *et al*, 2006) and nitrosamines (Ahotupa *et al*, 1987) are also reported to increase oxidative stress in different organs.

Many medications also contribute to elevations in ROS production. Common medications like acetaminophen (Jiang *et al*, 2015) and other non-steroidal anti-inflammatory drugs (Ghosh *et al*, 2015; Tomita *et al*, 2014) can increase hepatic and intestinal levels of ROS, respectively. Some cancer chemotherapeutic drugs increase ROS in normal cells causing dose limiting toxicities. Organ specific toxicities associated with chemotherapeutic agents such as 5-fluorouracil (5-FU) and cisplatin, is due to increases in ROS in specific cell types (Focaccetti *et al*, 2015, Lamberti *et al*, 2012; Minotti *et al*, 2004; Qian *et al*, 2018; Zhang *et al*, 2017; Zhang *et al*, 2009a). In particular, the chemotherapeutic agent doxorubicin has been shown to cause ROS-related cardiotoxicity.

1.2.5. The mechanism of toxicity of doxorubicin

Doxorubicin is a chemotherapeutic agent that is widely used for different cancer types (Wells *et al*, 2009). It exerts its anti-cancer biological activity by intercalation into DNA and inhibiting topoisomerase-II (Top2) (Gewirtz, 1999; Tewey *et al*, 1984; Thorn *et al*, 2011). Doxorubicin binds both DNA and Top2 (particularly Top2α) to form a Top2-doxorubicin-DNA cleavage complex to cause cell death. Despite its wide implementation in various cancer therapy regimens, its dosage is limited by cardiotoxicity and other organ toxicity (Chatterjee *et al*, 2010; Tangpong *et al*, 2011). Although other mechanisms have been proposed (Minotti *et al*, 2004; Zhang *et al*, 2012; Zhang *et al*, 2009b), it is generally believed that the main cause for cardiotoxicity is the over production of ROS in heart mitochondria (Berthiaume and Wallace, 2007; Doroshow, 1983; Singal and Iliskovic, 1998).

Many direct and indirect mechanisms have been investigated to explain the elevation in ROS levels following treatment with doxorubicin (Kim *et al*, 2006; Tsang *et al*, 2003; Wei *et al*, 2015). The production of ROS in heart cells, which are rich in mitochondria, is thought to be mediated by redox-cycling activity caused by the interaction of doxorubicin with complex I

(Davies and Doroshow, 1986; Tokarska-Schattner *et al*, 2006). The increase in mitochondrial superoxide levels and ROS was observed in many reports in different cell lines including cardiomyocytes (Branco *et al*, 2012, Mukhopadhyay *et al*, 2007; Mukhopadhyay *et al*, 2009; Octavia *et al*, 2012; Tsang *et al*, 2003). Also, ROS scavengers have been partially successful in reducing the cardiomyocyte toxicity of doxorubicin (Chacko *et al*, 2015), emphasizing the role of ROS in doxorubicin toxicity to cardiomyocytes.

In heart cells, doxorubicin is proposed to react with complex I resulting in the reduction of doxorubicin by the flavoproteins to form a radical semiquinone form (**Figure 1.2**). The semiquinone is oxidized by molecular oxygen to the quinone form and the superoxide radical which acts as a precursor to other ROS.

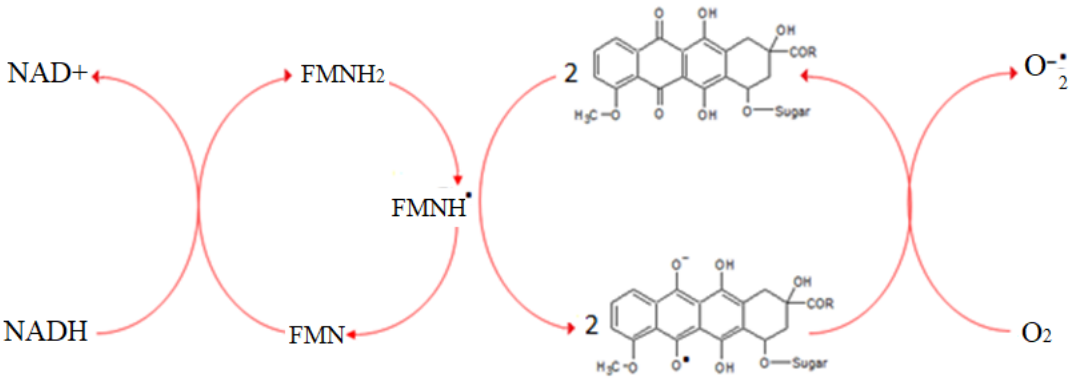

Figure 1.2: Cellular metabolism of doxorubicin and the formation of free radicals. Initially, doxorubicin is reduced by flavoproteins (such as mitochondrial complex I in heart cells), to form a radical semiquinone form. The fate of the semiquinone depends on the presence of oxygen, which is often high in cardiomyocytes. The semiquinone is oxidized in the presence of oxygen back to the quinone form. A superoxide radical is formed from the reaction which together with other ROS can react with proteins, DNA and lipids contributing to cellular toxicity. (Adapted from Davies and Doroshow, 1986; Tokarska-schattner *et al*, 2006).

The increase in mitochondrial ROS is presumed to be the main cause of toxicity in heart cells (Berthiaume and Wallace, 2007; Doroshow and Davies, 1986; Octavia *et al*, 2012; Singal and Iliskovic, 1998). Cardiomyocytes are rich in mitochondria (Stanley, 2004) and depend

principally on mitochondrial oxidative phosphorylation and complex I. The reaction of doxorubicin with this complex, then would cause redox-cycling activity and possibly a rapid increase in ROS upon exposure to doxorubicin. However, except in one (Mukhopadhyay *et al,* 2007), studies report increases after longer periods of incubations ranging from 12-48 hours (h) using concentrations between 1 and 5 µM (Bernuzzi *et al,* 2009; Cheung *et al,* 2015; Hosseinzadah *et al,* 2011; Tan *et al,* 2010). Such prolonged exposures with doxorubicin suggests apoptosis as a mechanism of ROS increase (Akopova *et al,* 2012, Chen et al, 2003) rather than a direct redox-cycling activity in the heart.

The usage of H9c2 cells as an *in vitro* model to evaluate the cardiotoxicity of many compounds, including doxorubicin, is widely accepted (Enayetallah *et al*, 2013). Much of the research on cytotoxicity, ROS and mitochondrial superoxide generation, as well as effects on mitochondrial membrane potential (MMP) with doxorubicin has involved undifferentiated H9c2 cells (Choi *et al*, 2007; Deus *et al,* 2015; Mukhopadhyay *et al*, 2007; 2009). The mechanism of doxorubicin cytotoxicity may be different between actively dividing cells and differentiated cardiomyocytes. In actively dividing cancer cells the mechanism is primarily by DNA intercalation and interference with DNA replication (Thorn *et al*, 2011), while the mechanism for cardiotoxicity is thought to be mitochondrial redox-cycling and ROS production (Berthiaume and Wallace, 2007; Doroshow and Davies, 1986; Octavia *et al,* 2012; Singal and Iliskovic, 1998). The literature indicates that differentiated H9c2 have phenotypes more similar to mature cardiomyocytes *in vivo* and thus would more accurately represent the mechanism of doxorubicin-induced cardiotoxicity (Branco *et al*, 2012; Branco *et al*, 2015).

1.2.6. Scavenging of ROS by antioxidant agents

The human diet contains a wide array of antioxidant chemicals that have attracted attention and efforts to identify, characterize and evaluate their toxicity and efficacy (Devasagayam *et al*, 2004; Grabacka *et al*, 2014; Huh *et al*, 2004; Miki *et al*, 2012; Sies and Stahl, 1995). These antioxidants have the ability to scavenge radicals and may assist in treating or preventing many diseases caused by oxidative stress (Hajhashemi *et al*, 2010; Pham-Huy *et al*, 2008).

Several epidemiological studies showed that ingestion of antioxidant compounds or diets containing antioxidants has beneficial anti-inflammatory, anti-atherosclerotic, antitumor, antimutagenic, anticarcinogenic, antibacterial and antiviral activities (Hertog *et al*, 1995; Mitscher *et al*, 1996; Sala *et al*, 2002; Sun *et al*, 2002; Yang *et al*, 2001). Whether these observations can be shown in interventional controlled studies is still controversial (Baynes, 1999; 1991; Chang *et al*, 1993; Halliwell and Gutteridge, 1990; McLennan *et al*, 1991; Young *et al*, 1995). Despite the many challenges, the low toxicity profile of anthocyanidins, their numerous clinical applications, low cost, and broad availability could encourage further investigation into their possible clinical applications.

Interventional studies with dietary antioxidants have shown limited benefit due to a number of factors that are often poorly acknowledged in the design of these studies. Factors that can contribute to the limited activity include: 1) Low oral bioavalability associated with a majority of flavonoid antioxidants due to low intestinal absorption and high first pass metabolism (Thilakarathna and Rupasinghe, 2013); 2) Instability of some antioxidants, such as certain flavonoids, in the gastrointestinal tract resulting in tissues levels too low to exert an activity (Braune *et al*, 2001; Fleschhut *et al*, 2006; Ramesova *et al*, 2012); 3) Limited distribution and accumulation of antioxidants into mitochondria to address excessive mitochondrial ROS (Fiorani

et al, 2010; Peng, 2012); 4) The low potency of many natural antioxidants and/or the extremely rapid and high damaging effects of oxidants may hinder their bioactivity (Cadenas and Davies, 2000; Fridovich, 1986; Halliwell and Gutteridge, 1990; Milani *et al*, 2011; Powers and Jackson, 2008), requiring the ingestion of high quantities of antioxidant-rich food to reach a therapeutic effect (Hagiwara *et al*, 2001; Pojer *et al*, 2013); and 5) A limited knowledge of the pathophysiology of disease (Diaz-Hung and González Fraguela, 2014) and of antioxidant pharmacology (Covey *et al*, 2006) has underestimated their efficacy. These observations stress the importance of evaluating available antioxidants to comprehensively understand their behaviour and to reveal lead compounds for the synthesis of new agents with enhanced bioactivities. For example, the ability to accumulate in the mitochondria is evidently a crucial feature to improve the bioactivity of antioxidants in situations involving mitochondrial oxidative stress. Therefore, emphasis has been directed towards characterising new antioxidants with ability to accumulate into mitochondria.

1.2.7. Non mitochondria-targeted antioxidants

Antioxidants are widely used for their possible health benefits (Injac and Strukelj, 2008; Devasagayam *et al*, 2004). Antioxidant vitamins, particularly vitamin E and C, have received considerable attention due to their high bioavailability and potential to scavenge ROS (Conti *et al*, 2016; Fahn *et al*, 1992; Lan and Jiang, 1997; May, 1999; Odunze *et al*, 1990; Roghani and Behzadi, 2001; Sano *et al*, 1997; Wang and Quinn, 2000).

The polyphenol, resveratrol has shown moderate potency in lowering ROS levels in *in vitro* studies. Further, resveratrol restores the normal level of endogenous antioxidants by inducing expression of glutathione and antioxidant enzymes via activation of the redox sensitive transcription factor nuclear erythroid-related factor 2 (Nrf2) (Kode *et al*, 2008). For example,

resveratrol was able to increase the expression of MnSOD in mouse brains (Robb *et al*, 2008) leading to decreased lipid peroxidation (Baur *et al*, 2006; Khanduja *et al*, 2004).

Many other antioxidants have been investigated for their bioactivity. For example, dietary co-enzyme Q10 (CoQ10, or ubiquinone) also successfully demonstrated antioxidant and neuroprotective activities in mice (Wadsworth *et al*, 2008). Endogenous CoQ10 is localized in the inner mitochondrial membrane where it acts as an electron carrier from complex I and complex II in the ETC and transfers electrons to complex III. Acetyl-L-carnitine (ALCAR) (Ames and Liu, 2004) and R-alpha lipoic acid (RLA) (Maczurek *et al*, 2008) were also investigated for their activity as antioxidants. RLA is reduced to dihydrolipoic acid which has antioxidant activity. The combination of both RLA and ALCAR decreased ROS mediated damage, reduced mitochondrial damage and improved cognitive and motor functions in rats (Aliev *et al*, 2009; Haenen and Bast, 1991; Long *et al*, 2009).

In general, *in vitro* studies indicate high concentrations of these chemicals provide significant protection from elevated ROS. Nevertheless, disappointing results were found in many *in vivo* studies (Etminan *et al*, 2005; Padayatty *et al*, 2003; Parkinson Study Group, 1993; Scheider *et al*, 1997; Seidl and Potashkin, 2011; Weber *et al*, 2006; Zhang *et al*, 2002).

1.2.8. Mitochondria-targeted antioxidant therapy

Since mitochondria are a major site for ROS production (Ott *et al*, 2007), targeting this organelle is anticipated to increase the effectiveness of antioxidants in conditions of mitochondrial oxidative stress (Oyewole and Birch-Machin, 2015; Smith and Murphy, 2011). However, limited reports have compared the bioactivity for mitochondria-targeted to non-targeted antioxidants in ROS-linked illnesses. One study (Jauslin *et al*, 2003) showed the enhanced activity of mitochondria-targeted antioxidants over the untargeted antioxidants in protecting against oxidative

stress in Friedreich Ataxia fibroblasts. However, evidence for the improved bioactivity of mitochondrial-targeted antioxidants is very limited. Various strategies have been evaluated to enhance the mitochondrial accumulation of potential antioxidants. One approach that is generally accepted is conjugating an antioxidant to a positively charged lipophilic molecule which accumulates in the mitochondria. The positive charge is attracted by the mitochondrial matrix negative charge caused by the large mitochondrial membrane potential ($\Delta\Psi m$) of 150-180 mV. Many antioxidants have been conjugated to a triphenylphosphonium (TPP) cation (Liberman *et al*, 1969; Murphy and Smith, 2007; Ross *et al*, 2005), which has the suitable chemical features (positive charge and lipophilicity) to enable it to accumulate in mitochondria (100- to 500-fold higher concentration than the cytoplasm) (Smith *et al* 1999, 2003). Based on this approach, several mitochondria-targeted antioxidants with good bioavailability were synthesized including MitoQ, MitoVitE, and MitoTEMPOL (Murphy and Smith, 2007; Ross *et al*, 2005). Treatments with these compounds resulted in significant protection from neurodegenerative and cardiovascular diseases in different mouse models (Fetisova *et al*, 2010; Hobbs *et al*, 2008; Owada *et al*, 2017; Sheu *et al*, 2006; Smith and Murphy, 2010; Zang *et al*, 2012).

1.2.8.1. MitoVitE

MitoVitE (mitotocopherol) is TPP+ conjugated to an α-tocopherol moiety by a two-carbon chain in place of the phytyl side chain. It was found to be effective in protection against oxidative stress-induced aortic endothelial cell apoptosis (Davidson, 2010; Li, 2013). It accumulates in the inner membrane of the mitochondria of different tissues and protects the cells from lipid peroxidation and oxidative stress (Smith *et al*, 1999; Smith *et al*, 2003; Smith and Murphy, 2011). In an *in vitro* study on fibroblasts from Friedrich Ataxia patients, MitoVitE protected the cells from oxidative stress-induced cell death (Jauslin *et al*, 2003). Animal models showed protection

by MitoVitE against cardiac damage in septic pneumonia animal models (Zang *et al*, 2012). Despite these favourable effects, MitoVitE showed neurotoxicity at high doses in some animal models explaining the possible reason for the limited number of human clinical trials (Covey *et al*, 2006).

1.2.8.2. MitoTEMPOL

MitoTEMPOL consists of TPP+ conjugated with a stable piperidine nitroxide radical TEMPOL (4-hydroxy-2,2,6,6,tetramethyl-piperidine-1-oxyl) designed to target the mitochondria. In many cellular models, MitoTEMPOL was able to protect cells from oxidative stress (Lim *et al*, 2011; Kizhakekuttu *et al*, 2012). In addition, a few *in vivo* evaluations have shown protective effects against cardiovascular diseases (Cho *et al*, 2013; Pung *et al*, 2012).

1.2.8.3. Other "Mito" compounds

Many "mito" compounds have been developed. MitoApocynin (conjugated with the NADPH oxidase inhibitor and antioxidant, apocynin), MitoPBN (conjugated with a carbon-centered radical reactor, phenoxy-butyl-nitrone) (Barclay and Vinqvist, 2000) and MitoPeroxidase (conjugated with the glutathione peroxidase-like actor, ebselen) (Mugesh *et al*, 2001) are compounds that conjugate TPP+ with different antioxidants. These conjugates accumulate in mitochondria and exert an activity in some *in vivo* animal models (Ghosh *et al*, 2016) but these molecules require evaluation of their effectiveness in human studies targeting different diseases (Jin *et al*, 2014). Another conjugate, SkQ1, a plastoquinone covalently bound to TPP+ that acts as a potent antioxidant in isolated mitochondria (Antonenko *et al*, 2008) and cell cultures (Skulachev *et al*, 2011) also shows promise in reducing oxidative stress in different animal models of disease (Agapova *et al*, 2008; Anisimov *et al*, 2008; Bakeeva *et al*, 2008; Neroev *et al*, 2008).

1.2.8.4. Szeto-Schiller (SS) tetrapeptides and alternative targeting approaches

Many side effects of TPP+ have been reported (Murphy, 2008; Trnka *et al*, 2015). For this reason, different strategies that target the mitochondria have been adopted. Dependent on the mitochondrial potential, the Szeto-Schiller (SS) tetrapeptides are believed to target the mitochondria due to their aromatic-cationic motif (Zhao *et al*, 2004; 2003). The most currently studied compounds of this group are SS-20 and SS-31. They are selectively localized to the inner mitochondrial membrane (Zhao *et al*, 2005) and have a dimethyltyrosine (Dmt) residue, which acts as a free radical scavenger (Szeto *et al*, 2008). Promising results have been shown for the peptide's antioxidant potency in neuronal *in vitro* studies as well as one animal study (Reddy *et al*, 2006; Yang *et al*, 2009; Zhao *et al*, 2005). However, whether its antioxidant activity or other unknown mechanism is responsible for the neuroprotection is undetermined (Yang *et al*, 2009).

1.2.9 Flavonoids

Positive outcomes in treating/preventing many mitochondrial ROS related diseases *in vitro* and *in vivo* provide potential evidence for the benefit of targeting the mitochondria. However, disadvantages exist with the available mitochondria targeting moieties, such as TPP+, as these compounds can lead to toxicity. Moreover, some of the available mitochondria-targeted antioxidants have apparent low potency. This can be inferred from the high concentrations required in *in vitro* studies. Therefore, an urgent need for the development of other mitochondrial targeted antioxidants with good potency, low cost and low toxicity is required. The flavonoids, particularly the anthocyanin subclass, may serve as a natural alternative to target the mitochondria.

Flavonoids are found in many fruits, vegetables and other foods consumed regularly by humans. Due to their strong *in vitro* antioxidant potency, these compounds have been tested for their anti-carcinogenic, anti-inflammatory, anti-mutagenic and cellular protection activity

(Darvesh *et al*, 2010; Havsteen, 2002; Hu 2007; Kumar and Pendey, 2013; Middleton *et al* 2000; Xiao *et al*, 2011; Yao *et al*, 2004). Epidemiological evidence suggests flavonoid rich diets lower risks of cardiovascular disease, type 2 diabetes, neurological disease, and cancer (Bazzano *et al*, 2003; Dauchet and Dallongeville, 2008; Eichholzer *et al*, 2001; Garcia-Closas *et al*, 1999; Hertog *et al*, 1997; 1993; Mink *et al*, 2007; Zunino, 2009).

The cytoprotective effect of some flavonoids against doxorubicin has been tested *in vitro* or *in vivo* (eg. Chen *et al*, 2013; Choi *et al*, 2007; Chularojmontri *et al*, 2013; Dong *et al*, 2014; Han *et al*, 2012; Kaiserova *et al*, 2007; Mandziuk *et al*., 2015a; 2015b; Mojzisova *et al*, 2009; van Acker *et al*, 2001; Wang *et al*, 2013). However, some of these studies (eg. Choi *et al*, 2010) used crude extracts rather than pure compounds. In addition, only a few studies (eg. Kaiserova *et al*, 2007; van Acker *et al*, 2001) conducted a comparative analysis between different classes of flavonoids. Such studies are crucial in understanding the structure-activity relationship in decreasing mitochondrial ROS, or designing new compounds, with a better bioactivity profile.

1.2.9.1. Structure/Subclasses

The basic structure of flavonoids contains two benzene rings and one heterocyclic pyran or pyrone ring (**Figure 1.3**). The roughly 6400 natural flavonoid compounds found in various plants share the same structure with different functional groups attached to the benzene and the heterocyclic rings. Depending on the hydroxylation pattern, conjugation between the aromatic rings, methoxy groups and glucosidic moieties, the compounds are subdivided into six major subclasses. These subclasses include flavones, flavonols, flavanones, flavanols (catechins), anthocyanidins and isoflavones (Beecher, 2003). Two related subclasses, which include chalcones and dihydroflavonols, are also found in nature (Heim *et al*, 2002). Flavonoids are primarily found in nature in their glucosylated form. The carbohydrate moieties are usually attached at locations

3 and 7. These carbohydrates include D-glucose, L-rhamnose, D-glucorhamnose, D-galactose, lignin, and D-arabinose (Heim *et al*, 2002).

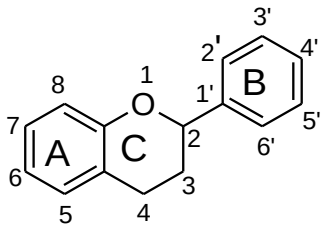

Figure 1.3: Basic flavonoid structure. The presence and location of the different functional groups forms the wide variety of flavonoid compounds (Adapted from Heim *et al*, 2002).

1.2.9.2. Flavonoid antioxidant properties

Dietary plant compounds, especially flavonoids and other polyphenols, have been widely investigated for their antioxidant activity. Despite their low bioavailability, the potent antioxidant activity of flavonoids has been supported by evidence for their protection against oxidative stress related diseases (Darvesh *et al*, 2010; Havsteen, 2002). The protective effect observed by a wide range of studies encouraged further research into the health benefits of these chemicals.

Flavonoids are believed to protect against oxidative damage by scavenging free radicals and chelating transition-metals involved in free radical production (Aruoma, 2003). Flavonoids can donate a hydrogen atom from an aromatic hydroxy group to a free radical. The process forms a stable phenolic delocalized radical and reduces the reactive oxygen radical (Rice-Evans *et al*, 1996).

Flavonoid (OH) + $R^{\bullet}$ ⟶ Flavonoid($O^{\bullet}$) + RH

Free radicals such as hydroxyl, lipid alkoxyl, peroxyl and superoxide and other ROS such as hypochlorous acid can all be scavenged by flavonoids (Heim *et al*, 2002; Rice-Evans *et al*, 1996). Quercetin and rutin also can lower ROS by chelating transition metal ions thus decreasing their ability to promote reactive species formation (Afanasev *et al*, 1989). Also, flavonoids such

as quercetin, myricetin and fisetin can induce the endogenous antioxidant enzymes such as glutathione-S-transferase, thus causing a reduction in ROS (Elliott *et al*, 1992; Filipe *et al*, 2002).

In vivo and *in vitro* studies suggest that the antioxidant activity of flavonoids may protect against oxidative stress related diseases (Middleton *et al*, 2000; Rein *et al*, 2000). In cardiovascular disease, the ability of flavonoids to inhibit the production of lipid hydroperoxides mitigates the development of coronary artery disease (de Whalley *et al*, 1990; Middleton *et al*, 2000; Nijveldt *et al*, 2001). The antioxidant activity of flavonoids also has benefit in liver (Peres *et al*, 2000; Pisonero-Vaquero *et al*, 2015), neurological (Vauzour *et al*, 2008) and muscular (Malaguti *et al*, 2013) disorders. In addition to their antioxidant activity, flavonoids show antimutagenic, anticarcinogenic, anti-allergic, and anti-inflammatory effects (Darvesh *et al*, 2010; Havsteen, 2002; Middleton *et al*, 2000; Middleton and Kandaswami, 1992; Nijveldt *et al*, 2001; Obrenovich *et al*, 2010). These properties may be exploited to mitigate the negative effects of other chemotherapeutic agents, as exemplified by the cardioprotective effects of anthocyanidins (such as cyanidin) and flavonols (such as quercetin) against doxorubicin cardiotoxicity in one *in vitro* and *in vivo* studies (Choi *et al*, 2007; Dong, 2014; Kaiserova *et al*, 2007; Sadzuka *et al*, 1997). These results provide important evidence that flavonoids can be utilized to promote human health. However, these studies fail to compare the activities of anthocyanidins with other flavonoids subclasses. Such comparison is highly crucial in understanding the significance of certain structural features present in anthocyanidin. In addition, these studies evaluate the protective activity of anthcyanidins when cells are incubated with doxorubicin for extended periods (24-48 h). The extended incubations with doxorubicin apoptosis mediated increase in ROS levels instead of redox-cycling mechanism.

1.2.9.3. Flavonoids and mitochondria

An inability to accumulate into mitochondria may explain the lack of activity of some antioxidants. Mitochondriotropic compounds may overcome this limitation and several studies suggest the ability of some flavonoids to accumulate into isolated mitochondria (Cavallini *et al*, 1978; Dragicevic *et al*, 2011; Haraguchi *et al*, 1996; Trumbeckaite *et al*, 2006) and mitochondria of cultured cells (Dragicevic *et al*, 2011). Their accumulation was associated with reductions in lipid peroxidation following exposure to of isolated mitochondria to pro-oxidants (eg. Elingold *et al*, 2008; Santos *et al*, 1998; Ratty and Das, 1988). Also, flavonoids were able to inhibit membrane permeability transition in Ca^{2+} induced mitochondrial swelling and inhibition of protein sulfhydryl oxidation (Santos *et al*, 1998). Some flavonoids were also able to inhibit NADH-oxidase activity in mitochondria which may inhibit ROS generation (Hodnick *et al*, 1994; Santos *et al*, 1998). Several flavonoids such as quercetin and epicatechin, cooperate with ascorbate to protect mitochondria-mimetic membranes from cytochrome c-catalyzed lipid peroxidation (Bandy and Bechara, 2001). Although the accumulation of quercetin in mitochondria was found to be significant *in vitro* (Fiorani *et al*, 2010; Mattarei *et al*, 2008) it is not clear whether quercetin accumulates in sufficient quantities in tissue mitochondria, particularly in the heart, to protect cells from mitochondrial insults (de Oliveira *et al*, 2016). Apart from the work of Peng (2012), the intracellular distribution of cyanidin has not been evaluated.

1.2.9.4. Anthocyanins

Anthocyanins are flavonoids found in fruits and vegetables as water soluble glucosides of polyhydroxy and polymethoxy derivatives of 2-phenylbenzopyrylium or flavylium salts (**Figure 1.4)** (Wallace, 2013). The glucosylated or nonglucosylated forms are named anthocyanins and anthocyanidins, respectively (**Figure 1.4)**. They act as natural pigments in plants and give them

their blue, purple, and red colors. Six anthocyanins are largely found in nature, namely, glucosides of the anthocyanidins cyanidin, delphinidin, malvidin, pelargonidin, peonidin, petunidin. The wide range of compounds differs in the number and location of hydroxyl, methylated and glucoside groups. These chemicals have attracted considerable interest for their potent antioxidant activity when tested in many different *in vitro* and *in vivo* assays (Andres-Lacueva *et al*, 2005; Hassimotto *et al*, 2008; Neto, 2007; Serraino *et al*, 2003). Previous studies in our laboratory (Peng, 2012) suggest that their potential favourable activity compared to other flavonoid subclasses is most likely caused by their accumulatation in mitochondria where they can exert their antioxidant activity.

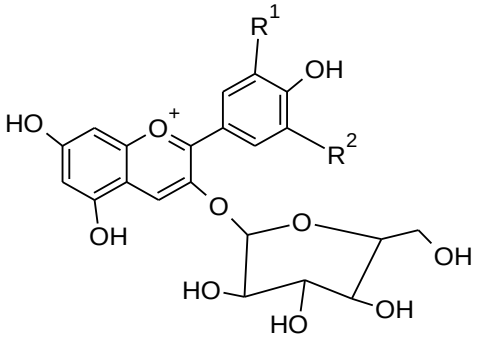

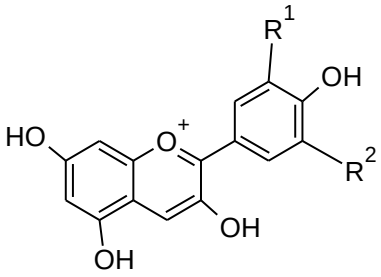

R1	**R2**	**Anthocyanidin 3-glucoside) (Anthocyanin)**
H	H	Pelargondin-3-glucoside (Pelargonin)
OH	H	Cyanidin-3-glucoside (Cyanin)
OCH_3	H	Peonidin-3-glucoside (Peonin)

R1	**R2**	**Anthocyanin aglycone** (Anthocyanidin)
H	H	Pelargonidin
OH	H	Cyanidin
OCH_3	H	Peonidin

OH	OH	Delphinidin-3-glucoside (Delphin)	OH	OH	Delphinidin
OCH_3	OH	Petunidin-3-glucoside (Petunin)	OCH_3	OH	Petunidin
OCH_3	OCH_3	Malvidin-3-glucoside (Malvin)	OCH_3	OCH_3	Malvidin

Figure 1.4: General structure of anthocyanins. The presence and location of the different functional groups forms the wide variety of anthocyanin compounds (Adapted from Sancho and Pastore, 2012).

1.2.9.4.1. Anthocyanins and mitochondria

Since the involvement of mitochondrial ROS is apparent in many diseases and conditions, targeting this organelle by antioxidants is crucial. However, achieving an ideal antioxidant with potential treatment activity has been a challenge. The chemical structure should have sufficient lipophilicity and a positive charge at physiological pH (Graham *et al*, 2009). Interestingly, both structural features are found in anthocyanidins. Therefore, these compounds are presented as a widely available and inexpensive antioxidant. The antioxidant activity and the therapeutic potential of anthocyanins have been well documented (Lila 2004; Prior *et al*, 2001; Zhao *et al*, 2013; Zheng *et al*, 2003). Work from our laboratory (Peng, 2012) showed that the anthocyanidin, cyanidin, accumulated in the mitochondria to a greater extent than cyanidin-3-glucoside, quercetin and quercetin-3-glucoside. Being widely available, these compounds might serve as an inexpensive alternative to synthetic mitochondriotropic antioxidants and have therapeutic benefit in conditions such as doxorubicin-induced mitochondrial damage in the heart.

The attraction of amphiphilic compounds such as anthocyanidins into the mitochondria may be influenced by the mitochondrial membrane potential (MMP). This charge is believed to increase the accumulation of lipophilic cations inside the mitochondria by 10 fold for every 61 mV increase (Murphy, 2008). In addition to the MMP, the unique phospholipid cardiolipin, found in large quantities in the inner mitochondria membrane (Houtkooper and Vaz, 2008) possesses a negative charge (Paradies *et al*, 2014), which further facilitates the accumulation of lipophilic cationic compounds.

Flavonoids differ in their pKa value which determines the charge they possess at physiological pH. A suitable pKa is required to enable the flavonoids to form a positive charge thus allowing their accumulation in the mitochondria. With pKa values for anthocyanin flavylium ions of 5.3-5.9 (Borkowski *et al*, 2005), the equilibrium between the different forms of cyanidin favors the formation of flavylium cation along with the neutral quinoid form at physiological pH (**Figure 1.5**). With regard to C3G however, the highly hydrophilic glucoside molecule attached to the anthocyanidin may impede its entrance to the mitochondria. Therefore, the aglycone possesses the favorable charge with reasonable lipophilicity to passively cross the mitochondrial membrane. This may present an explanation for the higher cytoprotective activity for cyanidin compared to C3G against doxorubicin-induced cytotoxicity and lipid peroxidation observed previously in H9c2 cardiomyocytes (Choi *et al*, 2007) and against different pro-oxidants in other cell lines (Adhikari *et al*, 2005; Chun *et al*, 2003; Jang *et al*, 2005; Lazze *et al*, 2003).

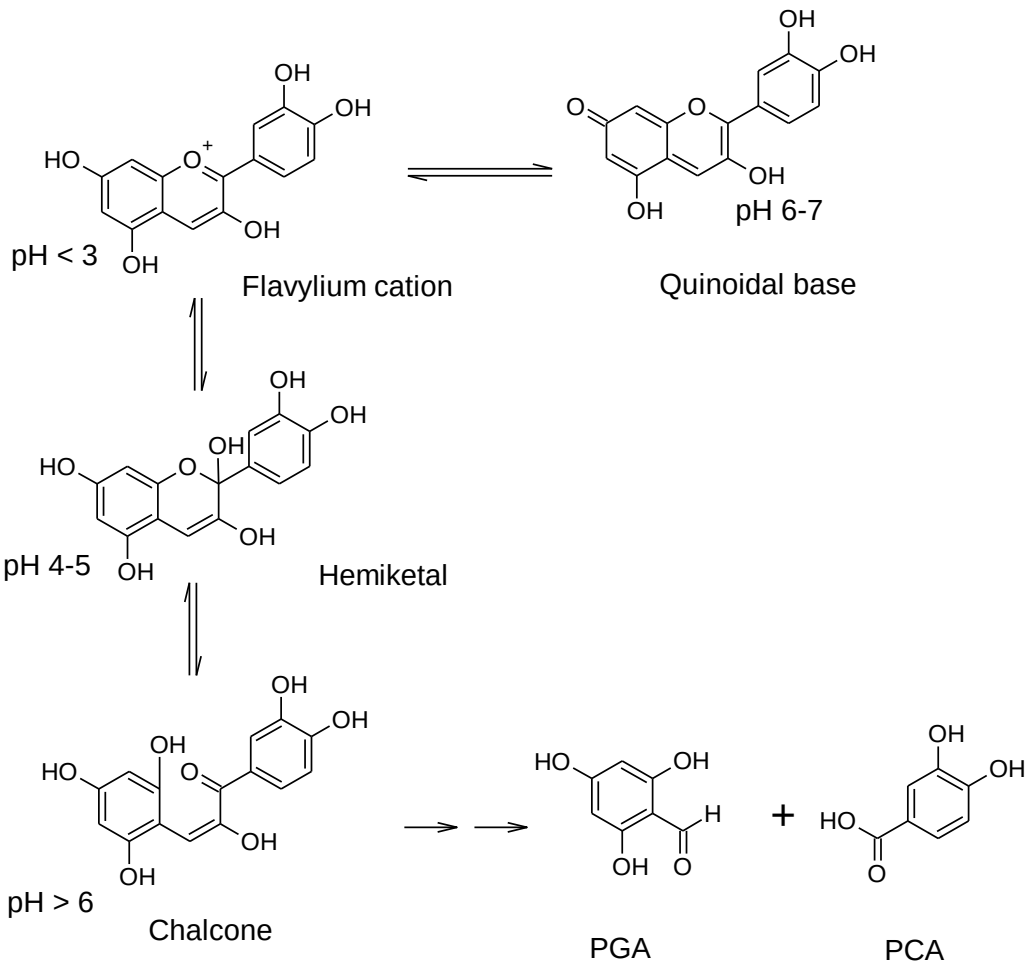

Figure 1.5: Proposed degradation pathway for anthocyanins. Cyanidin parent compound, flavylium ion (287 Da), is speculated to degrade rapidly to protocatechuic acid (PCA) (154 Da) and phloroglucinaldehye (PGA) (154 Da) by passing through different intermediate compounds namely, hemiketal (304 Da), chalcone (304 Da). Quinoidal base (286 Da) is also proposed as a product of the degradation. 99% of the compound is assumed to be found in the indicated form at the indicated pH. (Adapted from Borkowski *et al*, 2005; Fang, 2014; Kamiloglu *et al*, 2015).

In contrast, the subclasses, flavonols and flavanols with pKa's of ~6 and ~4, respectively (Escandar and Sala, 1991; Lemanska *et al*, 2001; Jovanovic *et al*, 1994), would form a mixture of anions and neutral molecules at neutral pH. Despite their known strong antioxidant potency, relative stability and amphiphilic nature, the negatively charged flavonoids at physiological pH (quercetin, catechin) (Chebotarev and Snigur, 2015) may have less mitochondrial uptake and

activity compared to cyanidin. Despite these favourable structural features, anthocyanidins including cyanidin are believed to have low systemic bioavailabilities, which may cause a limited clinical outcome. However, should the low quantities of an anthocyanidin accumulate in key organelles (such as the mitochondrial inner membrane), it could have substantial biological effects.

1.2.9.4.2. Systemic exposure following oral or IV administration

Anthocyanins, particularly C3G, are rapidly and directly absorbed across the intestine causing a fast increase in plasma levels (Hassimotto *et al*., 2008; Mazza *et al*., 2002) but only to reach a low plasma bioavailability (0.02%) (Abourashed, 2013; de Ferrars *et al*, 2014) with a low plasma half-life ($t_{1/2}$ 0.36 h) (Czank *et al*, 2013; de Ferrars *et al*, 2014; Fang, 2014; Prior *et al*, 2010; Seeram *et al*, 2001; Tsuda *et al*, 2000; 1999; Vanzo *et al*, 2011; Vitaglion *et al*, 2007). The low bioavailability is often assumed to be due to rapid degradation in physiological environments (McGhie and Walton, 2007; Wallace and Giusti, 2013), as observed in many *in vitro* experiments (Kay *et al*, 2009; Liu *et al*, 2014b; Yang *et al*, 2018). However, some studies suggest that they may be more bioavailable than previously thought (Kay *et al*, 2017; Lila *et al*, 2016). Despite these reports, observations from *in vivo* work provide some evidence that C3G, once introduced to the blood, does not immediately degrade to PCA and PGA. For example, the fast disappearance of anthocyanins from plasma is accompanied by the fast appearance of C3G/anthocyanins in brain, kidney, liver and urine after an oral ingestion (Bub *et al*, 2001; de Ferrars *et al*, 2014; Kalt *et al*, 2008; McGhie and Walton, 2007, Matsumoto *et al*., 2001; Mazza *et al*, 2002; Talavera *et al*, 2005; Vanzo *et al*, 2011). Also, limitations in available analytical techniques have possibly resulted in underestimation of the stability of anthocyanins (Lila *et al*, 2016). Additionally, one group (Peng, 2012) were able to detect cyanidin in the heart of injected mice 30 min after its administration. Combined, these reports provide evidence that anthocyanins and possibly

anthocyanidins do not degrade immediately after administration. Therefore, further research on their stability is needed in different *in vitro* settings which might be extrapolated to *in vivo* physiological environments.

1.2.9.4.3. Anthocyanin stability in in vitro physiological environments

Few studies have addressed the stability of anthocyanins in different *in vitro* settings relevant to biological activities (Kay *et al*, 2009; Kern *et al*, 2007; Seeram *et al*, 2001). A series of degradation experiments for cyanidin and C3G in different environments were performed (Kay *et al*, 2009). In summary, a loss of ~15% and ~90% of original C3G and cyanidin, respectively were reported within 3 h when incubated in phosphate buffered saline (PBS) (37°C, pH 7.4). The major degradation products detected were PCA and PGA. The degradation process is speculated to pass through many intermediate chemicals leading to the two compounds (**Figure 2.5)** (Fang, 2014). The production of PCA and PGA is presumed to occur rapidly and irreversibly (Fang, 2014; Kay *et al*, 2009). A similar lack of stability in cell culture media was also observed by other groups (Kern *et al*, 2007; Seeram *et al*, 2001). Such studies have led to a general belief that the bioactivity of dietary anthocyanins is likely to be mediated by their degradation products particularly, PCA and PGA (Kay *et al*, 2009).

1.2.9.4.4. Biological activity of Anthocyanins

Anthocyanins may exert their biological activity as ROS scavengers (Chun *et al*, 2003, Wallace and Giusti, 2013). In addition to their antioxidant activity, some anthocyanins such as cyanidin have strong anti-inflammatory activity. Indeed, cyanidin showed higher potency against cyclooxygenase activity than the relatively potent anti-inflammatory drugs naproxen, ibuprofen and aspirin (Wang *et al*, 1999). In addition, a few anthocyanins were reported to protect DNA from oxidative damage (Sarma and Sharma, 1999) by forming a stabilized DNA triplex (Mas *et*

al, 2000). Anthocyanins may also preserve the activity of GSH and inhibit cardiolipin oxidation and mitochondrial fragmentation in certain neuronal cells (Kelsey *et al*, 2011). Due to these activities, anthocyanins may be able to exert many health benefits (Tsuda *et al*, 1999; Tsuda 2012).

1.2.9.4.5. The cytoprotective effects of anthocyanins against ROS related diseases

Due to their antioxidant activity, anthocyanins may protect from many diseases related to ROS such as cancer (chemotherapeutics), Parkinson's disease, microbial infections, inflammatory diseases, ocular and cardiovascular diabetic complications, and neurodegenerative disorders (Al-Awwadi *et al*, 2005; Chen *et al*, 2005; Dai *et al*, 2009; Kong *et al*, 2003; Mazza *et al*, 2002; Mink *et al*, 2007; Nasri *et al*, 2011; Neto, 2007; Olsson *et al*, 2004; Sasaki *et al*, 2007; Thomasset *et al*, 2009; Tsuda *et al*, 2003). In addition, the protective ability of anthocyanin-rich extracts against doxorubicin-induced ROS to mitigate its cardiotoxicity has been investigated mostly by *in vitro* (Hosseini *et al*, 2017; Tenore *et al*, 2013) and a few *in vivo* (Ashour *et al*, 2011; Choi *et al*, 2010; Diamanti *et al*, 2014; Hassanpour *et al*, 2011) studies. The use of extracts in these studies limits the ability to identify the causative bioacitive compound(s). Two studies have shown the protective effect of pure anthocyanidins or an anthocyanin-rich extract against doxorubicin-induced oxidative damage in H9c2 cells (Choi *et al*, 2007; Huang *et al*, 2016). However, to our knowledge, the protective activity of anthocyanins has not been compared with other subclasses of flavonoids to highlight the importance of their structural features (i.e. positive charge and suitable lipophilicity).

1.2.10. The usage of antioxidants with cancer chemotherapeutics

Elevated ROS is important in cancer cell proliferation and survival (Kumari *et al*, 2018; Liou and Storz, 2010). Therefore, depleting their concentration by antioxidants can inhibit cancer cell proliferation (Dong *et al*, 2016; Zhang *et al*, 2016). Therefore, antioxidants have been

employed for the purpose of lowering ROS levels to inhibit cancer cell proliferation. However, a concern stems from the ability of cancer cells to produce further ROS thus limiting the effectiveness of the antioxidants. Although promising, evidence for the effectiveness of antioxidants in cancer treatment, are limited (Seeram *et al*, 2006; Simone *et al,* 2007; Singh *et al*, 2018; Yang *et al,* 1998).

In addition, when used with chemotherapeutics, antioxidants have been shown to protect different cell types from the toxicity of the drugs (Singh *et al*, 2017). ROS-induction by some chemotherapeutics is involved in their mechanism of cytotoxicity in cancer cells (Alexandre *et al*, 2006; Llobet *et al*, 2008; Qanungo *et al*, 2005; Shankar *et al*, 2008; 2007; Yokoyama *et al*, 2017). Consequently, antioxidants might lower ROS levels and 'protect' these cells from chemotherapeutics. Collectively, the use of antioxidants in cancer therapy with or without chemotherapeutics is debatable (Fuchs-Tarlovsky, 2013).

1.3. HYPOTHESIS AND OBJECTIVES

Our interest in anthocyanidins is rationalized by their potential ability to accumulate into mitochondria enabling them to exert a potent antioxidant effect comparable to that of known antioxidants such as vitamin E, ascorbic acid and β-carotene (Kowalczyk *et al,* 2003; Rice-Evans *et al,* 1996; Wang *et al,* 1999) and to other flavonoid subclasses (Rice-Evans *et al,* 1996). Of the many different anthocyanidins, cyanidin has gained considerable interest for its potent antioxidant ability compared to other members of the subclass (Choi *et al,* 2007; Khoo *et al,* 2017). Also, the paradox between cyanidin's enhanced bioactivity and its limited stability warrants further investigation into factors influencing its stability and degradation.

1.3.1. Hypotheses

1) Cyanidin provides the strongest antioxidant and cytoprotective ability against a mitochondrial insult (doxorubicin) in cardiomyocytes compared to its glucosylated form (C3G), quercetin (flavonol) and catechin (flavanol).

2) Reduction in cardiomyocyte toxicity is caused by parent compound, intermediate compounds, and breakdown products, PCA and PGA.

3) Cyanidin will accumulate to a greater extent into mitochondria of cardiomyocytes than C3G, quercetin and catechin.

4) Cyanidin will not interfere with the cytotoxic effect of doxorubicin against cancer cells.

5) Cyanidin does not degrade immediately when dissolved in physiological solutions.

1.3.2. Objectives

Objective one: Measure the protective effect of cyanidin and its metabolites, C3G, quercetin and catechin against doxorubicin-induced cytotoxicity in differentiated H9c2 cells using the SRB and MTT assays.

Objective two: Identify the mechanism(s) by which doxorubicin causes cytotoxicity and how flavonoids exert their cytoprotective activity against doxorubicin in differentiated H9c2 cells.

Objective three: Demonstrate the mitochondrial accumulation of cyanidin in differentiated H9c2 cells.

Objective four: Determine if cyanidin enhances or inhibits the cytotoxicity of doxorubicin against K562 and HepG2 cell lines.

Objective five: Evaluate the stability and breakdown of cyanidin in different biological fluids, including plasma, PBS and cell culture media.

CHAPTER TWO: METHODOLOGY

2.1. MATERIALS AND CELL LINES

Human hepatoma (HepG2) and myelogenous leukemia (K562) cell lines were a kind gift from Drs. Dimmock and Wasan, respectively. The rat cardiomyoblast (H9c2) (CRL-1446) cell line was purchased from American Type Culture Collection (ATCC®, Manassas, VA). Fetal bovine serum (FBS) (12-483-020) and 3-(4,5-dimethylthiazol-2-yl)-2,5-diphenyltetrazolium bromide (MTT) (298-93-1) were purchased from Thermofisher® (Waltham, MA). DMEM/High Modified (SH30604.01) RPMI-1640 medium (SH30255.01), PBS (SH30256.01) and trypsin 0.25% (SV30031.01) were purchased from HyClone (South Logan, UT). Human serum off-clot (823192) was purchased from BM biochemical (Santa Ana, CA). Protocatechuic acid (PCA) (0393-05-90) was purchased from HWI Analytik BmbH (Rulzheim, Germany). Doxorubicin (15007) was purchased from Cayman Chemical (Ann Arbor, MI). Penicillin-streptomycin (A5955), catechin (C1251), quercetin (Q4951), 2,4,6-trihydroxybenzaldehyde (phloroglucinaldehyde) (PGA) (T65404), (4-(2-hydroxyethyl)-1-piperazineethanesulfonic acid (HEPES) (H3375), sulforhodamine B (S1402) and dimethyl sulfoxide (DMSO) (0909S) were all purchased from Sigma-Aldrich (St. Louis, MO). Cyanidin (0909S) and kuromanin (C3G) (0915S) were both purchased from Extrasynthese (Genay, France). 18 megaΩ milliQ water was used in sample preparations. Protocatechuic acid (PCA) (0393-05-90) was purchased from HWI Analytik BmbH (Rulzheim, Germany). Doxorubicin (15007) was purchased from Cayman Chemical (Ann Arbor, MI). LC-MS grade acetonitrile (A955-4) and water (W6-4) were purchased from Fisher Chemical.

2.2. PROTECTION AGAINST DOXORUBICIN-MEDIATED CYTOTOXICITY OF DIFFERENTIATED H9C2 CELLS BY CYANIDIN, QUERCETIN, CATECHIN AND C3G.

One of our objectives was to determine the cytoprotective effects of cyanidin and the other flavonoids against doxorubicin-mediated cytotoxicity. To achieve this, we initially determined the concentration- and time-dependent effects of doxorubicin on cell survival, mitochondrial functions (MTT and MMP assays), intracellular ROS generation, mitochondrial superoxide generation, and cellular morphology. These determinations were followed by the evaluation of the ability of flavonoids to protect against doxorubicin-induced changes.

2.2.1. H9c2 culture and differentiation

H9c2 cells were stored in liquid nitrogen until required. Passages 4-6 were used throughout all experiments. Undifferentiated H9c2 cells were cultured in T75 flasks (Corning®, NY) in 15 mL of their recommended growth medium, DMEM/high glucose supplemented with 10% fetal bovine serum (FBS) and 1% penicillin-streptomycin (PEN/STREP), and left overnight to attach (37°C, 5% CO_2). The medium was changed every second day until confluency was reached.

For differentiation, the existing medium was removed, and differentiation medium was added to cells for 7 days. DMEM/High glucose supplemented with 1% FBS, 1% penicillin and 1 nM retinoic acid was used as the differentiation medium (Branco *et al*, 2012). The medium was changed on days 3 and 6. Changes in the morphology of the cells was monitored throughout the 7 days to confirm the differentiation. Undifferentiated cells appeared mononucleated and spindle in shape (Kimes and Brandt, 1976), while differentiated ones were long and multinucleated with thin branched cardiomyotubes (Pereira *et al*, 2011).

2.2.2. Detection of cell survival using the sulforhodamine B assay

Cytotoxicity was measured using the sulforhodamine B (SRB) assay (Orellana and Kasinski, 2016; Vichai and Kirtikara, 2006). This assay quantitates the amount protein present in wells and assumes a correlation with cell viability at the time of the assay. A stock solution of SRB was prepared in 1% acetic acid at a concentration of 0.5 mg/mL. The SRB assay was initiated by fixing the adherent cells with the addition of 100 µL of 20% trichloroacetic acid (TCA) to the existing 100 µL medium in each well with adherent cell lines. This was followed by incubation for one hour at 4°C. Non-adherent cells required the addition of 60% TCA for 2 h at the same temperature (Kim *et al*, 1996). The TCA fixed cells were washed with tap water and left to air dry. 100 µL of stock SRB solution was then added and left to incubate for 30 min at room temperature. Cells were washed with 1% acetic acid to allow the binding of SRB to the protein and to remove unbound dye. Cells were allowed to air dry. 200 µL of 10 mM Trizma base (pH 10) was added to each well to dissolve the bound dye. A Biotek plate reader (Winooski, VT) was used to detect the absorbance of SRB at 510 nm. The percentage of adherent cell protein in treated wells was referenced to the control wells for determination of percentage of cell survival.

$$\text{Percentage of cell survival} = 100 - \left(\frac{Absorbance(control) - Absorbance\ (treatment)}{Absorbance\ (control)}\ \text{X}\ 100\right)$$

2.2.2.1. Evaluation of cytotoxicity of doxorubicin in differentiated H9c2 cells

The IC_{50} value was initially calculated to establish an idea of the toxicity of doxorubicin against differentiated H9c2 cells and to determine the appropriate concentrations for usage in subsequent assays. 1.0×10^4 H9c2 cells were seeded in a 96-well plate and allowed to differentiate for 7 days (Section 2.2.1). The cells were then exposed to different concentrations of doxorubicin in the range of 0.1 - 10 µM (with a final concertation of DMSO less than 0.05%) for 24 h. Once

the exposure period was complete, the SRB assay was initiated to determine the adherent cell density (Section 2.2.2).

The change in cell morphology after incubation with doxorubicin was also detected by imaging using a ZOE microscope. Differentiated H9c2 cells were exposed to doxorubicin (1 µM) (DMSO less than 0.05%) in differentiation medium. Wells with differentiation medium without doxorubicin (with similar DMSO percentage) were used as a negative control. Since doxorubicin is known to cause cytotoxicity, no positive control was needed. Cells were imaged after 3, 6, 12 and 24 h of incubation. Several images were taken at each time. Plates were returned to the incubator until the next specific period of incubation. The same wells were imaged after each time to record the change in cell number and morphology with time.

To further understand the cytotoxic behaviour of doxorubicin on cardiomyocytes, 1.0×10^4 H9c2 cells were seeded in each well in a 96-well plate and allowed differentiate as per Section 2.2.1. Differentiated H9c2 cells were incubated with 1 µM of doxorubicin for 3, 6, 12 and 24 h or 5 µM for 3 and 6 h in differentiation medium (DMSO less than 0.05%). Cell survival was then measured using SRB assay immediately after the exposure period or after a further 24 h incubation in fresh differentiation medium. Wells with cells in differentiation medium without doxorubicin (with similar DMSO percentage) were used as a negative control. Since doxorubicin is known to cause cytotoxicity, no positive control was needed.

2.2.2.2. Evaluation of the effects of cyanidin with doxorubicin on cell survival in undifferentiated H9c2 cells

Undifferentiated H9c2 cells were first used to confirm the protective activity of cyanidin against doxorubicin as reported previously (Choi *et al*, 2007). 1.0×10^4 undifferentiated H9c2 cells were seeded in a 96-well plate in their respective growth medium (100 µL) (DMEM/high glucose-

HyClone) supplemented with 10% FBS and 1% PEN/STREP and left over night to attach (37°C, 5% CO_2). The cells were then exposed to doxorubicin (1 µM) alone for 24 h (DMSO less than 0.05%). Doxorubicin was then removed and fresh medium containing cyanidin (50 or 100 µM) was added for another 24 h (DMSO less than 0.4 %). The percentage of cell viability was then assessed as detailed in the SRB assay (Section 4.2.2.). Control wells also received vehicle (<0.05% DMSO) treatments.

2.2.2.3. Evaluation of the effects of flavonoids with doxorubicin on cell survival in differentiated H9c2 cells

The detection of doxorubicin's cytotoxicity against differentiated H9c2 cells was followed by determination of the cytoprotective effects of the flavonoids against doxorubicin-mediated cytotoxicity. For this purpose, different treatment patterns were used to assess the cytoprotective effects. 1.0×10^4 H9c2 cells were seeded in a 96-well plate and differentiated for 7 days (Section 2.2.1.). Differentiated cells were then subjected to different patterns of treatments followed by the SRB assay to determine percentage of cell viability. Throughout all patterns used, DMSO never exceeded 1.2%. Control wells also received vehicle (<0.05% DMSO) treatments. The different treatment patterns are explained:

A) Co-treatment: This experimental design was used to explore if cyanidin is able to protect differentiated H9c2 cells from direct and immediate (rather than delayed) cytotoxicity of doxorubicin. Differentiated H9c2 cells were incubated with 100 µL of the differentiation medium containing doxorubicin (1 µM) with or without cyanidin (50 or 100 µM) for 24 h at 37°C and 5% CO_2 (DMSO was less than 0.05%). Control wells received only equivalent amounts of medium with DMSO. After 48 h cytotoxicity was determined using the SRB assay.

B) Pre/co-treatment: This experimental setting was conducted to verify if co-treatment with cyanidin, starting 1 h prior to doxorubicin exposure (to allow intracellular loading of cyanidin) was able to protect differentiated H9c2 cells from cytotoxicity of doxorubicin. Differentiated H9c2 cells were initially incubated with 100 µL of differentiation medium containing cyanidin (50 or 100 µM) (DMSO less than 0.4%) for 1 h (at 37°C and 5% CO_2). This was followed by the addition of doxorubicin (1 µM) (4 µL of 25 µM) to the same medium (total DMSO less than 0.5%). Both treatments were incubated together for 24 h at 37°C and 5% CO_2. Some wells received only doxorubicin treatment to assess the protective ability of cyanidin. Control wells received only equivalent amounts of medium with DMSO. Cytotoxicity was determined using the SRB assay.

C) Multiple treatments of cyanidin: This experimental setting was conducted to verify if cyanidin pulses are able to protect differentiated H9c2 cells from direct cytotoxicity of doxorubicin. Differentiated H9c2 cells were treated with doxorubicin (1 µM) and cyanidin (10 µM) and left to incubate in differentiation medium for 24 h. While doxorubicin (1 µM) was added only once, cyanidin was added every 8 h for 24 h (total of 3 additions) (at 37°C and 5% CO_2) (DMSO equalled 1.2%). The treatments were added with 100 µL of differentiation medium. Some wells received only doxorubicin. Control wells received only equivalent amounts of medium with DMSO. Cytotoxicity was determined using the SRB assay.

D) Co-treatment and delayed assessment: This experimental setting was conducted to verify if cyanidin is able to immediately protect differentiated H9c2 cells from the rapid cytotoxicity caused by doxorubicin but observed at a delayed time. Differentiated cells were incubated with doxorubicin (1 µM) with or without cyanidin (50 or 100 µM) in 100 µL differentiation medium for 24 h. Both treatments were replaced by 100 µL fresh DMEM containing no treatments. The cells were incubated for another 24 h followed by the initiation of SRB assay. A similar procedure

was also followed using C3G, catechin and quercetin. Control cells received only medium on the first 24 h followed by its replacement with another batch of fresh medium.

E) Post-treatment: This experimental setting was conducted to verify the ability of cyanidin to protect differentiated H9c2 cells from delayed cytotoxicity of doxorubicin. Differentiated cells were incubated with 100 µL of differentiation medium containing doxorubicin (1 µM) treatment alone for 24 h. This was followed by the removal of the treatment and the addition of 100 µL DMEM/high glucose-HyClone fresh medium containing cyanidin (50 or 100 µM). Doxorubicin-containing medium was switched to differentiation medium containing no cyanidin to assess the protective activity. Control cells received only medium for the first 24 h followed by its replacement with another batch of fresh medium. Cytotoxicity was determined using the SRB assay. The same procedure was also followed using C3G, catechin and quercetin.

2.2.3. Determination of cell viability by the 3-[4,5-dimethylthiazol-2-yl]-2,5 diphenyl tetrazolium bromide (MTT) assay

The MTT assay measures the activity of mitochondrial reductases which reflects mitochondrial energy metabolism level (Mosmann, 1983). H9c2 cells were seeded at 1.0×10^4 cells per well in a 96-well plate in DMEM (supplemented with 10% FBS and 1% penicillin-streptomycin) and left overnight to attach. A stock solution of MTT was first prepared in the medium at a concentration of 5 mg/mL. After the treatment period was complete, 20 µL MTT solution was added to each well (1 mg/mL final concentration) and left to incubate for 3 h at 37°C. The medium was then removed and 200 µL of DMSO was added to each well to dissolve the formazan crystals. Absorbance was then measured for each well at 570 nm using a plate reader (Biotek Instrument, Winooski, VT).

2.2.4. Evaluation of the effects on intracellular ROS

For measurements of intracellular ROS, H9c2 cells were plated in a black 96-well plate with a transparent bottom at 1.0×10^4 cells/well, and allowed to differentiate for 7 days (Section 4.2.1.). The cells were then treated with 1 µM of doxorubicin for 0.5, 1, 3, 6, 12 or 24 h or 5 µM for 30 or 60 min (37°C and 5% CO_2). In addition, to measure of the protective effects of the flavonoids against the observed doxorubicin-induced increase in ROS, cells were treated with doxorubicin (1 µM) with or without a flavonoid (cyanidin, quercetin, catechin or C3G) (100 µM) for 12 or 24 h. The incubations were followed by the measurement of intracellular ROS levels using 2'-7'-dichlorodihydrofluorescein diacetate (DCFH-DA) dye. The treatments were removed and the cells were washed once with fresh medium. The dye was added at a concentration of 5 mg/mL in DMEM (without phenol red) for 30 min. The fluorescence produced was detected at excitation and emission wavelengths of 485 and 528 nm, respectively, using a plate reader (Biotek Instrument, Winooski, VT). When indicated, the SRB assay was initiated immediately after measuring the fluorescence intensity of DCF. The fluorescence intensity measured for a certain well was normalized to the absorbance value measured after the completion of the SRB assay for the same well.

2.2.5. Evaluation of the effects on mitochondrial superoxide

This experiment was conducted to determine the conditions at which doxorubicin induced an immediate and delayed increase in mitochondrial superoxide. The experiment was initiated by seeding H9c2 cells in a black 96-well plate and allowing their differentiation similar to Section 2.2.1. Differentied 1.0×10^4 H9c2 cells per well (in a black 96-well plate with transparent bottom) were incubated with doxorubicin at a concentration of either 1 µM for 0.5, 1, 3 and 6 h or 5 µM for 30 min (37°C and 5% CO_2). Differentiated cells were also treated with doxorubicin of a specific

concentration (1 µM) with or without a flavonoid (cyanidin, quercetin, catechin or C3G) (100 µM) in 100 µL differentiation medium for 3, 6 or 12 h. After incubation, the cells are washed once with DMEM medium. MitoSOX was dissolved in DMEM (without FBS and without phenol red) at a final concentration of 5 µM (100 µL) and loaded to each well. The plate was incubated for 30 min at (37°C and 5% CO_2). The wells were then washed twice with 100 µL PBS. 100 µL of PBS were added to each well followed by the measurement of the fluorescence intensity at excitation and emission wavelengths of 530 and 590 nm, respectively, using a plate reader (Biotek Instrument, Winooski, VT). After the measurement of mitochondrial superoxide generation, the SRB assay was initiated by the addition of 100 µL TCA (20%) to each well which also contained 100 µL PBS. When indicated in the results, the fluorescence value from each well was normalized to the SRB value of the same well.

2.2.6. Evaluation of the effects on mitochondrial membrane potential (MMP)

This experiment was conducted to determine if doxorubicin had an immediate and/or a delayed effect on MMP. H9c2 cells were seeded in a black 96-well plate and allowed to differentiate as in Section 2.2.1. The cells were incubated with doxorubicin at a concentration of either 1 µM for 3, 6 and 12 h or 5 µM for 30 min (at 37°C). These experiments were also followed by measurements to determine the protective effects of the flavonoids (cyanidin, quercetin, catechin and C3G) against doxorubicin's effects on MMP. Cells were treated with doxorubicin (1 µM) with or without the tested flavonoid (100 µM) for 12 h in differention medium. The incubation was followed by the measurement of MMP levels using tetramethylrhodamine ethyl ester (TMRE). The treatments were removed and the cells were washed once with 200 µL of DMEM. TMRE dye was added to the cells at a concentration of 5 µM in DMEM (without phenol red) and incubated for 30 min. The cells were washed twice with 100 µL PBS. PBS (100 µL) was then added to each

well followed by the measurement of the fluorescence at excitation and emission wavelengths of 500 and 590 nm, respectively, using a plate reader (Biotek Instrument, Winooski, VT). After the measurement, cells were fixed by the addition of 100 µL TCA (20%) to each well for 1 h at 4°C followed by the conduction of SRB assay (Section 4.2.2.). When indicated, the fluorescence value for TMRE from each well was normalized to the SRB value of the same well.

2.2.7. Determination of mitochondrial morphology using electron microscopy (EM)

The effect of doxorubicin on the morphology of the mitochondria in H9c2 was previously determined using electron, confocal and light microscopy (Jakobs *et al*, 2011; Sardao *et al*, 2009). We used EM to determine the ability of cyanidin to inhibit the detrimental effects of doxorubicin on mitochondrial morphology. 5.0×10^5 H9c2 cells were plated in a T25 flask using DMEM and allowed to differentiate for 7 days (Section 4.2.1.). Flasks were divided into four groups. Flask one received doxorubicin (1 µM) with cyanidin (100 µM) and left to incubate for 24 h. The medium was then removed, fresh differentiation DMEM containing no doxorubicin or cyanidin was added and the cells were left to incubate for another 24 h. Flask two received only doxorubicin and the cells were left to incubate for 24 h. The DMEM containing the agent was removed and replaced by differentiation DMEM containing cyanidin (100 µM). The cells were then incubated for 24 h. Flask three received only differentiation DMEM containing doxorubicin (1 µM) for 24 h. After the removal of the medium, fresh differentiation DMEM was added and the cells were left to incubate for 24 h. Flask four (control) received no treatment but the medium was replaced after 24 h with fresh media.

Once the treatment periods were over, the DMEM was removed and cells were washed with FBS-free DMEM medium. Cells were fixed using 2% glutaraldehyde in 0.1 M sodium phosphate buffer (pH 7.2) for 4 h at 4°C. Some cells started to float by this step, however, scraping was

required to ensure the detachment of most cells. The cells were taken into a 1.5 mL tube and centrifuged at 1000 RPM for 2 min. The fixative liquid was removed and the pellet was washed 4 times with 0.1 M sodium phosphate buffer. The pellet was sent to the Western College of Veterinary Medicine Imaging Centre for further processing and EM imaging.

2.3. EFFECTS OF CYANIDIN AND QUERCETIN ON DOXORUBICIN CYTOTOXICITY IN HEPG2 AND K563 CELL LINES

2.3.1. Culturing HepG2 and K562 cells.

HepG2 and K562 were cultured in DMEM/high glucose-HyClone supplemented with 10% FBS and 1% PEN/STREP using T75 flasks. HepG2 cells were left overnight to attach (37°C, 5% CO_2) and medium was changed every second day until confluency. The K562 cells, which are nonadherent, were left overnight to grow. 2-3 mL of medium was added to the culture every 3 days until the cells were highly dense. HepG2 cells were subcultured by trypsinizing the cells and dividing them to 3-4 new flasks. Cells were then left to attach overnight. K562 cells present in 10-12 ml medium were subcultured by their transfer to a 50 ml falcon tube followed by centrifugation to form a pellet. The supernatant (old medium) was replaced by a fresh medium (20 ml). The volume was then split to 2-3 T75 flasks (around 6-7 ml per flask). All experiments were conducted with passages 10-15.

2.3.2. SRB assay to determine the cytotoxicity against HepG2 and K562 cells

The IC_{50} value was initially calculated to establish an idea of the toxicity of doxorubicin against HepG2 cells in addition to establishing the appropriate concentrations for use in subsequent assays. 1.0×10^4 HepG2 cells per well were seeded in a 96-well plate using normal DMEM and left overnight to attach. Cells were then exposed to different concentrations of doxorubicin in the range of 0.000305–20 µM for 72 h. A similar procedure was followed using K562 cells. However, they

were seeded at 5.0×10^4 cells per well and left to incubate over night at 37°C to attach. Cells were then incubated with doxorubicin (1 µM) with or without a flavonoid (cyanidin or quercetin) at concentrations of 50 or 100 µM for 72 h. The flavonoids were added either one time (single treatment) or every 24 h for 72 h (multiple treatments). After the completion of a treatment condition, the SRB assay was conducted as detailed in Section 3.1.2 to quantify cell viability of HepG2. A simiar SRB procedure was also followed for K562 cells except the requirement of a centrifugation step at 1200 RPM for 5 min before the removal of medium from each well and the incubation with 60% TCA (prepared in water) for 2 h at 4°C (Kim *et al*, 1996).

2.3.3. (3-[4,5-dimethylthiazol-2-yl]-2,5 diphenyl tetrazolium bromide) (MTT) assay using HepG2 and K562 cells.

MTT was used to detect if the cytotoxicity is preceded by changes in metabolism activity. 1.0×10^4 cells HepG2 cells were seeded in a black 96-well plate and left to attach overnight as detailed in Section 2.2.6. Cells were then exposed to 1.5 µM doxorubicin with or without cyanidin or quercetin 50 or 100 µM added every 24 h for 72 h. A similar procedure was followed for K562 cells. However, they were seeded at 5.0×10^4 cells per well and left to incubate over night at 37°C then exposed to 1.0 µM of doxorubicin with or without similar additions of cyanidin or quercetin. MTT assay was conducted as detailed in Section 2.2.3. However, K562 cells were centrifuged before each wash to limit the removal of cells.

2.3.4. Measurement of MMP in HepG2 and K562 cells

The experiment was conducted to determine if cyanidin or quercetin can potentiate the effect of doxorubicin on MMP in HepG2 and K562 cells. 5.0×10^3 HepG2 cells were plated (and allowed to attach) in each well in a black 96-well plate (with transparent flat bottom) as detailed in Section 2.2.6. This was followed by treatment with doxorubicin (1 µM) with or without a

flavonoid (100 µM) for 24 h. 1.0×10^4 K562 cells were also plated onto a black 96-well plate and allowed by the exposure to doxorubicin and a flavonoid (cyanidin or quercetin) for 12 h. Once the incubations were complete, the medium containing all treatments was removed. Except for the centrifugation of K562 cells before each wash, a procedure similar to that detailed in Section 2.2.6. was followed to determine MMP.

2.3.5. Measurement of ROS in HepG2 and K562 cells

The experiment was conducted to determine if cyanidin or quercetin can potentiate the effect of doxorubicin on ROS in HepG2 and K562 cells. 1.0×10^4 HepG2 cells were plated in each well in a black 96-well plate as detailed in Section 2.2.4. After their attachment, the cells were exposed to doxorubicin (1.5 µM) with or without a cyanidin or quercetin (100 µM) for 24 h. Similarly, 5.0×10^4 K562 cells were plated in a black 96-well plate. Cells were exposed to doxorubicin 1.0 µM with or without a similar addition of cyanidin or quercetin for 24 h. Once the incubation was complete, the medium containing all treatments was removed. Except for the centrifugation of K562 cells before each wash, a procedure similar to that detailed in Section 2.2.4. was followed to determine ROS.

2.3.6. Measurement of DNA fragmentation in HepG2 and K562 cells

The COMET assay was conducted for quantitative determination of DNA fragmentation (Olive and Banáth, 2006). HepG2 or K562 (5.0×10^4 cells) were plated in a 6-well plate and left overnight. Cells were treated with doxorubicin at a concentration of 1.0 µM or 1.5 µM for HepG2 or K562, respectively, for 72 h. Cells were then trypsinized and diluted to 10×10^3 cells/mL with PBS (without any divalent ions). 400 µL of the prepared cell mixture were mixed with 1% low temperature melting point agarose (prepared and cooled to 40°C). The mixture was pipetted onto a slide and left to cool at 4°C for 2 h to ensure solidification of the gel. The slides were then

submerged in alkaline lysis buffer (1.2 M NaCl, 100 mM Na_2EDTA, 0.1% sodium lauryl sarcosinate, 0.26 M NaOH (pH > 13) overnight at 4°C. The slides were then rinsed three times with rinsing buffer (0.03 M NaOH, 2 mM Na_2EDTA (pH ~12.3) for 20 min each at room temperature. An electrophoresis was conducted at 20 Volts and 40 mA for 30 min. 0.5 µg/mL of DAPI solution was prepared in PBS. 200 µL of the DAPI solution was added to each slide and left to incubate for 5 min. A ZOE imager was used to capture the image of the DNA on the slides. Comet shapes containing DNA with tails and heads were formed. DNA fragmentation percentage was determined by calculating the ratio of the total fluorescence intensity of the tail to that of tail and head.

2.4. DEGRADATION OF CYANIDIN IN DIFFERENT PHYSIOLOGICAL MEDIA

The objective of these evaluations was the investigation of the degradation of cyanidin when added to physiological-like liquids (at neutral pH). These liquids include PBS (pH 7.4), the cell culture medium DMEM (with and without 10% FBS), human serum and HEPES buffer. The extent and the rate at which the parent compound degraded to PCA and PGA in physiological media was evaluated.

2.4.1. Evaluation of cyanidin degradation in PBS, DMEM, human serum and HEPES buffer using UV-vis spectrometry

UV-Vis spectrometry was used to determine the rate at which the absorbance of cyanidin changed. This provided a preliminary understanding about the rate of degradation/ transformation of these compounds without giving details about the nature of the products produced. All flavonoids were dissolved in DMSO at 25 mM and diluted to a final concentration of 100 µM in the different media with a final volume of 1 mL in a plastic cuvette just before UV-Vis measurement. Stock solutions in DMSO were stored at -80°C in 6 µL aliquots, and freshly thawed

just before use. Experiments were conducted in PBS (pH 7.4 and 2.4), DMEM cell culture medium with and without 10% FBS, human serum or 25mM HEPES buffer (pH 7.4). The experiments were conducted at 25°C. Initially, a complete UV-Vis (200-800nm) scan was determined for each sample at 0 min using a Beckman Coulter spectrophotometer. The λ_{max} for cyanidin was recorded at 585 nm in all media used.

The determination of the rate of change in absorbance was later evaluated using a Beckman Coulter spectrophotometer. For these measurements, cyanidin (100 µM) was added with a cuvette plunger and inserted into a cuvette containing the medium. This occurred while the instrument was initiated to record the change in absorbance at 585 nm every 1 sec for the first 10 min. This ensured the detection in the change in absorbance at the very initial instant. After 10 minutes, the measurement of the change in absorbance at intervals of 20 min (at 25°C) was carried out. The recording of the changes continued until a plateau was reached at the lowest absorbance value. A similar procedure was followed with quercetin, catechin and C3G. However, the absorbance was measured at 400 nm, 280 nm and 580 nm wavelengths for quercetin and catechin, and C3G, respectively.

2.4.2. Evaluation of cyanidin degradation in PBS (pH 7.4) using HPLC with UV-vis detection

HPLC was used to provide a better understanding of the nature of the chemical degradation/transformation of cyanidin. The HPLC system used was from Agilent Technologies comprising an L-6200A pump and an L-4500 diode array detector. The analysis was performed using an Agilent Eclipse XDB-C18 column (150 × 4.6 mm, 5µm). All liquids used were HPLC grade. To determine the behaviour of cyanidin at physiological pH, HPLC was run at pH 7.4 (mobile phases were set at 7.4). For this, a mobile phase with no FA was used. Samples were diluted to a final concentration of 100 µM in PBS just before injection.

Cyanidin was dissolved in PBS (pH 7.4) and immediately the initial sample was injected onto the column (time zero). The sample injection volume was 30 µL. The remaining sample in PBS was left at room temperature and evaluated for degradation and product formation at different times. The injection was repeated at time periods of 2, 4 and 8 h. The mobile phase solvents were water (A) and acetonitrile (B). The mobile phase started with 10% B from 0 to 2 min. The percentage of B was at 70% from 2 to 20 min. Flow rate was 1 mL min^{-1} and column temperature was 25°C.

The presence of cyanidin flavylium ion was initially observed using the previously determined at λ_{max} = 525 nm in acidic pH buffer solution (PBS pH 2.3). The λ_{max} previously determined for PCA (λ_{max} = 292 nm), PGA (λ_{max} 315 nm) and cyanidin (λ_{max} 585 nm) at neutral pH were used. Therefore, the diode array detector was set to detect the absorbance at these wavelengths.

2.4.3. Degradation of cyanidin evaluated using mass spectrometry

Samples of a stock solution were diluted to 10 µM in water with 10% methanol to ensure optimal ionization. Immediately after the preparation, samples were directly injected onto an Applied Biosystems MDS SCIEX 4000 quadrupole linear ion trap (QTRAP) mass spectrometer at a rate of 10 µL/min using a Hamilton syringe and Harvard syringe pump. Stock solutions of cyanidin dissolved in pure DMSO at 25 mM and stored at -80°C were used to make working solutions for the different experiments. To enhance ionization in the mass spectrometer, samples were prepared in LC-MS grade water (with 10% methanol) at a concentration of 10 µM. To determine the degradation/transformation of cyanidin, injections were repeated after various time points from solutions standing at room temperature. Chalcone and the hemiketal have the same molecular weight of 304 Da; cyanidin flavylium ion and quinoid form have molecular weights of

287 and 286 Da, respectively. Q1 MS negative mode using turbo spray as an ion source was used to detect ions at m/z 303 and 286. CUR, IS, GS1, DP and EP were set at of 10.00 V, -4500.00 V, 14.00 psi, -60.00 V and -10.00 V. MS/MS in the negative mode with a turbo spray was used to determine the product ions of 303 Da. Curtain gas (CUR) and nebulizing gas (GS1) were set at 14.0 pound per squar inch (psi) while curtain and drying gas (GS2) was set at 10.0 psi. Ion spray voltage (IS), declustering potential (DP) and entrance potential (EP) were set at -4500.00 volts (V), 6.00 V, -60.00 V, respectively. Collision energy (CE) and collision gas (CAD) were set at -24.00 eV and 6.00 psi, respectively. MS/MS in the negative ion mode with a heat nebulizer was also used to perform product ion scan at m/z 153. CUR, GS1 and GS2 were set at 20.0 psi, 22.0 psi and 15.0 psi, respectively. DP and EP were set at -60.00 V and -10.00 V, respectively. CE, collision cell exit potential (CXP) and CAD were set at -25.00 V, -10 V and 6.00 V, respectively. Temperature of ion source (TEM) and nebulizer current (NC) were set at 500.00^{o}C and -3.00 V, respectively.

2.5. MEASUREMENT OF INTRACELLULAR CYANIDIN CONCENTRATIONS

The determination of the uptake of cyanidin by differentiated H9c2 cells was attempted. Different analytical methods were employed for this purpose. In order to detect the cellular uptake of cyanidin, determination of the optimal extraction solvent was required initially. The solvent characteristics were required to favour three main features of cyanidin; stability, absorptivity and fluorescence capability. In addition, disruption of the cell membranes was crucial to allow extraction from cells. Therefore, the behaviour of cyanidin in different solvents was evaluated. Acetonitrile (ACN) (supplemented with 0.1% formic acid (FA)), methanol (supplemented with 0.1% FA), DMSO and PBS (supplemented with 0.1% FA and 0.1% tween-20) are solvents normally used for extraction purposes.

2.5.1. Determination of the absorptivity, stability and fluorescence characteristics of cyanidin in different extraction solvents.

To determine its absorptivity, cyanidin was dissolved in acetonitrile (ACN) (supplemented with 0.1% FA), methanol (supplemented with 0.1% FA), PBS (supplemented with 0.1% tween-20 and 0.1% FA) or DMSO at different concentrations. A standard curve was initially established by defining the absorbance as a function of the concentration. This was established by measuring the absorbance of cyanidin when dissolved in the different solvents at different concentrations (3.9, 7.81, 16.62, 31.25, 62.5, 125, 250 μM). The absorbance was measured at the predetermined λ_{max} (550 nm) for cyanidin in its respective solvent. Only standard curves generated with R^2 above 0.980 were accepted. The absorbance values of unknown solutions fell in the linear range of the standard curve.

The stability of cyanidin was determined by dissolving it at a concentration of 100 μM in different solvents (namely, ACN supplemented with 0.1% FA, methanol supplemented with 0.1% FA, PBS supplemented with 0.1% tween-20 and 0.1% FA, or DMSO) and incubating it for 60 min at room temperature. The absorbance at λ_{max} (550 nm) was measured at time zero and after completion of the incubation using a Biotek spectrometer plate reader (Winooski, VT). The percentage decrease in the absorbance was calculated.

To determine its fluorescence behaviour in the different solvents, cyanidin was added to a solvent followed by measuring its excitation/emission fluorescence spectrum using a spectrofluorometer (PerkinElmer, LS55, Waltham, MA). Once measure, the wavelengths combination with the highest fluorescence intensity was further confirmed using Biotek spectrometer plate reader (Winooski, VT).

2.5.2. Determination of cyanidin uptake using UV-vis spectroscopy

The determination of cellular uptake of cyanidin in differentiated H9c2 cells was initially attempted using its UV-Vis absorbance characteristics. 1.0×10^4 H9c2 cells were seeded onto a 96-well plate and allowed to differentiate for 7 days. Cells were then incubated in the differentiation medium with cyanidin (100 µM) at 37°C 5% CO_2 for 10 min. The medium containing cyanidin was removed and the cells were washed twice with PBS to eliminate the extracellular cyanidin. 50 µL ACN 0.1% FA was added to the wells to extract cyanidin. Cells were left to incubate for 30 min at 4°C to complete the extraction. Using a Biotek reader, the absorbance was recorded at the predetermined λ_{max} for cyanidin in ACN 0.1% FA (550 nm). Wells containing cells with no treatment were subjected to the same procedure and used as a control. In addition, the Biotek spectrometer UV-vis absorption spectra at a wavelength range of 200 – 800 nm were recorded after the completion of the incubation for cyanidin-treated and non-treated wells in the same treatment procedures.

In other experiments, H9c2 cells were cultured in T75 flasks and allowed to differentiate for 7 days. Cells were then trypsinized and centrifuged at 1200 RPM (4°C) to form a pellet. A final volume of 50 µL of cyanidin (100 µM) was incubated with the pellet for 10 min at 37°C. The pellet was then centrifuged and washed with PBS twice. The supernatant was then removed followed by the addition of ACN (0.1% FA) (50 µL). The pellet was subjected to vortexing and sonication in a bath sonicator for 5 min (kept at 4°C with ice) followed by incubation for 30 min (at 4°C) then by centrifugation in a benchtop microcentrifuge (1.0×10^4 RPM at 4°C). The supernatant was taken out (60 µL) and placed in a well of a 96-well plate. The process was also performed for a control with no cyanidin addition. Measurement of the absorbance spectra (200-800 nm) of samples was conducted using a Biotek spectrometer plate reader.

2.5.3. Determination of cyanidin uptake using its fluorescence characteristics

Fluorescence measurement is a sensitive and specific technique to detect chemicals. Hence, we used the fluorescence of cyanidin to detect its presence intracellularly. ACN (0.1% FA) extraction solvent was used to determine the cellular uptake of cyanidin in differentiated H9c2 cells using its fluorescence characteristics. 1.0×10^4 H9c2 cells were seeded onto a 96-well plate and allowed to differentiate for 7 days. Cyanidin (100 µM) was added to each well and left to incubate for 10 min (at 37°C and 5% CO_2). The incubation period was selected based on several considerations. Fiorani *et al*, 2010 was able to detect a similar flavonoid (quercetin) in Jurkat cells after just 10 min of incubation. In addition, degradative properties of cyanidin did not permit incubations for longer periods. The cells were washed twice with PBS followed by the addition of 50 µL ACN 0.1% FA to each well to extract cyanidin. Cells were left to incubate for 30 min at 4°C. Using a Biotek fluorometer, the fluorescence was measured for each well at excitation and emission wavelengths of 400 and 590 nm, respectively. These wavelengths were selected based on fluorescence intensity scans (**Appendix 1**). Control cells with no cyanidin addition were used as a control.

2.5.4. Determination of cyanidin H9c2 cellular uptake using HPLC and fluorescence detection

Another approach using HPLC and fluorescence detection was also employed to detect cyanidin in cellular extracts. This was conducted in two approaches. First, 10×10^4 cells were cultured in a 6-well plate and left to differentiate. Cells were then incubated with cyanidin (100 µM) in fresh differentiation medium for 10 min at 37°C. This was followed by the removal of the medium containing the cyanidin and washing the cells with PBS twice. 100 µL ACN (0.1%FA) was then added to each well and left to incubate for 30 min at 4°C. A cell scraper was then used

to ensure the collection of all cells. The cells and the supernatant were then collected into a 1.5 mL tube. The cells were centrifuged at 10×10^3 RPM for 5 min (4°C). The cell lysate was then taken to HPLC. Different mobile phases (including methanol with 0.1% FA, ethanol with 0.1% FA) and a range of gradient (between 10 and 90%) were attempted to optimise the detection of the peaks. The same fluorescence excitation/emission (400/590 nm) wavelengths which gave positive results in fluorescence plate reader were used

In another experimental approach, the differentiated H9c2 cells were trypsinized and centrifuged (1000 RPM for 5 min) to form a pellet. The pellet was then treated with cyanidin (100 µM) in 50 µL differentiation medium for 10 min at 37°C and 5% CO_2. The supernatant was removed, and cells were washed twice with PBS. 100 µL ACN (0.1% FA) was added to the pellet. The mixture was vortexed and sonicated in a bath sonicator for 5 min. The sample was centrifuged at 1.0×10^4 RPM in a benchtop microcentrifuge at 4°C. 30 µL of the supernatant was then injected to the HPLC. The HPLC system used was from Agilent Technologies comprising an L-6200A pump and an L-4500 diode array detector. The analysis was performed using an Agilent Eclipse XDB-C18 column (150 × 4.6 mm, 5µm). All liquids used were HPLC grade. To determine the behaviour of cyanidin at physiological pH, HPLC was run at pH 7.4. Samples were diluted to a final concentration of 100 µM using PBS just before injection, and a mobile phase with no FA was used. The mobile solvents were water (A) and acetonitrile (B). The mobile phase started with 10% B from 0 to 2 min. The percentage of B was at 70% from 2 to 20 min. Flow rate was 1 mL min^{-1} and temperature was 25°C. The presence of cyanidin flavylium ion was initially observed using the previously determined at λ_{max} = 525 nm in acidic pH buffer solution (PBS pH 2.3). The λ_{max} previously determined for PCA (λ_{max} = 292 nm), PGA (λ_{max} 315 nm) and cyanidin (λ_{max}

585nm) at neutral pH were used. Therefore, the diode array detector was set to detect the absorbance at these wavelengths.

2.5.5. Determination of cyanidin H9c2 cellular uptake using mass spectrometry

Since MS tends to have high sensitivity, determining the small amounts of intracellular cyanidin is highly achievable. Therefore, we employed the technique to detect intracellular cyanidin flavylium ion and the degradation products. To achieve this, H9c2 cells were cultured in a T75 flask and allowed to differentiate for 7 days (Section 4.2.1.). The cells were trypsinized and centrifuged to form a pellet. The supernatant was discarded, and the pellet was dispersed in a final 50 µL differentiation medium with cyanidin (100 µM) and incubated for 10 min at 37°C. The sample was also mixed every 3-4 min during the incubation by manually inverting it twice. The pellet was then centrifuged at 1.0×10^4 RPM for 5 min (4°C) and washed twice with PBS. 50 µL ACN (0.1% FA) was added to the pellet to extract cyanidin. The pellet was subjected to vortexing and sonication for 5 min followed by centrifugation at 1.0×10^4 RPM and 4°C. The lysate was then placed in a 1.5 mL tube and centrifuged at 1.0×10^4 RPM for 5 min at 4°C followed by running the supernatant through a syringe filter (pore size 0.45 µm) to remove all debris. The sample was immediately taken for MS measurement. Wells containing cells with no cyanidin addition were subjected to the same extraction procedure and used as a control. The mass spectrometer was set to detect 307 Da (chalcone or hemiketal), 286 Da (quinoidal), 287 Da (flavylium ion) and 154 Da (PCA and/or PGA). MS parameters were set similar to those used in Section 4.5.3.

2.6. Statistical analyses

All data were presented as means ± standard deviation (SD). Three different cell batches were used and for each batch, the experiment was conducted in quadruplicate. One way ANOVA followed by Tukey's post-hoc test was used to determine the significance of the effects between

multiple groups using GraphPad Prism 5 software (San Diego, CA). Using the same software, T-test was used to determine the significant effects between two groups. A p-value less than 0.05 was considered significant. IC_{50} values were determined by plotting the change in cell survival percentage with the increase in concentration. Nonlinear regression analysis (with variable slope model) was used to calculate the IC_{50}.

CHAPTER THREE: RESULTS

3.1. CHARACTERISATION OF DOXORUBICIN'S EFFECTS ON DIFFERENTIATED H9C2 CELLS.

3.1.1. Doxorubicin cytotoxicity in differentiated H9c2 cells

Initial optimizations were conducted to determine the concentrations required to investigate doxorubicin's effects on differentiated H9c2 cells. In differentiated H9c2 cells, the IC_{50} of doxorubicin was 0.88 ± 0.24 µM after 24 h incubation (**Figure 3.1**), which is consistent with an IC_{50} value of 1 µM reported previously using differentiated H9c2 cells after 24 h of incubation (Branco *et al*, 2012).

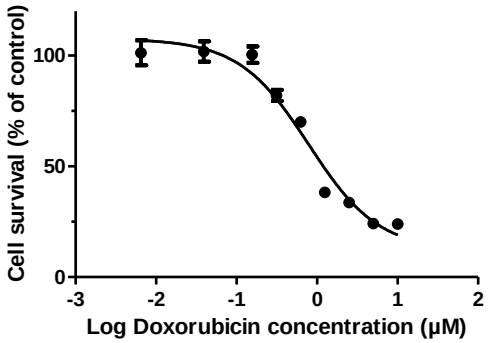

Figure 3.1.: Cell survival as a function of doxorubicin concentration in differentiated H9c2 cells after 24 h treatment. Differentiated H9c2 cells were treated with doxorubicin at concentrations of 0.1-10 µM and cytotoxicity determined by the SRB assay. Points represent mean ± SD. The IC_{50} (0.883 $\pm$ 0.242 µM) was determined by nonlinear regression analysis in GraphPad Prism. The experiment was repeated three times with 4 wells of cells per treatment.

Measurement of the IC_{50} was then followed with visually recording the effect of doxorubicin on H9c2 cellular viability over a period of time. Shown in **Figure 3.2**, 1 µM doxorubicin caused no apparent cell death (few floating round cells) when incubated with

differentiated H9c2 cells for 3 h or 6 h (**Figure 3.2b&d)** compared to control **(Figure 3.2a&c)**. Extensive cell death was apparent after 12 and 24 h of incubation (**Figure 3.2f&h**).

a.

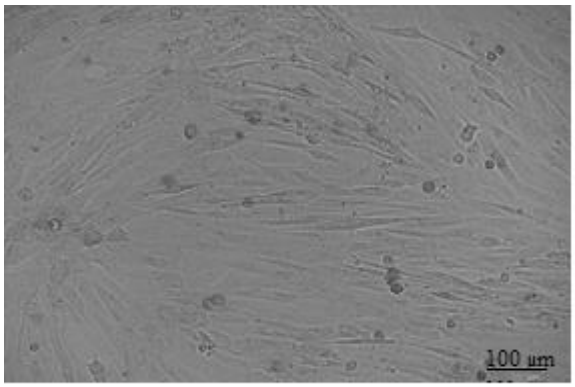

b.

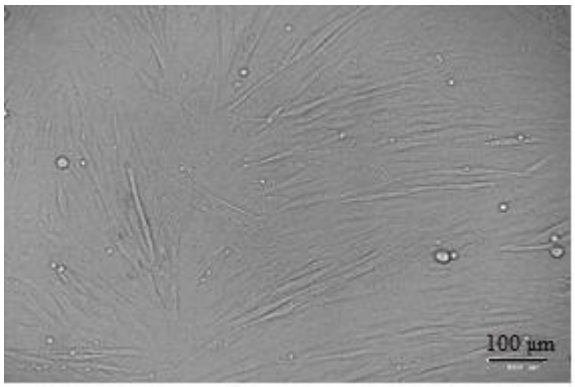

c.

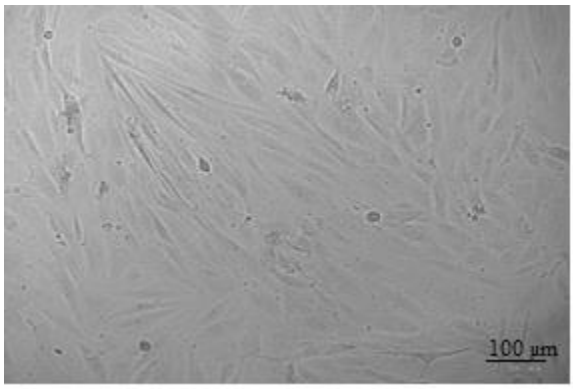

d.

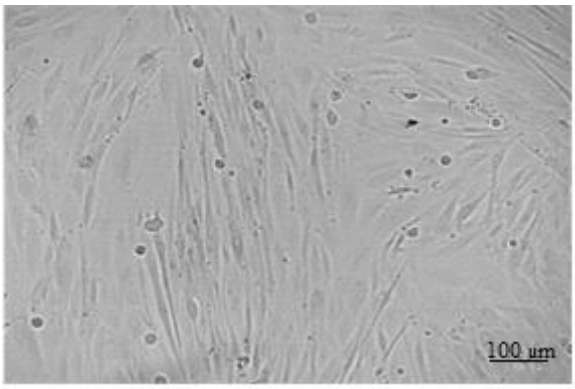

e.

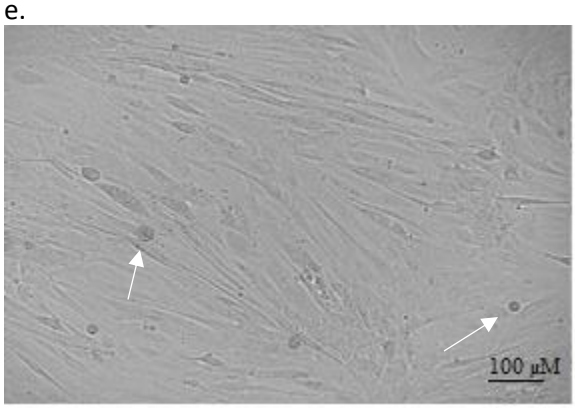

f.

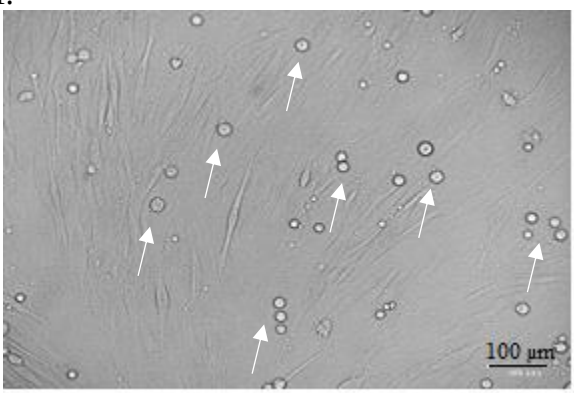

g. h.

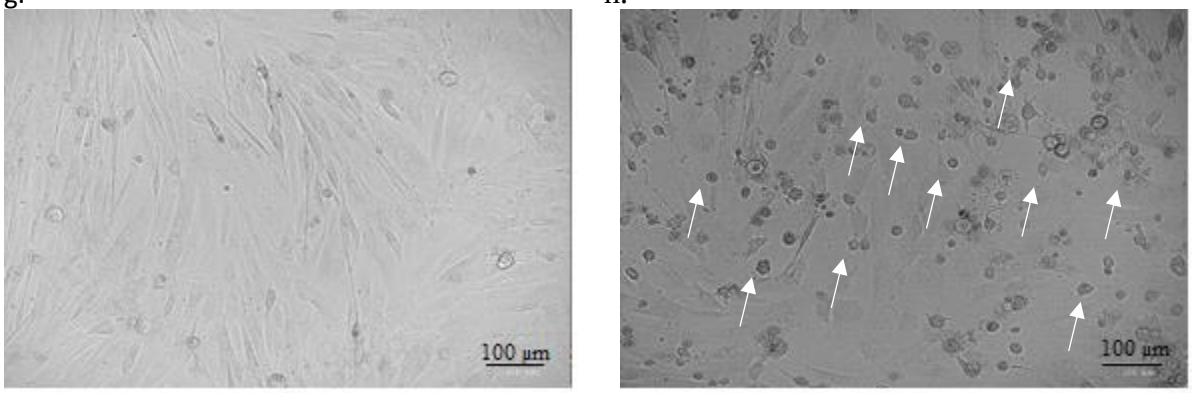

Figure 3.2. Cell morphology of differentiated H9c2 cells in the absence or presence of 1 µM doxorubicin. Cells were allowed to differentiate for 7 days then treated: for 3 h (**a**) without and (**b)** with doxorubicin (1 µM); for 6 h (**c**, control; **d**, doxorubicin); for 12 h (**e**, control; **f**, doxorubicin); and for 24 h (**g**, control; **h**, doxorubicin). Images were taken using the ZOE microscope at an objective magnification of 20X. White arrows point to the dead cells.

The SRB assay was used to quantify the early and late cytotoxic effects of low and high doxorubicin concentrations on the differentiated H9c2 cells. Cell survival remained high after 3 and 6 h of treatment with 1 µM doxorubicin (**Figure 3.3**). However, the percentage of cell survival decreased significantly by 14.5 and 59.0% at 12 and 24 h, respectively. A higher concentration of doxorubicin (5 µM) was attempted to capture the rapid effects on cell survival. However, no effect on cell survival after 3 and 6 h was apparent, but this concentration also caused significant decreases (by 14.5 and 77.1%) after 12 and 24 h of incubation.

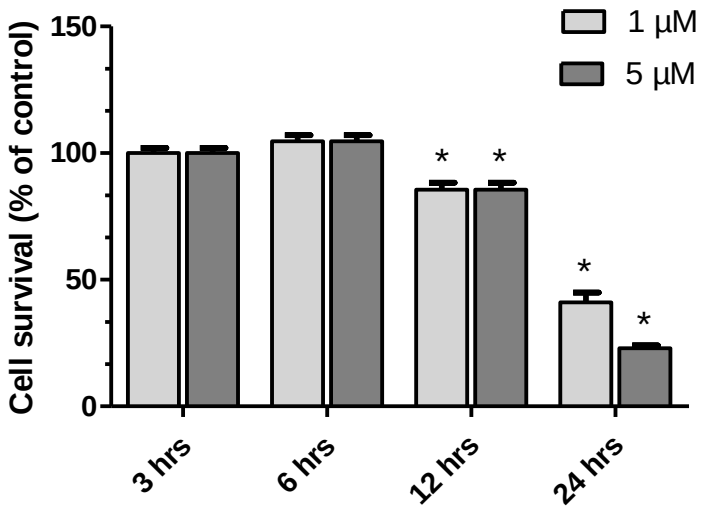

Figure 3.3: Survival of differentiated H9c2 cells with doxorubicin (1 or 5 µM) treatment for different exposure times. Differentiated cells were exposed to doxorubicin (1 or 5 µM) for 3, 6, 12 and 24 h followed by the SRB assay. Values are presented in relation to the survival of control cells (absence of doxorubicin) incubated for the corresponding times. Three different cell batches were used and for each batch the experiment was conducted in quadruplicate. Bars represent means ± SD. One way ANOVA with Tukey's post-hoc analysis was used to determine the significance of treated groups compared to the control group. * Indicates significantly different from the control group at $p < 0.05$.

To investigate delayed effects of doxorubicin on differentiated H9c2 cells, doxorubicin (1 µM) was added for 1, 3, 6, 12 and 24 h followed by its removal and addition of differentiation medium for 24 h. Under these experimental conditions, cell survival decreased only after incubation with 1 µM doxorubicin for 12 and 24 h (58.7 and 38.9% cell survival, respectively) (**Figure 3.4**). With 5 µM doxorubicin incubated for 1, 3 and 6 h followed by its removal and the addition of fresh differentiation medium for 24 h, the incubation periods of 3 and 6 h significantly decreased cell survival by 28.3 and 46.8%, respectively.

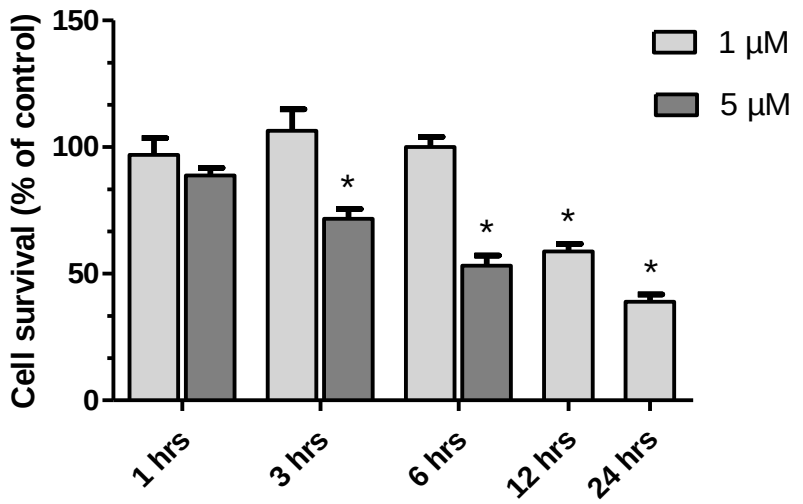

Figure 3.4: Survival of differentiated H9c2 cells after treatment with doxorubicin (1 or 5 µM) for different periods followed by incubation with fresh medium for 24 h. Percentage of cell survival was determined by the SRB assay after treatment with doxorubicin for different incubation periods. Values are presented in relation to the control. Three different cell batches were used and for each batch the experiment was conducted in quadruplicate. Bars represent means ± SD. One way ANOVA with Tukey's post-hoc analysis was used to determine the significance of the treated groups compared to the control group. * Indicates significant difference from the control group at $p < 0.05$.

3.1.2 Doxorubicin effects on cellular and mitochondrial ROS production

Different doxorubicin concentrations and incubation periods were investigated for effects on intracellular ROS and mitochondrial superoxide generation in differentiated H9c2 cells. At 1 µM, doxorubicin significantly increased mitochondrial superoxide generation at 3 and 6 h of incubation by 49.69 and 89.07%, respectively, but had no effect at earlier times (**Figure 3.5**). A higher concentration (5 µM) caused a rapid (30 min) and significant increase in superoxide generation by 72.61% (**Figure 3.5**).

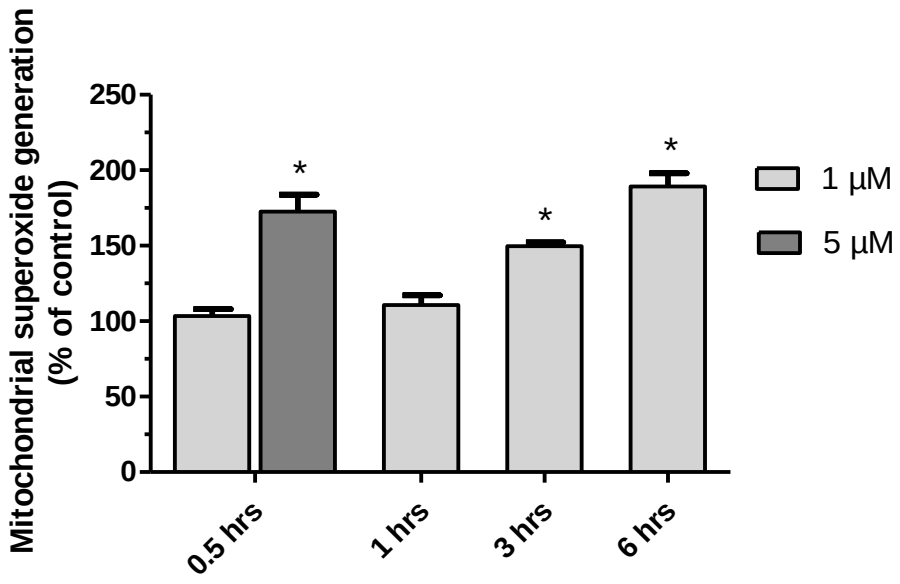

Figure 3.5: Effect of doxorubicin on mitochondrial superoxide. Differentiated H9c2 cells were exposed to doxorubicin (1 or 5 µM) for different incubation periods, and rates of mitochondrial superoxide generation were measured using MitoSOX dye. Values are presented in relation to negative control. Three different cell batches were used and for each batch the experiment was conducted in quadruplicate. Bars represent means ± SD. One way ANOVA with Tukey's post-hoc analysis was used to determine the significance of the treated groups compared to the control group. * Indicates a significant difference between the doxorubicin treated group and the control group.

In measurements of the effects of doxorubicin on intracellular ROS, no significant effects were observed after 30 and 60 min exposure using a low (1 µM) concentration (**Figure 3.6**). Incubation with 1 µM doxorubicin for 3, 6, 12 and 24 h however, produced significant increases in intracellular ROS generation by 22.7, 74.0, 75.4 and 57.9%, respectively (**Figure 3.6**). The incubation with higher concentrations of doxorubicin (5 and 20 µM) for 30 or 60 min also caused no significant increase in intracellular ROS generation (**Figure 3.6**).

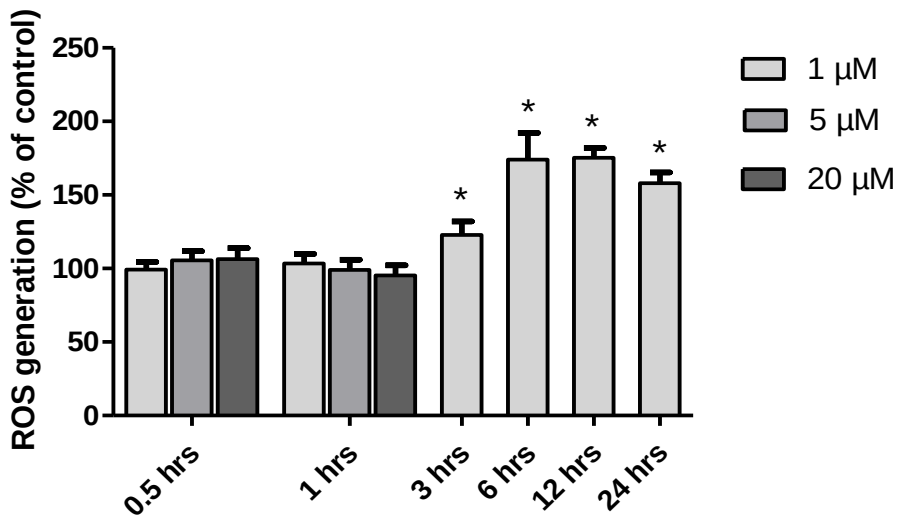

Figure 3.6: Effects of doxorubicin (1, 5 and 20 µM) incubation for different times on intracellular ROS generation. Differentiated H9c2 cells were incubated with doxorubicin (1, 5 or 20 µM) for different incubation periods followed by measurement of intracellular ROS generation using DCFH-DA dye. Values are presented in relation to the corresponding control. Three different cell batches were used and for each batch the experiment was conducted in quadruplicate. Bars represent means ± SD. One way ANOVA with Tukey's post-hoc analysis was used to determine significant differences from control groups. * Indicates a significant difference between the doxorubicin treated group and the control group.

3.1.3. Doxorubicin effects on mitochondrial function

The MTT assay was used to detect changes in the metabolic activity produced by doxorubicin in differentiated H9c2 cells. Doxorubicin (5 µM) treatment for 6 h significantly decreased MTT reductase enzyme activity by 34.1% **(Figure 3.7)**. Incubation periods of 1 and 3 h with doxorubicin caused no significant effect on MTT reduction.

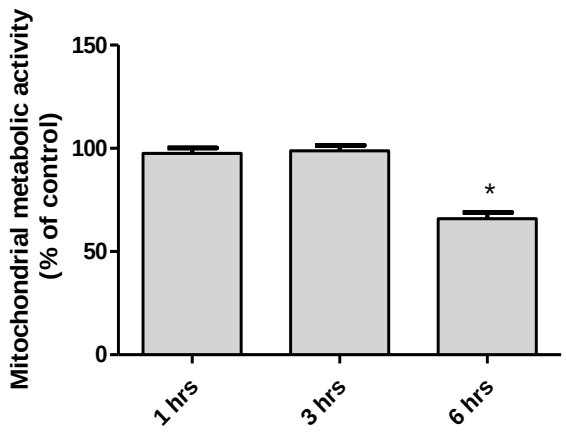

Figure 3.7: **Effect of doxorubicin for different time periods on metabolic activity.** Differentiated H9c2 cells were exposed to doxorubicin (5 µM) for 1, 3, or 6 h followed by the addition of MTT to detect metabolic activity. Values are presented in relation to the control (absence of doxorubicin). Three different cell batches were used and for each batch the experiment was conducted in quadruplicate. Bars represent means ± SD. One way ANOVA with Tukey's post-hoc analysis was used to determine the significance of the treated groups compared to the control group. * Indicates a significant difference between the doxorubicin treated group and the corresponding control group at that time.

Measurements of MMP were used to investigate the early (direct) and late (apoptosis-mediated) effects of doxorubicin on the MMP in differentiated H9c2 cells. No significant change in the MMP was observed after 3 or 6 h of 1 µM doxorubicin incubation (**Figure 3.8**). However, a significant decrease in the MMP was observed after a more prolonged exposure (12 h) (**Figure 3.8**). A higher concentration (5 µM) of doxorubicin was unable to decrease the MMP in a short (30 min) incubation period, but decreased MMP by 29.3 and 47.9% after 3 and 6 h, respectively **(Figure 3.8)**. Notably, 5 µM doxorubicin did not decrease cellular protein (SRB assay) at these time points (**Figure 3.3**).

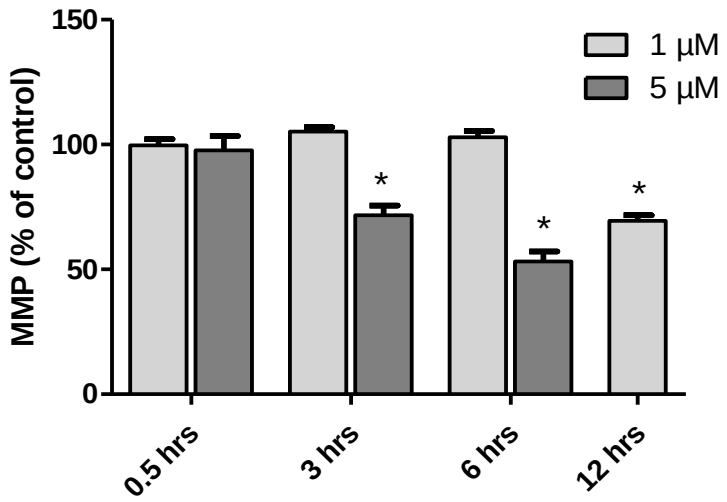

Figure 3.8: Effect of doxorubicin for different time periods on MMP. Differentiated H9c2 cells were exposed to doxorubicin (1 or 5 µM) for 0.5, 3, 6 and 12 h followed by the addition of TMRE probe for MMP measurement. Due to a decrease in cell number at 12 h of doxorubicin exposure (Fig. 5.3), the fluorescence intensities were normalized to the cell density (from SRB fluorescence). Values are presented in relation to the control (absence of doxorubicin). Three different cell batches were used and for each batch the experiment was conducted in quadruplicate. Bars represent means ± SD. One way ANOVA with Tukey's post-hoc analysis was used to determine significant difference between the doxorubicin and control group. * Indicates a significant difference between the doxorubicin treated group and the corresponding control group at that time.

3.2. PROTECTION BY DIFFERENT FLAVONOIDS AGAINST DOXORUBICIN-INDUCED CYTOTOXICITY, ROS GENERATION AND MITOCHONDRIAL DYSFUNCTION IN DIFFERENTIATED H9C2 CELLS

3.2.1. Protection against doxorubicin cytotoxicity.

In order to compare with the literature, the cytoprotective ability of cyanidin against doxorubicin was initially measured using undifferentiated H9c2 cells (Choi *et al*, 2007). A significant increase in cell survival (by 26.0 and 46.92%, respectively) was noticed when doxorubicin (1 µM) was incubated for a period of time followed by cyanidin (50 and 100 µM) treatment (**Figure 3.9)**. Treatment of differentiated H9c2 cells with doxorubicin (1 µM) and cyanidin (50 and 100 µM) following the same pattern significantly increased cell survival by 66.6 and 96.0% respectively (**Figure 3.9)**.

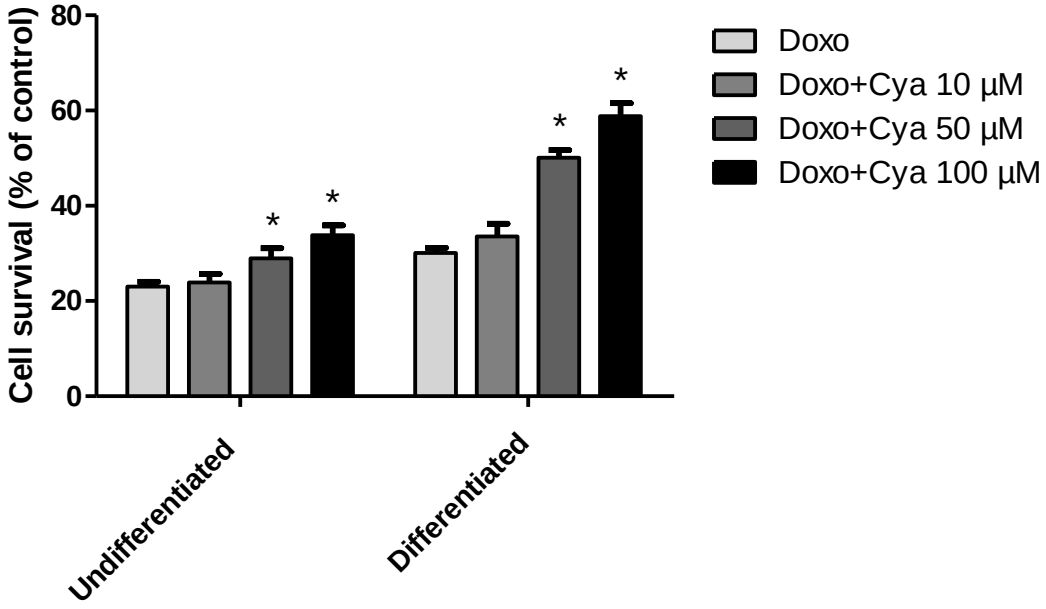

Figure 3.9: Cell survival of undifferentiated and differentiated H9c2 cells when treated with doxorubicin followed by cyanidin. Doxorubicin (1 µM) was added to undifferentiated and differentiated H9c2 cells and incubated for 24 h followed by its removal and addition of fresh medium containing cyanidin (10, 50 or 100 µM) and incubation for 24 h. Cell survival was then determined by the SRB assay. Values are presented in relation to the survival of control cells in the absence of treatments. Bars represent means ± SD. One way ANOVA with Tukey's post-hoc analysis was used to determine the significance of the difference between cyanidin treated groups

and the doxorubicin treated group. * Indicates a significant difference from the doxorubicin group at $p < 0.05$. Doxorubicin was significantly different from the control group. Doxo: doxorubicin.

Since proactive protection is more desirable than post-protection, cyanidin (100 µM) and doxorubicin (0.25, 0.50 or 1.00 µM) were co-administered to the differentiated H9c2 cells for 24 h. Under these experimental conditions, cyanidin failed to show significant protective ability (**Figure 3.10a)**. In addition, to ensure its presence in the cells, 1 h pre-incubation of cyanidin (100 µM) with the cells before the addition of doxorubicin (1 µM) was conducted. The result showed a lack of protection in this experimental condition (**Figure 3.10b**). In addition, no significant protection from doxorubicin (1 µM) was observed with multiple additions of cyanidin (10 µM every 8 h) (**Figure 3.10b)**.

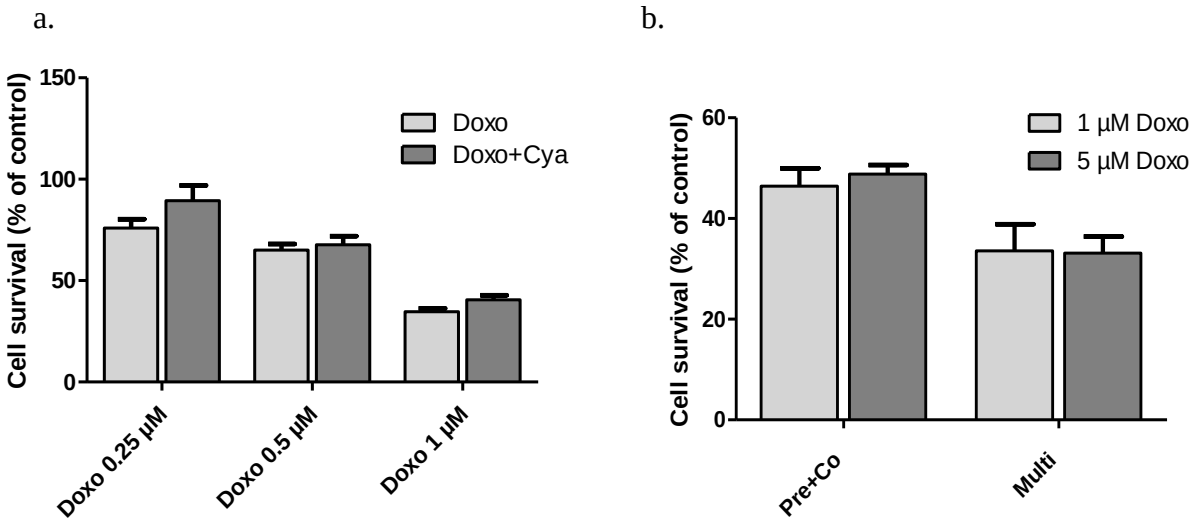

Figure 3.10: Cell survival of differentiated H9c2 cells when treated with doxorubicin and cyanidin together for 24 h. Differentiated H9c2 cells were treated with cyanidin and doxorubicin in different doses and patterns, and cell survival after 24 h was determined by the SRB assay. **a)** Cyanidin (100 µM) and doxorubicin (0.25, 0.5 or 1 µM) were added to the differentiated H9c2 cells together and incubated for 24 h. **b)** For the single treatment, cyanidin (100 µM) was pre+co-incubated (Pre+Co) with differentiated cells for 1 hr followed by the addition of doxorubicin (1 or 5 µM) and their co-incubation for 24 h. For the multi-treatments (Multi), cyanidin (10 µM) was initially added together with doxorubicin (1 or 5 µM), and then 10 µM cyanidin was added every 8 h until up to 24 h (3 additions). Values are presented in relation to the survival of control cells in the absence of treatments. Three different cell batches were used and for each batch the experiment was conducted in quadruplicate. Bars represent means ± SD. T-test was used to determine the significance of the effects between cyanidin treatment and the corresponding doxorubicin group. Doxorubicin was significantly different from the control group in all cases. Doxo: doxorubicin.

Using differentiated H9c2 cells, the protective effect of cyanidin was compared with other flavonoids (namely C3G, quercetin, and catechin) when applied after doxorubicin exposure (post-treatment pattern). Significant increases in cell survival were observed with cyanidin at 50 and 100 µM, quercetin at 100 µM and C3G at 100 µM **(Figure 3.11a).** The protective effect of cyanidin was also compared to that of its metabolites (PCA and PGA). Significant increases in cell survival were observed with cyanidin and the combination of its two degradation products in doxorubicin exposed differentiated H9c2 cells **(Figure 3.11b)**. However, cyanidin (50 and 100 µM) gave 13.1 and 19.9% greater survival than PCA+PGA (50 and 100 µM of each), respectively, with increased cell survival at 100 µM being significantly different.

a.

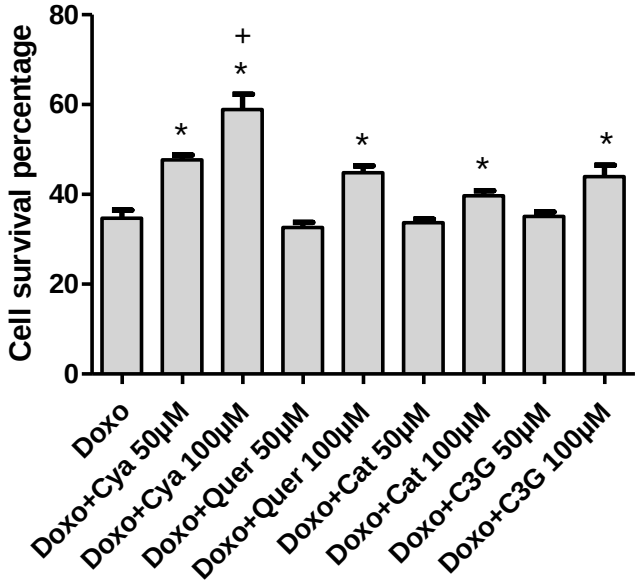

b.

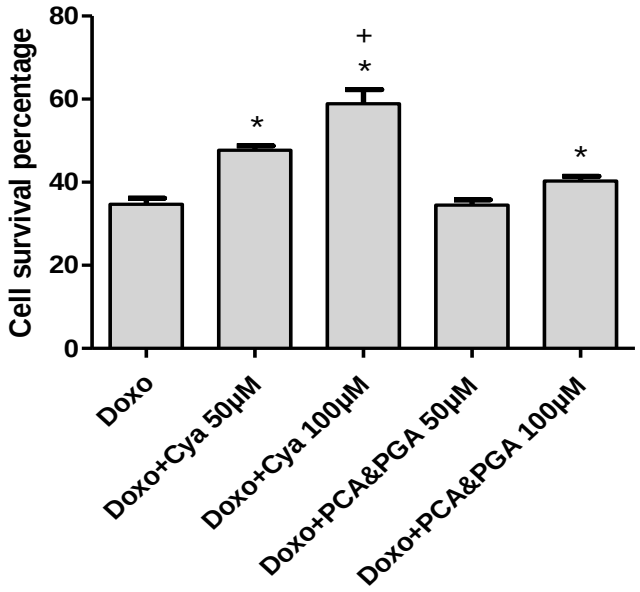

Figure 3.11: Cell survival of differentiated H9c2 cells when treated with doxorubicin followed by a flavonoid. A comparison between the protection ability of **a)** different flavonoids (50 or 100 µM) or **b)** cyanidin and PGA+PCA against doxorubicin's cytotoxicity. The PCA+PGA conditions received the indicated concentration of each compound. Cell survival was determined by the SRB assay. Values are presented in relation to the control survival. Bars represent means ± SD. One way ANOVA with Tukey's post-hoc analysis was used to determine the significance of the difference between flavonoid treated groups and the doxorubicin treated group. * Indicates a significant difference from the doxorubicin group at $p < 0.05$. Doxorubicin was significantly different from the control group. + indicates a significant difference from the "PCA&PGA 100µM" group. Doxo: doxorubicin, Cya: cyanidin, Quer: quercetin, Cat: catechin, C3G: cyanidin-3-glucoside.

Differentiated H9c2 cells were also treated with doxorubicin and cyanidin for a period of time followed by a 24 h drug free period. Cyanidin significantly increased cell survival by 15.1 and 21.7% at 12 h and 24 h, respectively (**Figure 3.12a)**. This was followed by the comparison of the cytoprotective effects of different flavonoids and cyanidin utilizing the same treatment pattern. All four flavonoids were able to significantly protect against loss of cell viability (**Figure 3.12b**), with cyanidin and quercetin giving the strongest survival (an increase by 34.0%). The protective effects of cyanidin were also compared to that of its metabolites (PCA and PGA) using the same

treatment pattern. Both cyanidin and its two degradation products significantly enhanced cell survival following exposure to doxorubicin **(Figure 3.12c)**. However, cyanidin (50 or 100 µM) significantly increased cell survival by 16.0% or 20.2% over PCA&PGA (50 or 100 µM), respectively.

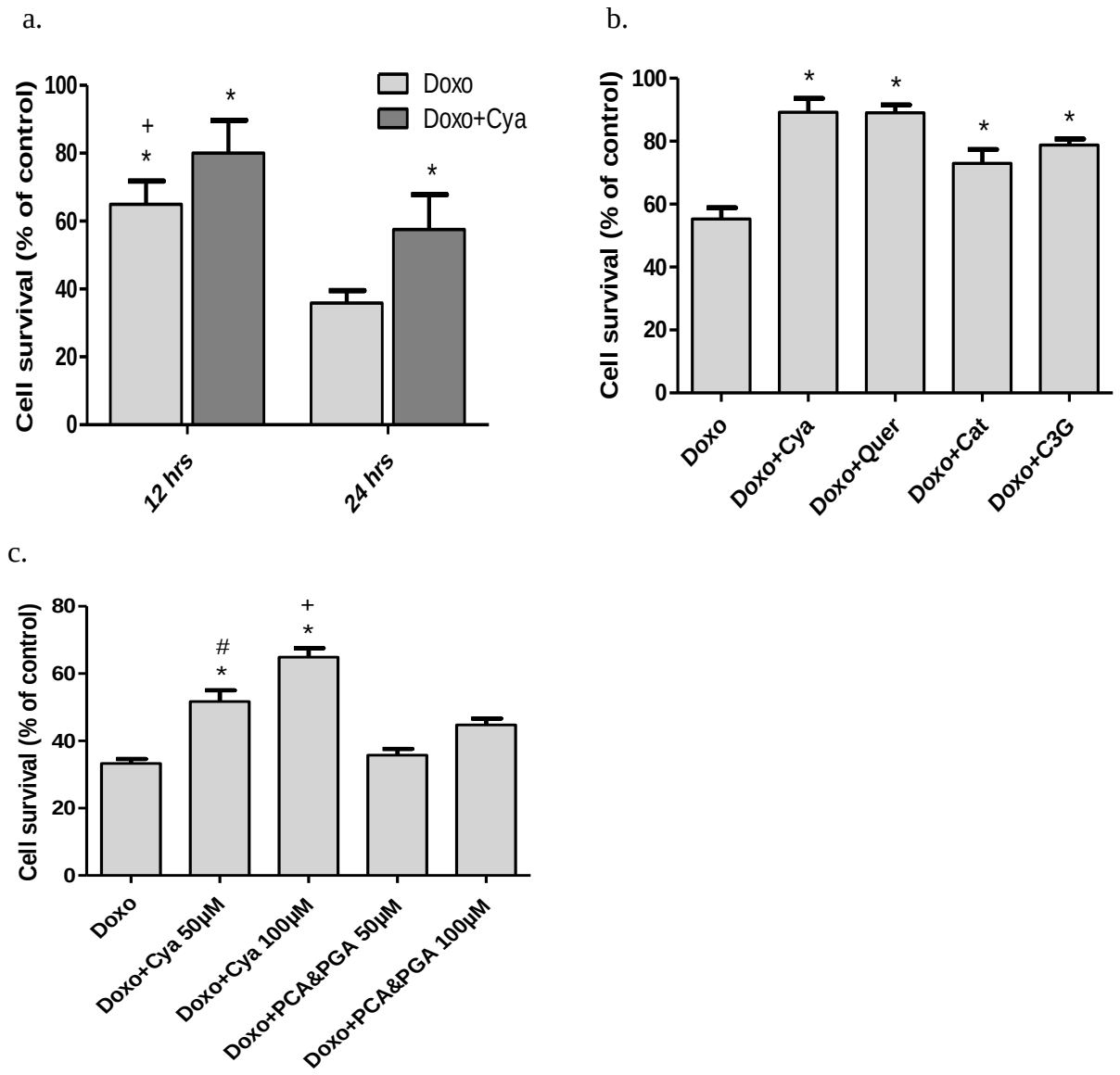

Figure 3.12: Delayed cytoprotective effects of flavonoids when added together with doxorubicin (1 µM) and replaced by fresh medium for another 24 h. Doxorubicin was co-treated with **a)** Cyanidin (100 µM) 12 or 24 h, **b)** Flavonoid (100 µM) for 24 h, **c)** PCA&PGA or cyanidin for 24 h, followed by a drug free 24 h period. The treatments were followed by a drug free 24h. Cell survival was then determined by the SRB assay. The PCA&PGA were added at 50 or 100 µM each. Cell survival was determined relative to control. Three different cell batches were

used and for each batch the experiment was conducted in quadruplicate. Bars represent means ± SD. One way ANOVA with Tukey's post-hoc analysis was used to determine the significance of the effects between groups (p value < 0.5). * Indicates a significant difference from the doxorubicin alone group. + indicate**s** a significant difference between the cytoprotection by cyanidin (100 µM) and that for PCA&PGA (100 µM). # indicates a significant difference between the cytoprotection by cyanidin (50 µM) and that for PCA&PGA (50 µM). Doxorubicin was significantly different from the control (absence of doxorubicin) group in all panels. Doxo: doxorubicin, Cya: cyanidin, Quer: quercetin, Cat: catechin, C3G: cyanidin-3-glucoside.

To capture the protective effect of the flavonoids at early stages, short incubations were performed with a high concentration of doxorubicin. All flavonoids were able to significantly protect the cells from doxorubicin (5 µM) when incubated together for 6 h followed by their replacement with fresh medium for 24 h (**Figure 3.13**). However, when the treatments lasted 1 h or 3 h, percentage of cell survival was similar across all treatments (**Figure 3.13**).

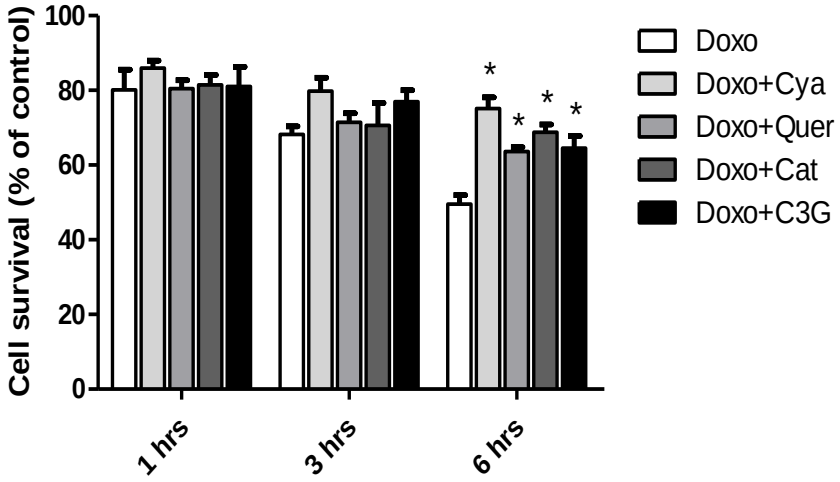

Figure 3.13: Delayed cytoprotective effects of flavonoids when added together with doxorubicin (1 µM) and replaced by fresh medium for another 24 h. Flavonoid (100 µM) co-treatments for 1, 3 or 6 h, followed by their removal and the addition of fresh medium for 24 h. Values are presented in relation to the control survival. Three different cell batches were used and for each batch the experiment was conducted in quadruplicate. Bars represent means ± SD expressed as a percentage of control cells. One way ANOVA with Tukey's post-hoc analysis was used to determine the significance of the effects between groups (p value < 0.5). For each time point, * indicates a significant difference between doxorubicin alone group and the flavonoid treated group. Doxorubicin was significantly different from the control (absence of doxorubicin)

group in all panels. Doxo: doxorubicin, Cya: cyanidin, Quer: quercetin, Cat: catechin, C3G: cyanidin-3-glucoside.

3.2.2. Protection against doxorubicin–induced mitochondrial and cellular ROS

These experiments were conducted to explore the protective effect of flavonoids on doxorubicin-affected mitochondrial superoxide and intracellular ROS generation in differentiated H9c2 cells following different concentrations and incubation periods. Cyanidin and C3G significantly decreased mitochondrial superoxide generation after 3 h by 33 and 23%, respectively, compared to doxorubicin alone, while quercetin and catechin had no significant effect **(Figure 3.14a)**. After 6 h, all of the flavonoids produced significant decreases (by 33.3, 22.1, 19.2 and 19.8% with cyanidin, quercetin, catechin and C3G, respectively), compared to doxorubicin alone **(Figure 3.14a)**. With 12 h incubation, only cyanidin showed a significant decrease in mitochondrial superoxide generation (by 19%) compared to doxorubicin alone **(Figure 3.14a)**. When the ability of the flavonoids to decrease the acute (30 min) doxorubicin (5 µM)-induced mitochondrial superoxide generation was measured, a significant decrease (by 55.8%) with cyanidin and quercetin was observed (**Figure 3.14b**).

a.

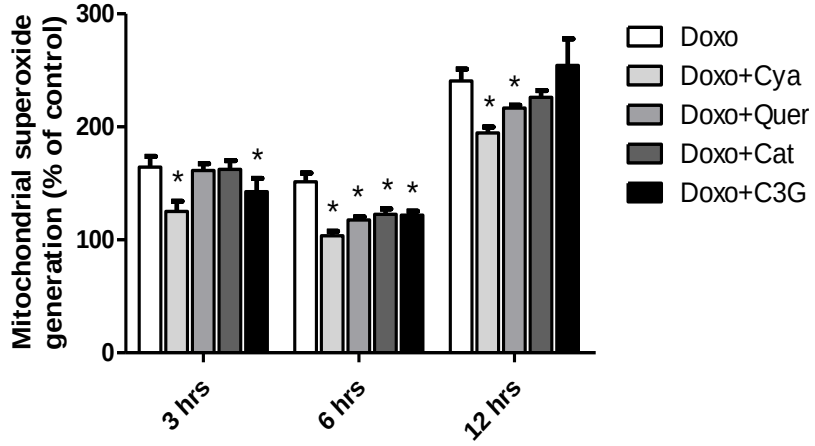

b.

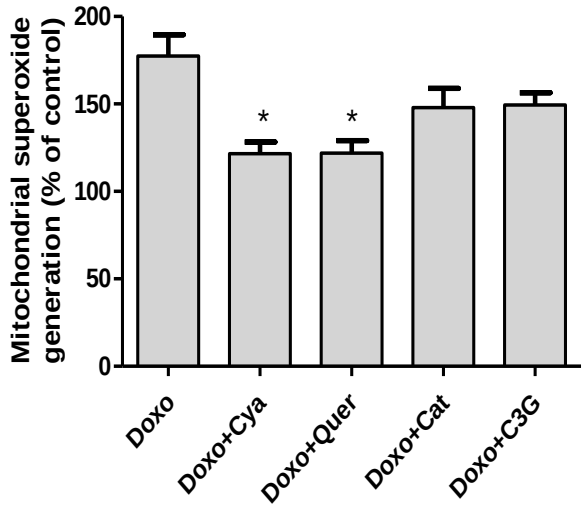

Figure 3.14: Effect of different flavonoids on mitochondrial superoxide generation induced by doxorubicin (1 or 5 µM). Differentiated H9c2 cells were incubated with doxorubicin **a)** 1 µM for 3, 6 or 12 h or **b)** 5 µM for 0.5 h with or without a flavonoid (100 µM). MitoSOX was used to measure the level of mitochondrial superoxide generation. The values were then normalised to SRB values. Values are presented in relation to the control cells. Three different cell batches were used and for each batch, the experiment was conducted in quadruplicate. Bars represent means ± SD. One-way ANOVA with Tukey post-hoc analysis was used to determine the significance of the effects between groups. * Indicates a significant difference from the doxorubicin-treated group ($p < 0.05$). Doxorubicin was significantly different from the control group. Doxo: doxorubicin, Cya: cyanidin, Quer: quercetin, Cat: catechin, C3G: cyanidin-3-glucoside.

Since measurements of intracellular ROS generation did not show significant increases by doxorubicin at early time points (**Figure 3.15**), the effects of flavonoids on doxorubicin-induced intracellular ROS were determined after 6 and 12 h. Only cyanidin caused a significant reduction in intracellular ROS generation by 35.0% when treated together with doxorubicin for 6 h **(Figure 3.15)**. When the incubation lasted 12 h, a slight, but significant decrease in doxorubicin-induced ROS was produced by cyanidin or quercetin.

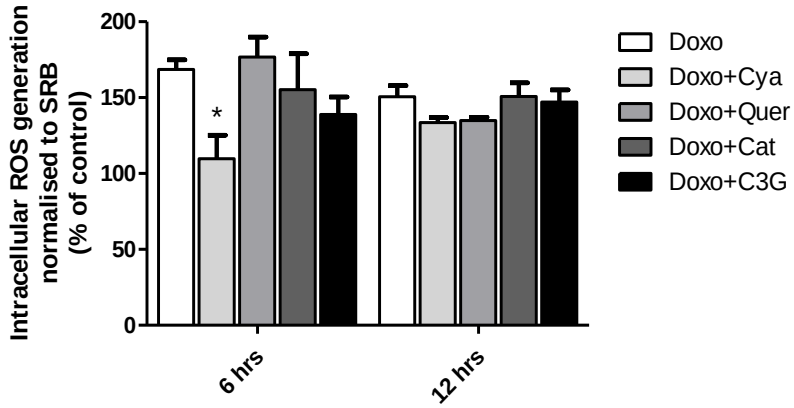

Figure 3.15: Effect of different flavonoids on intracellular ROS generation induced by doxorubicin (1 µM). Differentiated H9c2 cells were incubated with doxorubicin (1 µM) with or without a flavonoid (100 µM) for 6 or 12 h. Intracellular ROS generation was then measured using DCFH-DA. The results for intracellular ROS were normalized to the measured adherent cell density. Values are presented in relation to the control. Three different cell batches were used and for each batch, the experiment was conducted in quadruplicate. Bars represent means ± SD. One-way ANOVA with Tukey post-hoc analysis was used to determine the significance of the effects between groups. * Indicates a significant difference from the doxorubicin-treated group ($p < 0.05$). Doxorubicin was significantly different from the control group. Doxo: doxorubicin, Cya: cyanidin, Quer: quercetin, Cat: catechin, C3G: cyanidin-3-glucoside.

3.2.3 Protection by flavonoids against mitochondrial dysfunction and morphological changes induced by doxorubicin

Measurements of metabolic activity and MMP using MTT and TRME dyes, respectively, were employed to understand the ability of the flavonoids to protect against the effect of doxorubicin on metabolic functions. With the MTT assay, all flavonoids except C3G were able to increase mitochondrial function by 26.83, 18.99, and 18.5% for cyanidin, quercetin, and catechin, respectively, compared to doxorubicin (5 µM) alone when incubated together (**Figure 3.16a**). In measurements of MMP in cells treated with doxorubicin (1 µM) with or without a flavonoid (100 µM) for 12 h, the flavonoids were not able to ameliorate the decrease in MMP (**Figure 3.16b**).

a. b.

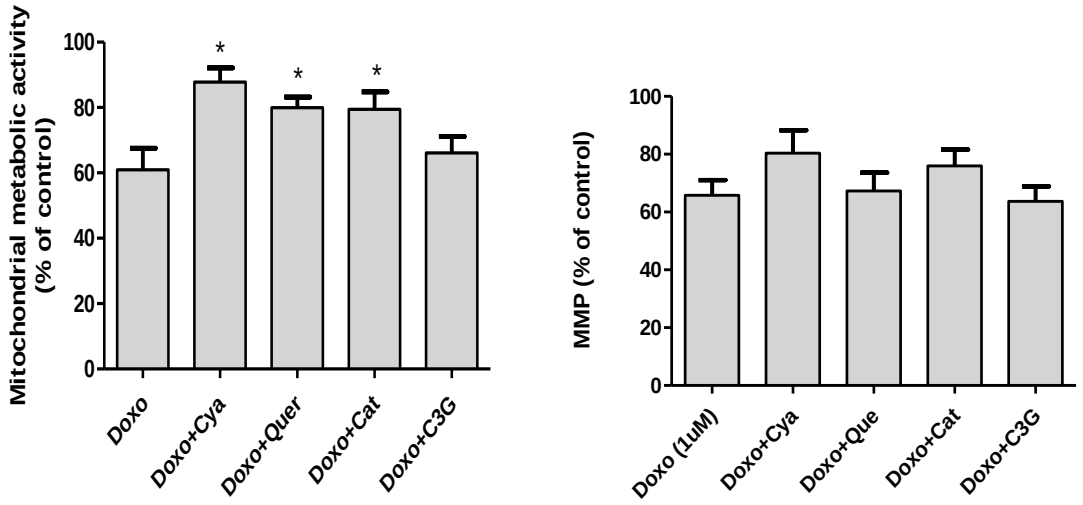

Figure 3.16: **Effects of flavonoids and doxorubicin on metabolic functions. a)** Doxorubicin (5 µM) with or without a flavonoid (100 µM) was incubated with differentiated H9c2 cells for 6 h. This was followed by the measurement of metabolic function using the MTT assay. **b)** Differentiated H9c2 cells were incubated with doxorubicin (1 µM) with or without a flavonoid for 12 h. MMP levels were then determined using TRME dye. Values are presented in relation to control cells in the absence of doxorubicin. Three different cell batches were used and for each batch, the experiment was conducted in quadruplicate. Bars represent means ± SD. One-way ANOVA with Tukey post-hoc analysis was used to determine the significance of the effects between groups. * Indicates a significant difference between the doxorubicin-treated group and the flavonoid-treated group (p value < 0.05). Doxorubicin was significantly different from the control group. Doxo: doxorubicin, Cya: cyanidin, Quer: quercetin, Cat: catechin, C3G: cyanidin-3-glucoside.

We also assessed the ability of cyanidin to protect against changes in mitochondrial morphology caused by doxorubicin using electron microscopy. Doxorubicin decreased the number of mitochondrial cristae (**Figure 3.17b**) compared to control cells (**Figure 3.17a**). Following treatment with cyanidin fewer changes in mitochondrial morphological features were observed with exposure to doxorubicin when given in either "post-treatment" or "co-treatment with delayed assessment" patterns (**Figure 3.17c&d**). However, all cyanidin-treated cells retained some mitochondrial damage from doxorubicin compared to the control cells (**Figure 3.17a**).

a.

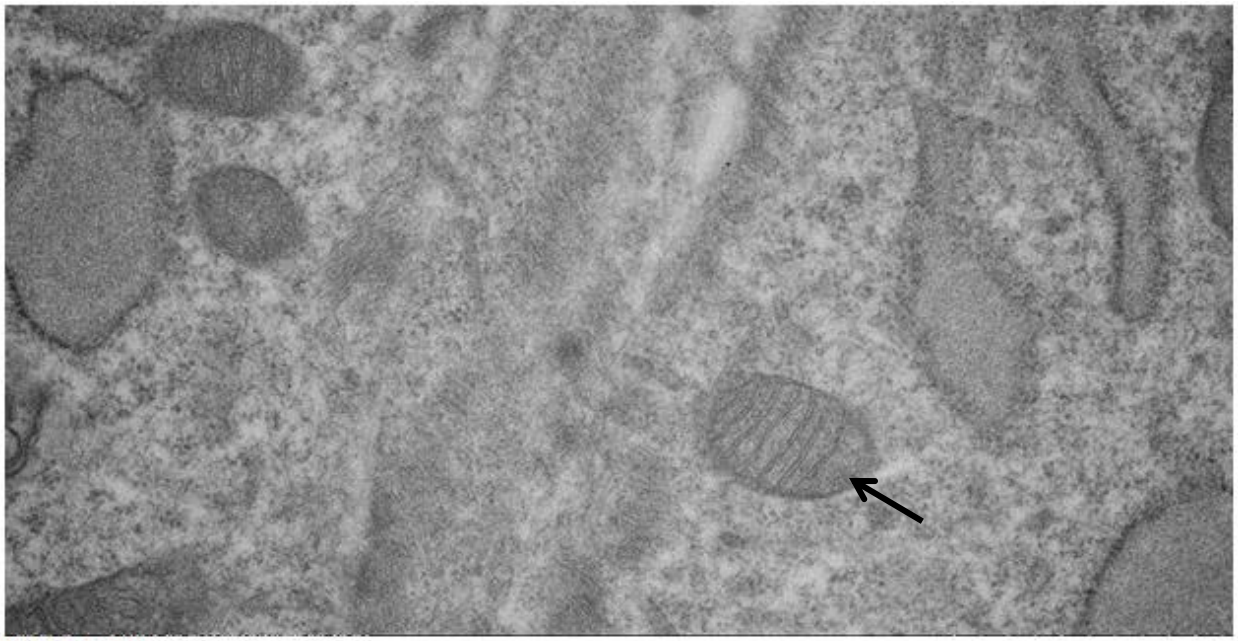

X25.0k Zoom

b.

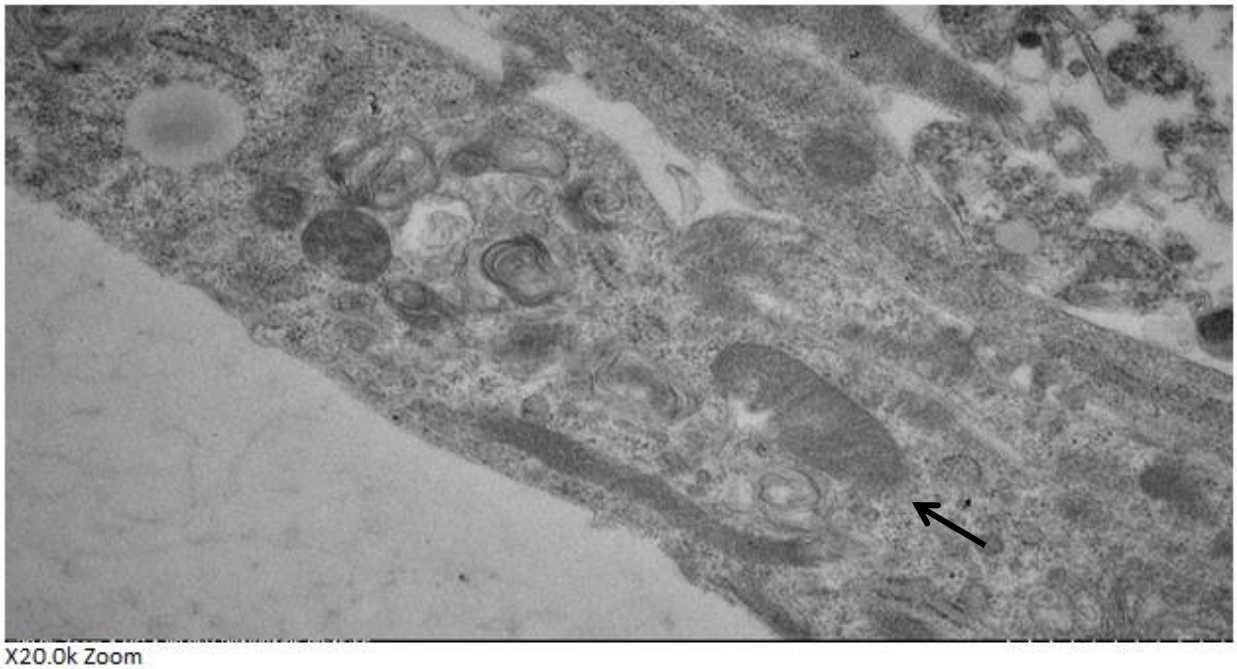

X20.0k Zoom

c.

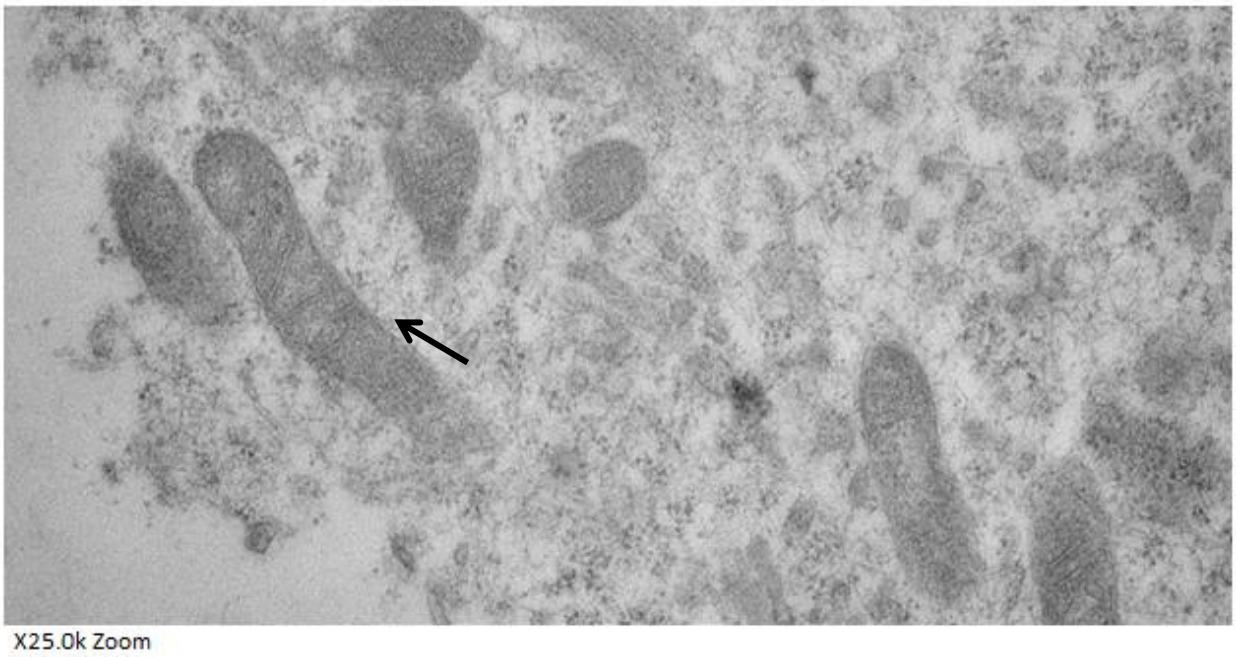

d.

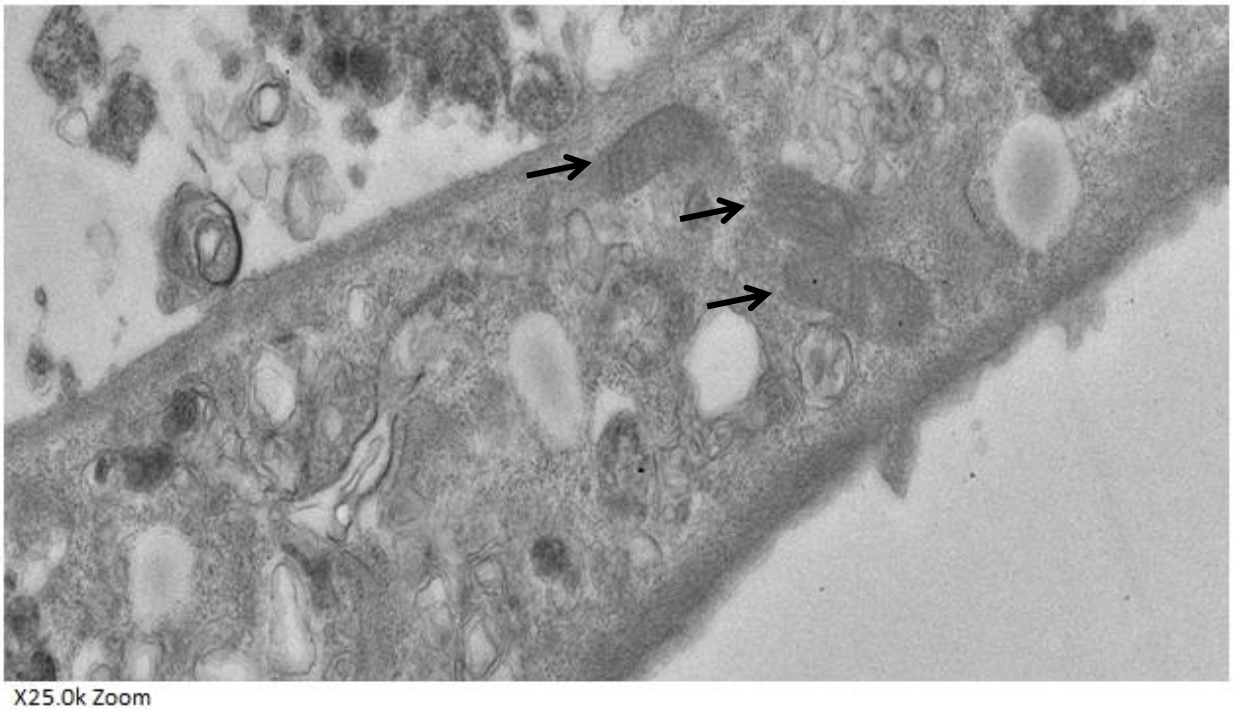

Figure 3.17: Mitochondrial morphology changes detected by EM. Differentiated H9c2 cells were incubated in differentiation medium with **a)** no treatment for 48 h (control) (an arrow pointing at a mitochondrion in this cell has a complete cristae indicating its healthy structure) **b)** doxorubicin (1 µM) for 24 h, followed drug free period (24 h) (an arrow shows a mitochondrion with disrupted cristae, and the image shows other disrupted mitochondria and intracellular damage) **c)** doxorubicin (1 µM) for 24 h followed by its removal and the addition of cyanidin (100

μM) for 24 h (The arrow shows a mitochondrion with partially restored cristae and the image shows other mitochondria in a similar condition) **d)** doxorubicin (1 μM) together with cyanidin (100 μM) for 24 h followed by a drug free period for 24 h (the arrows show mitochondria with mostly distinguishable cristae).

3.3. DETECTION OF INTRACELLULAR CYANIDIN

3.3.1. Absorptivity, stability and fluorescence characteristics of cyanidin in different solvents.

Initially, the stability and the UV-vis absorbance and fluorescence characteristics of cyanidin were identified in different solvents. Cyanidin's behaviour in these solvents determined the suitable extraction solvent for intracellular uptake measurements.

Absorptivity of cyanidin

The objective of this experiment was to determine the absorptivity of cyanidin when dissolved in different extraction solvents (PBS with 0.1% tween-20 and 0.1% FA, ACN with 0.1% FA, methanol with 0.1% FA, DMSO). The absorptivity at 550 nm was determined to be similar and ranged from 0.0016 μM^{-1} (PBS 0.1% tween-20 and 0.1% FA) to 0.0019 μM^{-1} (ACN 0.1% FA), **Figure 3.18**.

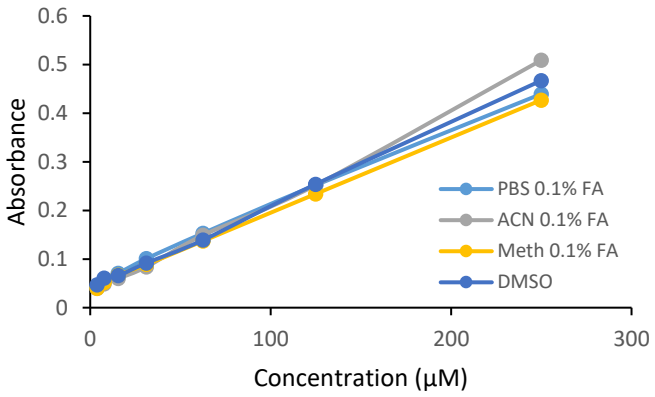

Figure 3.18: **Absorptivity at 550 nm of cyanidin in different solvents.** Cyanidin was dissolved in ACN (0.1% FA), methanol (0.1% FA), PBS (0.1% FA and 0.1% tween-20) or DMSO at different concentrations. The absorptivity was calculated as the slope of the line plotted from the concentration and absorbance at 550 nm.

Stability of cyanidin

The purpose of this evaluation was to determine the stability of cyanidin in different extraction solvents. Cyanidin was found to be highly stable in DMSO, and in ACN or methanol, each supplemented with 0.1% FA. Only 8, 10 and 12% decreases in absorbance at 550 nm after 60 min were observed at room temperature when cyanidin was dissolved in DMSO, ACN 0.1%FA and methanol 0.1% FA, respectively. However, a 27% decrease in absorbance after 60 min was observed when cyanidin was dissolved in PBS supplemented with 0.1% tween-20 and 0.1% FA.

Fluorescence characteristics of cyanidin

After measuring its fluorescence at different excitation and emission wavelengths, cyanidin (100 µM) had a maximum 7.30 fold increase in fluorescence intensity (Ex: 400 Em: 590) compared to the blank when dissolved in DMSO. Cyanidin (100 µM) had 3.80, 3.84 and 2.60 fold increases in fluorescence (Ex: 400 Em: 590) (**Appendix A**) over the solvents alone when dissolved in PBS (0.1% FA and 0.5% tween-20), ACN (0.1% FA) and methanol (0.1% FA).

Finally, the solvents which resulted in the highest cyanidin fluorescence intensity, the highest absorptivity and the highest stability was selected for cyanidin extraction measurements. Therefore, DMSO or ACN (0.1% FA) were used as extraction solvents to determine the cellular uptake of cyanidin in differentiated H9c2 cells using its fluorescence characteristics.

3.3.2. Determination of intracellular cyanidin using UV-vis and fluorescence spectroscopy, HPLC and MS

UV-vis spectroscopy

The detection of intracellular uptake of cyanidin in differentiated H9c2 cells seeded in a 96-well plate was initially attempted using UV-vis absorbance after incubation with 100 µM cyanidin for 10 min. Despite the high concentration of cyanidin in the medium that was retained throughout the 10 min experiment time (as shown in degradation experiments), no UV-vis

absorbance was detected in extracts from cyanidin-treated cells. That is, no difference in absorbance was recorded between the cyanidin treated and the control cells when extracted with DMSO or ACN (0.1% FA). In addition, to verify if any change to the λ_{max} might have occurred after the incubation with the cells, full absorbance scans were conducted on the cell lysate. No difference in absorbance spectrum was observed between the cyanidin-treated and control cells when extracted by ACN (0.1% FA). In addition, when cyanidin was incubated with pelleted H9c2 cells followed by the extraction with ACN (0.1% FA) and the measurement of UV-vis spectrum of the extract, no difference in the absorbance spectrum was detected compared to the control.

Fluorescence spectroscopy

Using DMSO as the extraction solvent, cyanidin was not detected in cyanidin treated-H9c2 cells (results not shown). We also utilized the fluorescence characteristics of cyanidin in ACN (0.1% FA) to detect its presence intracellularly. Using excitation and emission wavelengths of 400 nm and 590 nm, respectively, a difference in fluorescence intensity between the cyanidin-treated and control cells was observed (**Figure 3.19b)**. The standard curve obtained from plotting the concentration vs fluorescence intensity (**Figure 3.19a)** was employed to determine cyanidin's concentration in extraction solvent after treatment of cells. The concentration was found to be 29.9 µM in 50 µL of ACN (0.1% FA) after extraction (giving an amount of 0.430 µg). Knowing that the concentration of cyanidin added to the cells was 100 µM in 100 µL, the original amount of cyanidin is equal to 2.87 µg. This implies that 14.97% of the cyanidin was taken up by the cells. Importantly, incubating the cells with the cyanidin degradation products PCA and PGA followed by subjecting them to the same conditions showed no difference in fluorescence compared to control cells at these wavelengths (Ex: 400nm and Em: 590 nm), (**Appendix B**).

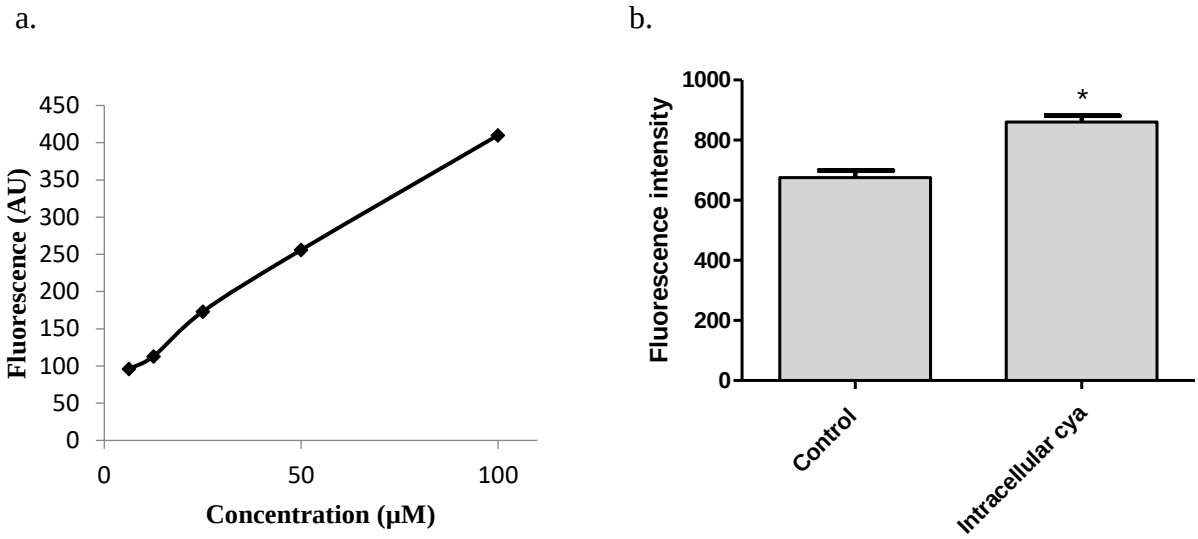

Figure 3.19: Intracellular cyanidin detection using fluorescence and ACN (0.1% FA). Determination of intracellular cyanidin was conducted using fluorescence (Ex: 400 and Em: 590) detection after extraction with ACN (0.1% FA). Fluorescence intensity of **a)** ACN (0.1% FA) cell extracts spiked with different concentrations of cyanidin to form a standard curve for cyanidin and **b)** lysate of differentiated H9c2 cells incubated with cyanidin (100 µM) in a 96 well plate for 10 min (37°C, 5% CO_2), followed by washing with PBS and extraction with ACN 0.1% FA. Fluorescence intensity was measured at (Ex: 400 and Em: 590). * Indicated a significant difference between the detected fluorescence intensity in cyanidin treated cells and the control. Cya: cyanidin.

HPLC detection

Using the two HPLC approaches (with UV-vis or fluorescence detection) the method failed to detect cyanidin or any of its products after cellular extraction with ACN (0.1% FA) (results not shown).

MS detection

The detection of the intracellular amounts of cyanidin, after incubation with pelleted cells for 10 min, was attempted using MS. MS failed to detect cyanidin in the samples extracted with ACN (0.1% FA). Results showed that the extract from control and treated cells had similar peaks with values of 154, 287 or 308 (negative mode). These results show the failure to detect PCA,

PGA, flavylium ion, hemiketal, or chalcone after treatment of differentiated H9c2 cells with cyanidin and their extraction with ACN (0.1% FA).

3.4. EVALUATION OF CYANIDIN AND QUERCETIN AS ANTI-CANCER POTENTIATORS OR INHIBITORS ON HEPG2 AND K562 CELLS IN THE PRESENCE AND ABSENCE OF DOXORUBICIN

3.4.1. Cytotoxicity effects of cyanidin and quercetin in HepG2 and K562 cells in the presence and absence of doxorubicin

The IC_{50} of doxorubicin was initially calculated for HepG2 and K562 cells using the SRB assay. The IC_{50} was 1.59 $\pm$ 0.22 and 1.17 $\pm$ 0.46 µM with HepG2 and K562 cells, respectively (**Figure 3.20**).

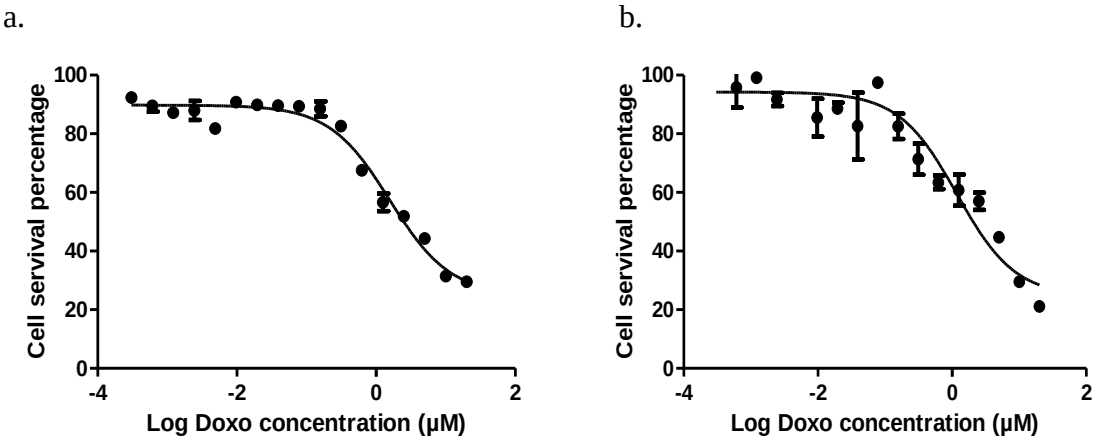

Figure 3.20: Dose-response curve for doxorubicin in HepG2 and K562 cells. a) HepG2 and **b)** K562 cells were incubated with doxorubicin at different concentrations for 72 h, and the SRB assay was used to determine cell density. Three different cell batches were used and for each batch the experiment was conducted in quadruplicate. Points represent means ± SD. Doxo: doxorubicin

The effect of cyanidin and quercetin on doxorubicin cytotoxicity to HepG2 and K562 cells was then evaluated. Cyanidin showed no effect on doxorubicin toxicity with either treatment protocol or cell line (**Figure 3.21a&b**). In HepG2 cells, quercetin produced no significant effect on cell survival when it was added only once with doxorubicin (**Figure 3.21a**). In K562 cells however, 100 µM quercetin produced a significant 7% decrease in survival compared to

doxorubicin alone (**Figure 3.21b**). With multiple additions, quercetin (100 µM each) significantly decreased HepG2 cell survival by 53.3%. In K562 cells, the multiple additions of 50 or 100 µM quercetin caused a significant decrease in cell survival by 23.6 or 34.6%, respectively (**Figure 3.21a&b)**.

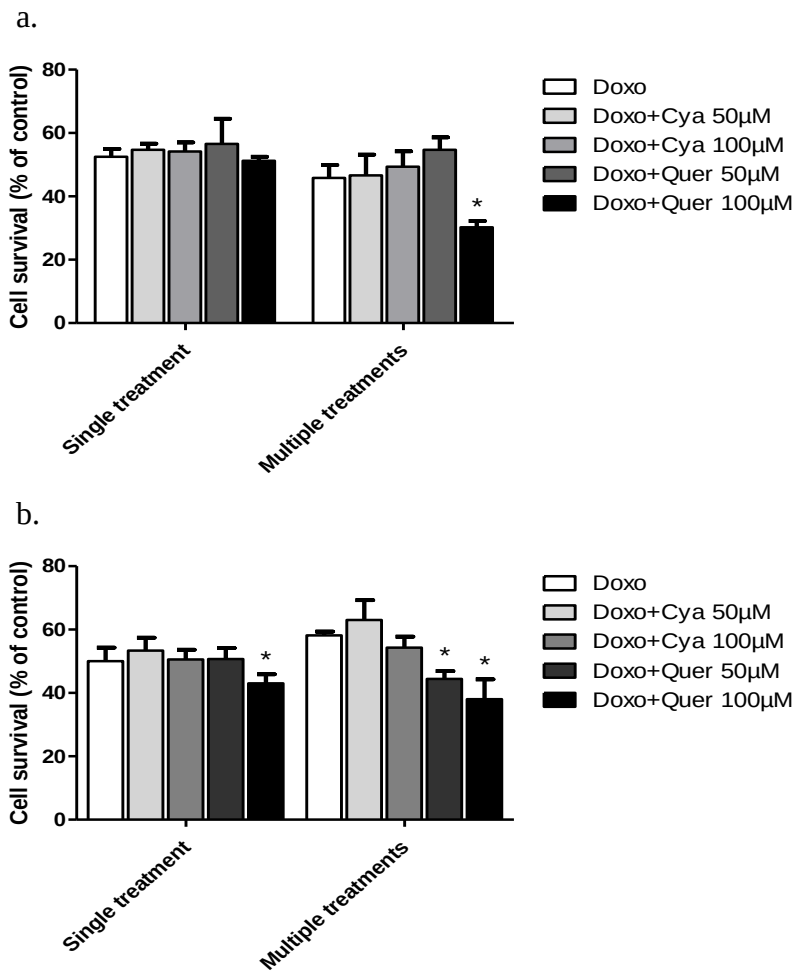

Figure 3.21: Effect of cyanidin and quercetin on the survival of HepG2 or K562 cells when treated with doxorubicin. Doxorubicin with or without the flavonoids was added to **a)** HepG2 or **b)** K562 cells. Cyanidin or quercetin (50 µM or 100 µM) were added either once (single treatment) or every 24 h for 72 h (total of 3 times addition) (multiple treatments). A concentration of 1 or 1.5 µM for doxorubicin for HepG2 or K562 cells. The SRB assay was used to quantify the cell survival percentage. Values are presented in relation to the control survival. Three different cell batches were used and for each batch the experiment was conducted in quadruplicate. One way ANOVA was used to determine the significance of the effects between groups using GraphPad Prizm. * Indicates a significant difference between the treated groups and the doxorubicin group. Doxorubicin was significantly different from the control group. Doxo: doxorubicin, Cya: cyanidin, Quer: quercetin, Cat: catechin, C3G: cyanidin-3-glucoside.

The cytotoxicity of cyanidin and quercetin against HepG2 or K562 cells were also evaluated when added without doxorubicin. Cyanidin showed no effect on cell survival in either cell line despite its addition every 24 h (for 72 h), (**Figure 3.22**). Quercetin, added at 100 µM initially and every 24 h over 72 h, significantly reduced cell survival by 37.7% in HepG2 cells, and by 25.0% in K562 cells (**Figure 3.22**).

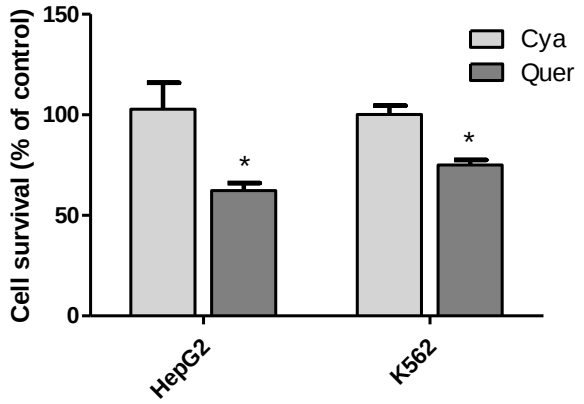

Figure 3.22: Effects of cyanidin and quercetin alone on HepG2 and K562 cell survival. Cyanidin or quercetin (100 µM additions) were added to HepG2 or K562 cells initially and every 24 h for 72 h (total of three additions). The SRB assay was employed to determine the cell survival. Values are presented in relation to the control survival. Three different cell batches were used and for each batch the experiment was conducted in quadruplicate. T-test was used to determine the significance of the effect between the treatment and control group using GraphPad Prism. * Indicates a significant difference between the treated group and the control group. Doxo: doxorubicin, Cya: cyanidin, Quer: quercetin.

3.4.2. Mitochondrial effects of cyanidin and quercetin in HepG2 and K562 cells in the presence and absence of doxorubicin

Quercetin or cyanidin were co-treated with doxorubicin to evaluate their possible potentiating or inhibitory activity on mitochondrial energy metabolism. While doxorubicin was added only once, the flavonoids were added initially and every 24 h for 72 h (total of three additions). Cyanidin showed no effect on doxorubicin toxicity in this experimental condition in either cell line (**Figure 3.23a&b**). With HepG2 cells, the co-treatment of doxorubicin and querctin

(100 µM × 3) caused a significant reduction in MTT by 67.4% (**Figure 3.23a**). With K562 cells, quercetin together with doxorubicin caused significant decreases in MTT (normalised to SRB-determined cellular protein) (by 12.7 and 43.8%) with 50 and 100 µM additions of quercetin, respectively, compared to doxorubicin alone (**Figure 3.23b**).

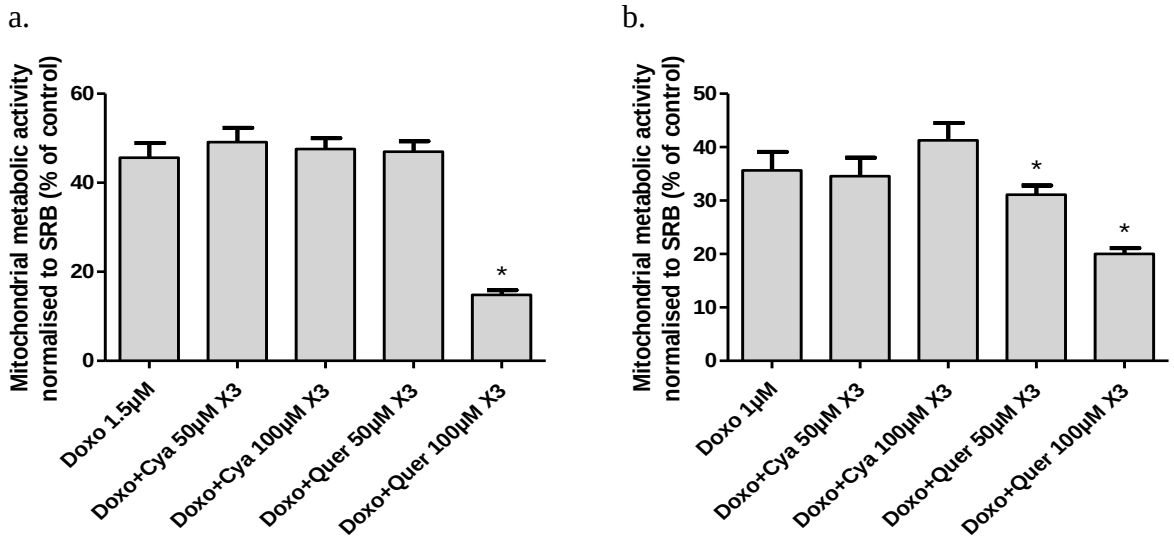

Figure 3.23: Effect of flavonoids on doxorubicin-induced changes in mitochondrial energy metabolism in HepG2 and K562 cells. Doxorubicin (1.5 µM for HepG2 and 1.0 µM for K562 cells) with or without one of the flavonoids (50 or 100 µM) was added to **a)** HepG2 or **b)** K562 cells. However, while doxorubicin was added only once initially, flavonoids (50 or 100 µM) were added initially and every 24 h for 72 h (3 total additions). MTT dye was then employed to quantify the metabolic activity. Values are presented in relation to the control MTT reduction values normalized to cellular protein determined by the SRB assay done in the same wells. Three different cell batches were used and for each batch the experiment was conducted in quadruplicate. One-way ANOVA with Tukey's post-hoc test was used to determine the significance of the effects between groups using GraphPad Prism. * Indicates a significant difference between the flavonoid treated group and the doxorubicin group. Doxorubicin was significantly different from the control group. Doxo: doxorubicin, Cya: cyanidin, Quer: quercetin.

The MMP assay was also used to explore the combined effects of cyanidin or quercetin with doxorubicin on mitochondrial function in HepG2 and K562 cells. In HepG2 cells treatment with doxorubicin (1 µM) without a flavonoid for 24 h significantly lowered MMP (**Figure 3.24a**). Cyanidin showed no effect, but quercetin significantly decreased MMP by 30.4% compared to HepG2 cells treated with doxorubicin alone. With K562 cells, cyanidin again had no effect but

quercetin caused a significant decrease (by 24.1%) after 12 h of treatment compared to doxorubicin (1.5 µM) alone (**Figure 3.24b**). As determined by the SRB assay, the density of cellular protein did not change after 24 h incubation using both cell lines (data not shown).

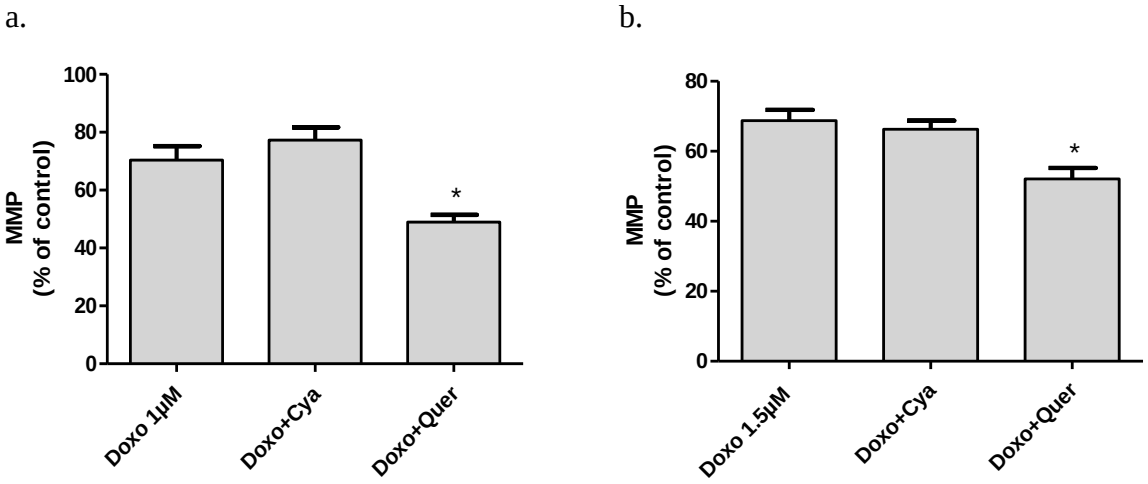

Figure 3.24: Effect of flavonoids on doxorubicin-induced changes to mitochondrial membrane potential (MMP) in HepG2 and K562 cells. Doxorubicin (1 µM) with or without one of the flavonoids (100 µM) was added to **a)** HepG2 or **b)** K562 cells, and incubated for 24 h or 12 h, respectively. MMP was then measured using TMRE dye. No effects on SRB were seen at these incubation times, so normalization to cell density was not needed. Three different cell batches were used and for each batch, the experiment was conducted in quadruplicate. Bars represent means ± SD. One-way ANOVA with Tukey's post-hoc analysis was used to determine the significance of the effects between groups. Doxorubicin was significantly different from the control. * Indicates a significant difference from the doxorubicin-treated group ($p < 0.05$). Doxo: doxorubicin, Cya: cyanidin, Quer: quercetin.

3.4.3. Effects of cyanidin and quercetin on doxorubicin-induced intracellular ROS generation in HepG2 and K562 cells

Assessments of intracellular ROS generation were conducted to understand the possible mechanisms involved in any inhibitory or potentiating effects of the flavonoids with doxorubicin. With HepG2 cells, quercetin significantly enhanced the effect of doxorubicin on intracellular ROS generation, while cyanidin failed to show such capability (**Figure 3.25**). With K562 cells, both flavonoids failed to cause any significant increase in ROS compared to doxorubicin alone (**Figure 3.25**).

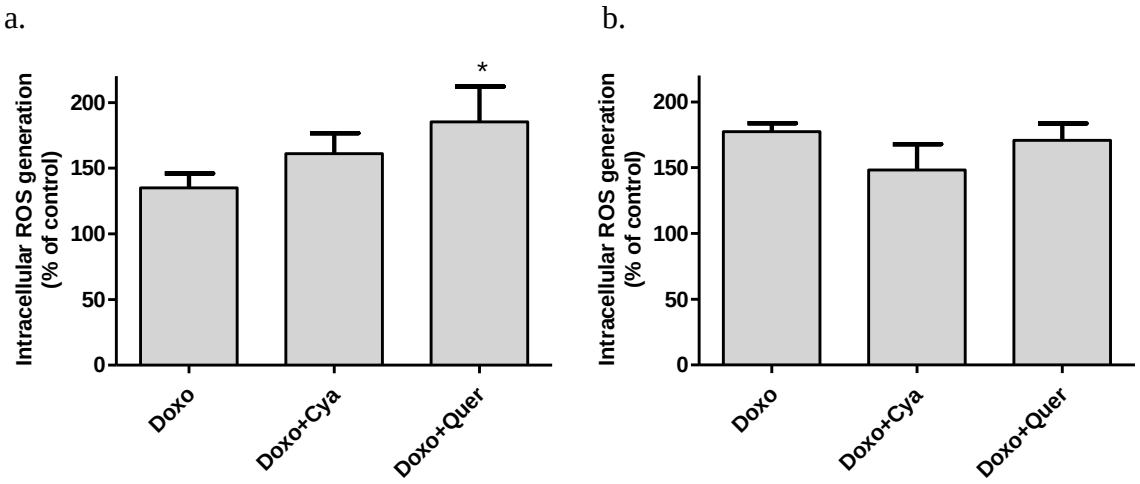

Figure 5.25: Effect of cyanidin and quercetin on doxorubicin-induced reactive oxygen species (ROS) in HepG2 and K562 cells Doxorubicin (1 µM) with or without one of the flavonoids (100 µM) was added to **a)** HepG2 or **b)** K562 cells and incubated for 24 h. Intracellular ROS generation was then measured using DCFH-DA dye. Values are presented in relation to the control. Three different cell batches were used and for each batch, the experiment was conducted in quadruplicate. Bars represent means ± SD. One-way ANOVA with Tukey's post-hoc analysis was used to determine the significance of the effects between groups. * Indicates a significant difference from the doxorubicin-treated group ($p < 0.05$). Doxorubicin was significantly different from the control group. Doxo: doxorubicin, Cya: cyanidin, Quer: quercetin.

3.4.4. Effects of cyanidin and quercetin on the ability of doxorubicin to cause DNA fragmentation in HepG2 and K562 cells

The COMET assay was conducted to evaluate the effect of cyanidin and quercetin on doxorubicin-induced DNA damage in HepG2 and K562 cells. The images in **Figure 5.26** show no COMET tail in the control HepG2 (panel **a**) or K652 (panel **e**) cells, but COMET tails are apparent in all of the conditions with doxorubicin. The quantified results of percent of DNA in the tail are shown in **Figure 5.26**. With HepG2 cells, exposure to doxorubicin (1 µM) for 72 h significantly increased the amount of fragmented DNA to 33.8% (**Figure 5.27)**. Quercetin significantly increased the fragmented DNA by 27.7% over doxorubicin alone. Cyanidin had no effect on DNA fragmentation caused by doxorubicin.

In K562 cells, doxorubicin for 72 h caused an increase in DNA fragmentation to 26.1±7.4% (**Figure 3.25**). Cyanidin had no significant effect on DNA fragmentation compared to doxorubicin alone, however, quercetin increased the fragmentation by 46.4%.

a.

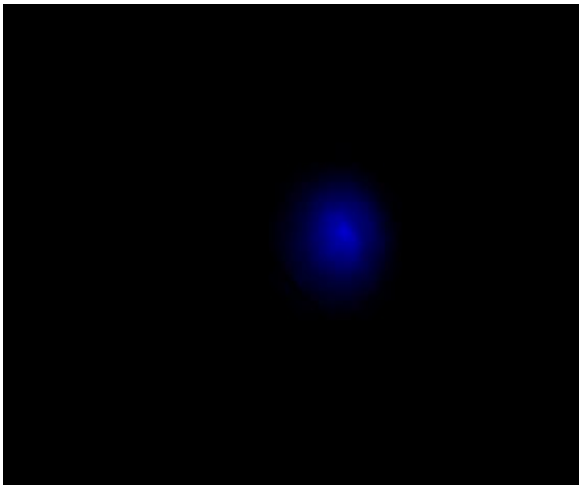

b.

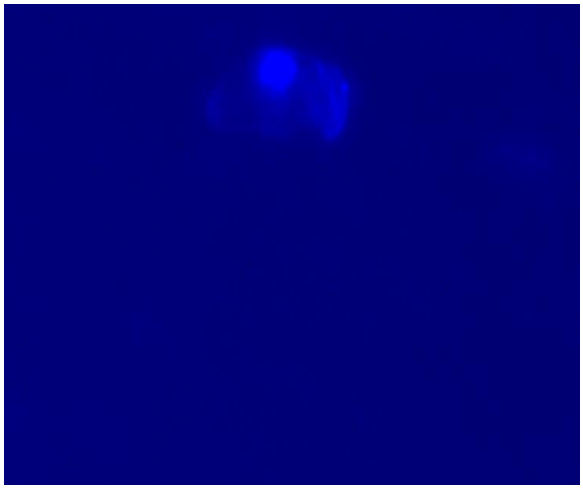

c.

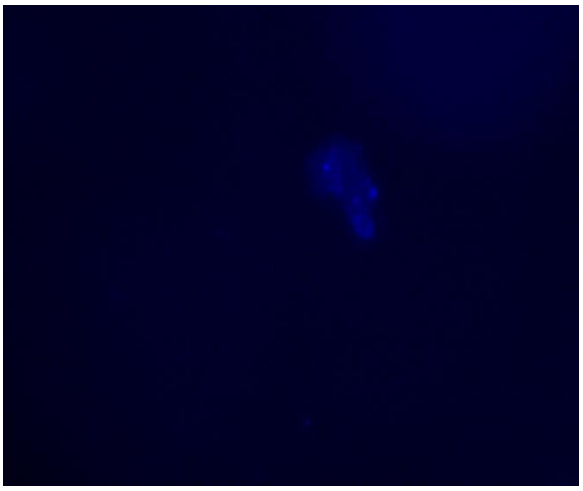

d.

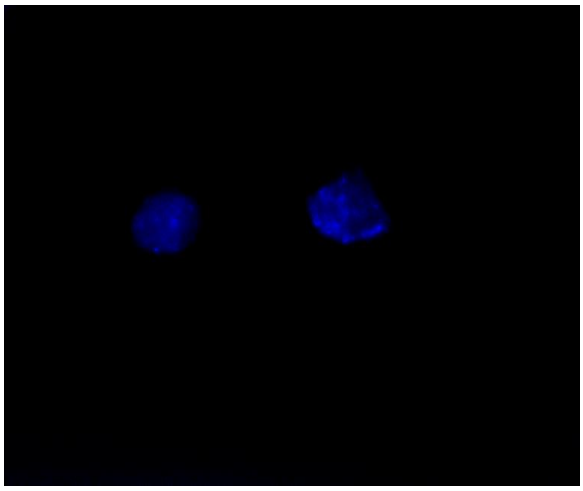

e.

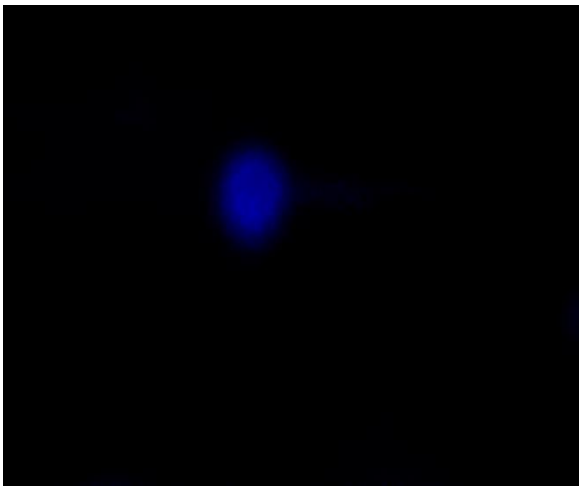

f.

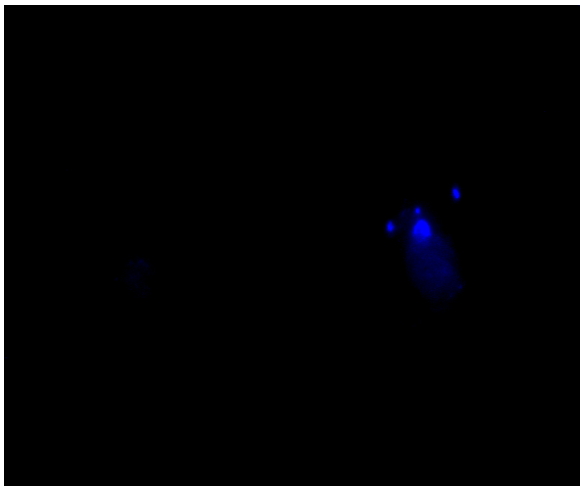

g.

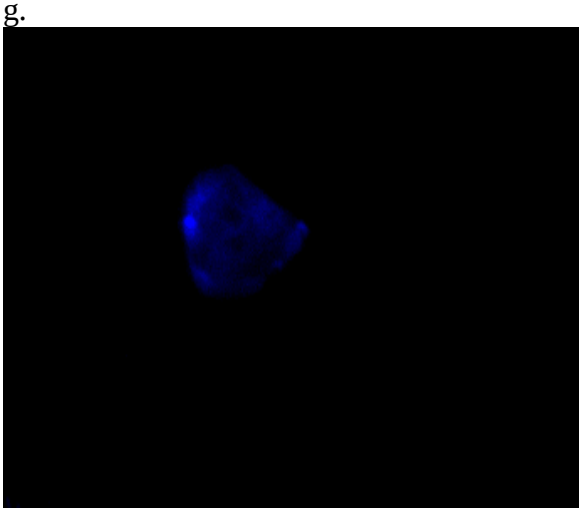

h.

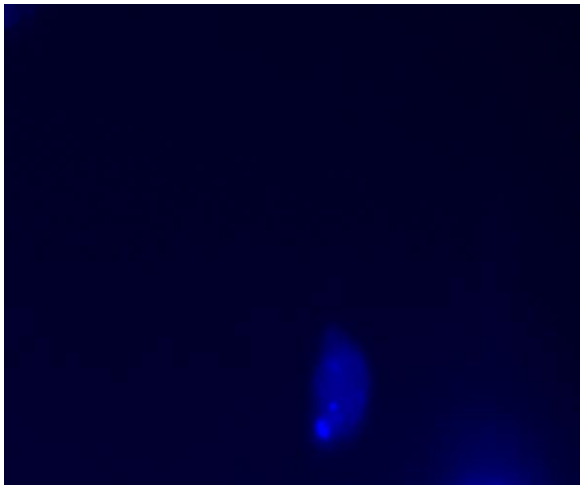

Figure 3.26: Effects of cyanidin and quercetin on doxorubicin-induced DNA fragmentation in HepG2 and K562 cells. HepG2 cells were incubated for 72 h with **a)** no additions, **b)** doxorubicin (1 µM), **c)** doxorubicin (1 µM) and cyanidin (100 µM), or **d)** doxorubicin (1 µM) and quercetin (100 µM), followed by the COMET assay. K562 cells were treated for 72 h with **e)** no additions, **f)** doxorubicin (1 µM) **g)** doxorubicin (1 µM) and cyanidin (100 µM), or **h)** doxorubicin (1.5 µM) and quercetin (100 µM), followed by the COMET assay. Three different cell batches were used and for each batch. Shown are representative images of 7-10 cells from one experiment.

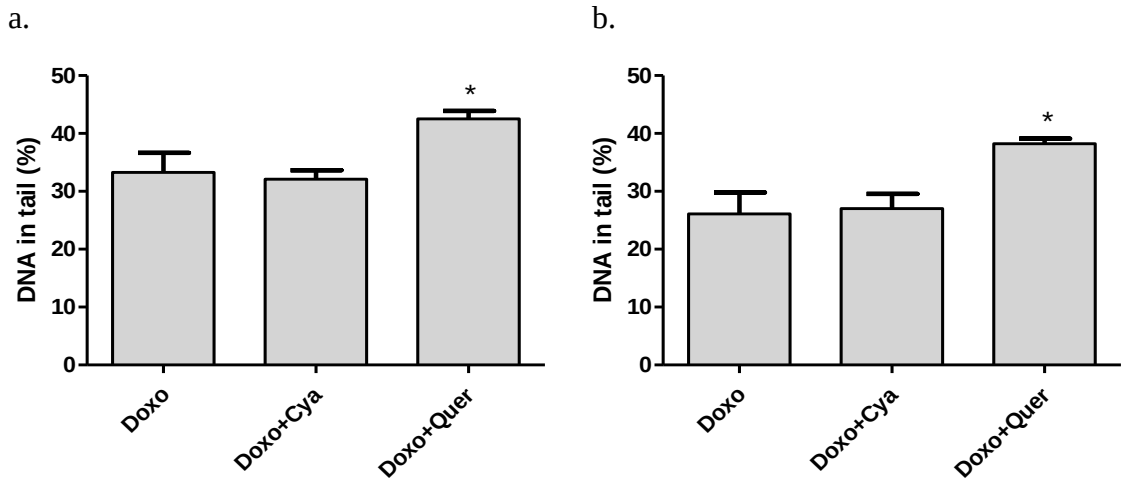

Figure 3.27: Effect of doxorubicin on DNA fragmentation with or without a flavonoid in HepG2 and K562 cells. a) HepG2 or **b)** K562 cells were exposed to doxorubicin with or without cyanidin or quercetin followed by COMET assay. Values are presented in relation to the control. Three different cell batches were used and for each batch, the experiment was conducted in quadruplicate. Bars represent mean ± SD. One-way ANOVA with Tukey's post-hoc analysis was used to determine the significance of the effects between groups. * Indicates a significant difference from the doxorubicin-treated group ($p < 0.05$). Doxorubicin was significantly different from the control group. Doxo: doxorubicin, Cya: cyanidin, Quer: quercetin.

3.5. DEGRADATION OF CYANIDIN

3.5.1 Comparison of rates of disappearance in different media using UV-vis measurements

Cyanidin

In order to determine its λ_{max}, absorbance spectrum of cyanidin was measured at the wavelength range of 200-800 nm (**Figure 3.28)**. The spectrum showed that the λ_{max} was 585 nm in the vible wavelength range. Cyanidin had similar spectra and λ_{max} values when dissolved in human serum, PBS, HEPES and DMEM (with and without 10% FBS).

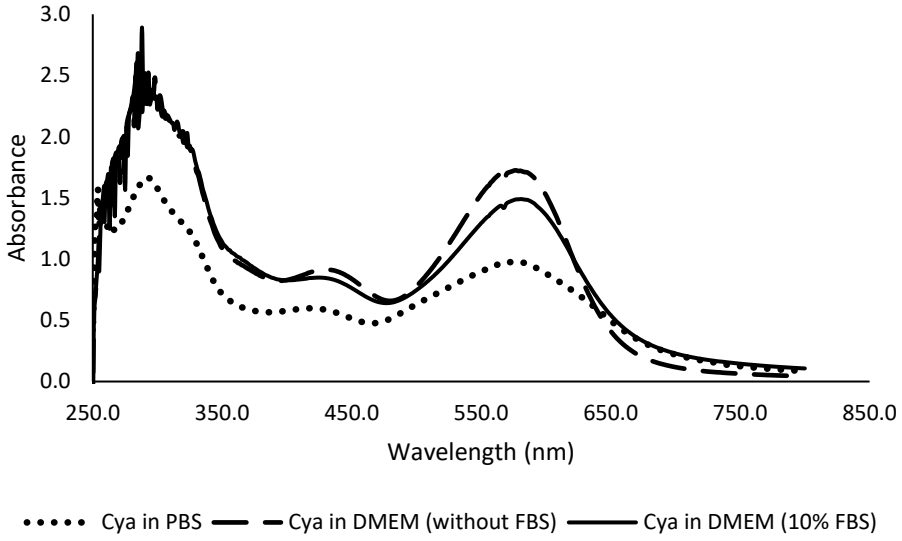

Figure 3.28: The absorbance spectrum of cyanidin in phosphate buffered saline (PBS) (pH 7.4), Dulbecco's Modified Eagle's Medium (DMEM) (without fetal bovine serum (FBS)) and DMEM. Cyanidin was dissolved in each solvent separately (pH 7.4) at a concentration of 100 µM followed by the absorbance spectrum measurement at wavelength ranges of 250-800 nm. Cya: cyanidin.

To determine its rate of disappearance, cyanidin (100 µM) was dissolved in different media and the change in absorbance was recorded over time at 585 nm (λ_{max}) using a Beckman spectrophotometer. **Figure 3.29** shows the degradation of cyanidin in PBS (pH 7.4), DMEM with and without 10% FBS, human serum and HEPES buffer. The $t_{1/2}$ values were different in all solvents, with human serum (43.2 $\pm$ 1.73 min) being significantly higher than when cyanidin was

incubated in other media. When PBS was used as a medium, cyanidin had the lowest $t_{1/2}$ of only 10.2 $\pm$ 0.56 min, and the reaction showed biphasic kinetics. Compared to PBS, cyanidin dissolved in HEPES had a significantly higher $t_{1/2}$ (32.6 $\pm$ 2.38 min). The $t_{1/2}$ of cyanidin when dissolved in DMEM with or without FBS had no significantly different values (21.6 or 18.7 min, respectively).

a.

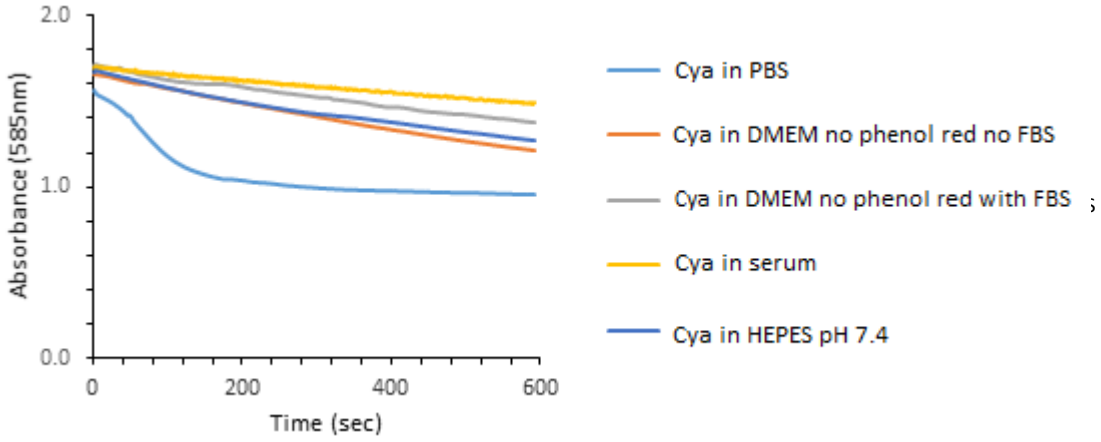

b.

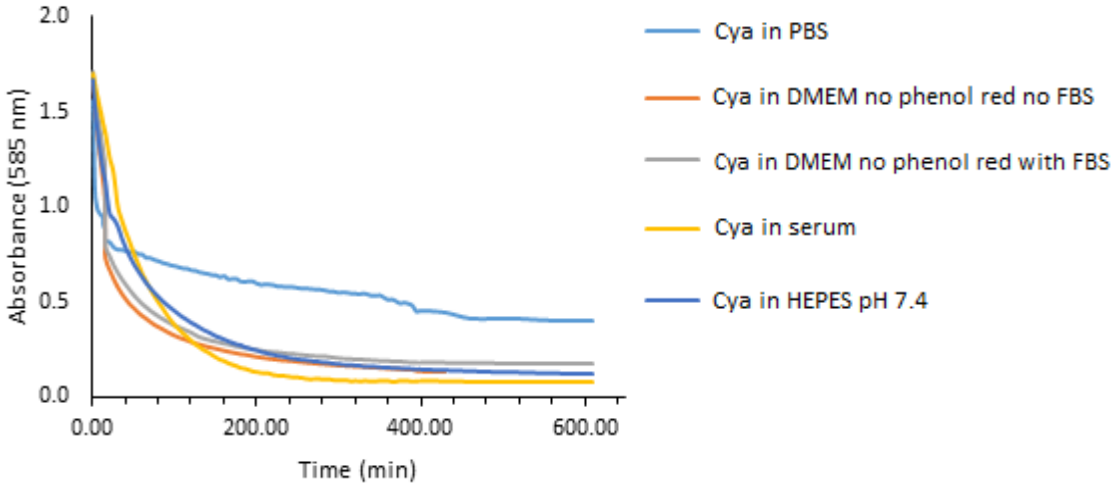

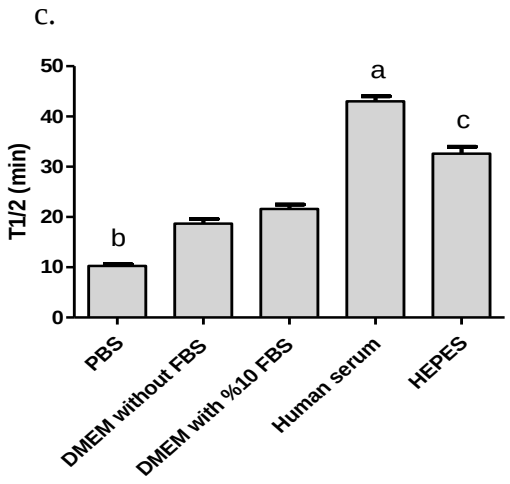

Figure 3.29: **Change in absorbance of cyanidin in different media**. The rates of degradation at room temperature of cyanidin in PBS pH 7.4, DMEM supplemented with 10% FBS, DMEM with no supplementation, human serum, and 25 mM HEPES buffer (pH 7.4) were determined using a spectrophotometer. Cyanidin was initially added to the medium at a concentration of 100 µM followed by the measurement of the absorbance at 585nm. Representative curves of kinetics at room temperature of the change in absorbance at 585 nm are shown of the same reaction over **a)** 600 sec and **b)** 600 min. **c)** Mean $\pm$ SD of $t_{1/2}$ cyanidin in different media calculated by GraphPad Prism software following a nonlinear exponential decay model. [a] Indicates a significant difference between human serum and all other groups. [b] Indicates a significant difference between PBS and all other media. [c] Indicates a significant difference between HEPES and all other media. Cya: cyanidin.

Quercetin

The absorption spectrum of quercetin (100 µM) when dissolved in PBS was determined using a Beckman spectrophotometer. The λ_{max} was found to be 400.0 nm (**Figure 3.30**). Quercetin had similar spectra and λ_{max} when dissolved in DMEM (with and without 10% FBS).

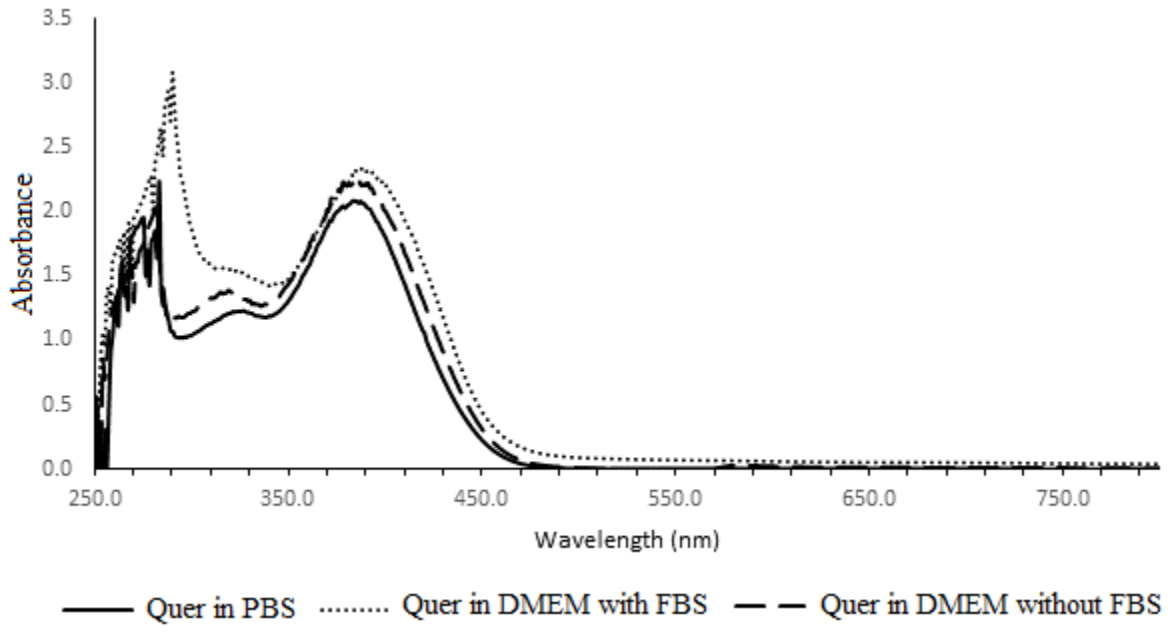

Figure 3.30: **Absorbance spectra for quercetin in different media**. Quercetin was added to different media at a concentration of 100 µM, and the absorbance spectrum was then measured.

The rate of change in absorbance (at 400 nm) differed when 100 µM quercetin was incubated in different media (**Figure 3.31**). The $t_{1/2}$ was 63.47 min and 29.61 min when quercetin was incubated in DMEM without FBS, and PBS, respectively. However, the $t_{1/2}$ for quercetin when dissolved in DMEM with 10% FBS was not measurable as the plateau was not reached despite the long incubation period (12 h) (**Figure 3.31**).

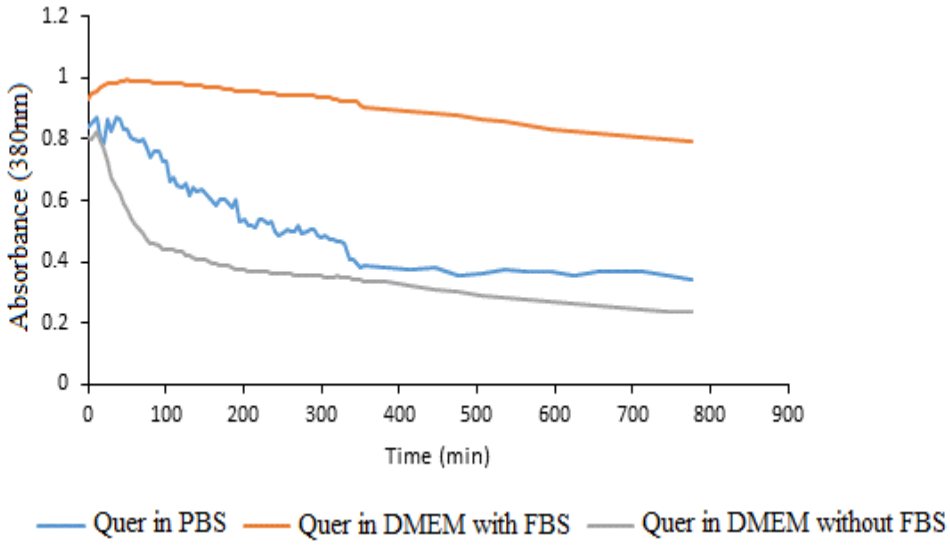

Figure 3.31: Change in absorbance at 380 nm of quercetin in different media. The rate of the decrease in the absorbance of 100 µM quercetin in PBS and DMEM (with or without FBS) at room temperature was measured in a spectrophotometer. Quer: quercetin.

Catechin

The catechin spectrum and λ_{max} were measured initially (**Figure 3.32a**) when dissolved in PBS and its λ_{max} was determined to be at 280.0 nm. Catechin had similar spectrum and λ_{max} when dissolved in DMEM (with and without 10% FBS). It had no apparent changes in absorbance at 280 nm when dissolved in PBS (pH 7.4) or DMEM (**Figures 3.32b)**.

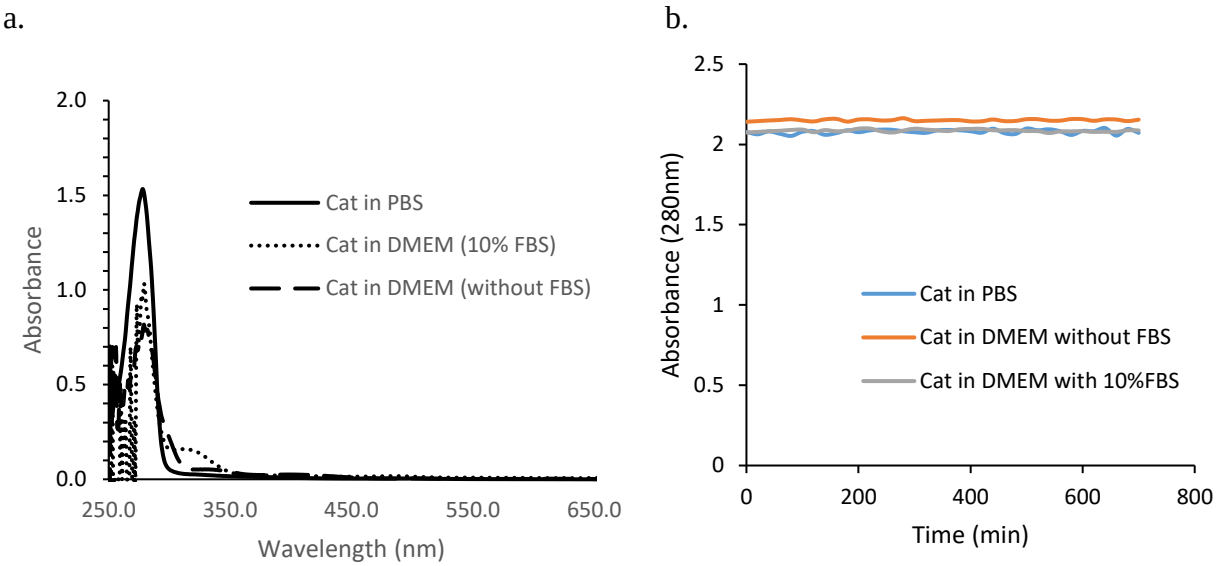

Figure 3.32: Change in absorbance of catechin in different media. a) Spectrum for 300 µM catechin when dissolved in PBS pH 7.4. **b)** The change in absorbance at 280 nm in different media at room temperature was measured over time using a plate reader. Cat: catechin.

Cyanidin-3-glucose (C3G)

The degradation of C3G in PBS and DMEM with or without FBS is relatively slow at room temperature (**Figure 3.33a**), with 22%, 25% and 35% of the initial C3G absorbance was lost after 16 h when dissolved in PBS, DMEM without FBS and DMEM with FBS (**Figure 3.33b**), respectively.

a.

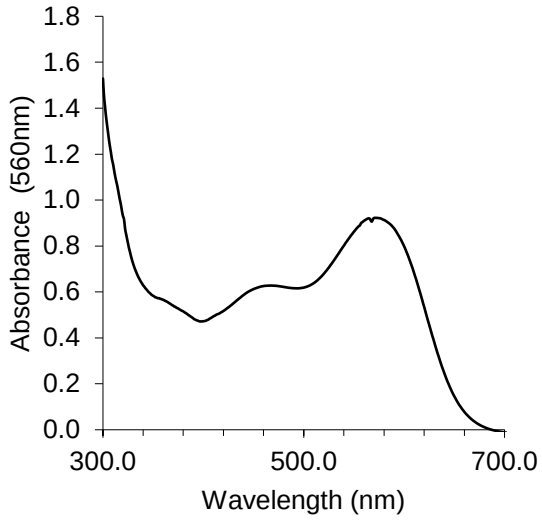

b.

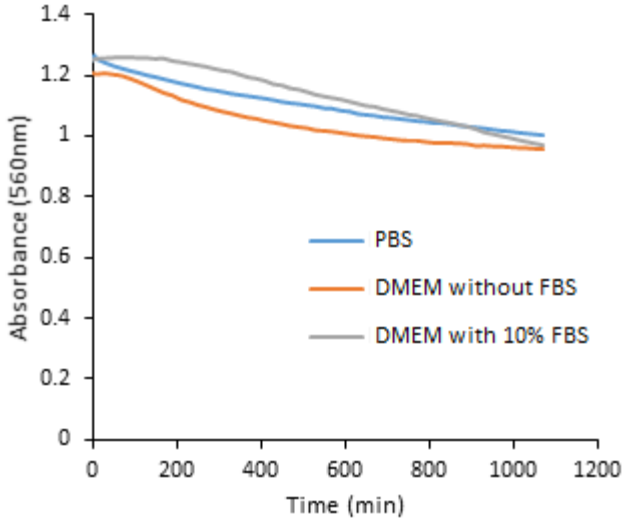

Figure 3.33: Change in absorbance of cyanidin-3-glucose (C3G) in different media a) Spectrum for C3G (100 µM) when dissolved in PBS pH 7.4. **b)** C3G (100 µM) was incubated at room temperature in PBS (pH 7.4), and DMEM with or without 10% FBS and absorbance (at 580 nm) was measured at 20 min intervals in a plate reader. The experiment was terminated after 16 h with no apparent plateau in absorbance values.

3.5.2. HPLC analyses of cyanidin degradation and formation of degradation products

The objective of this experiment was to determine the change in the concentration of cyanidin and its degradation products (PCA and PGA) with time. Initially, cyanidin was detected immediately after its addition to PBS (pH 7.4) (**Figure 3.34a)**. After 30 min at room temperature, a decrease (by about 99%) in the peak area at retention time 5.018 min was noticed (**Figure 3.34b**).

a.

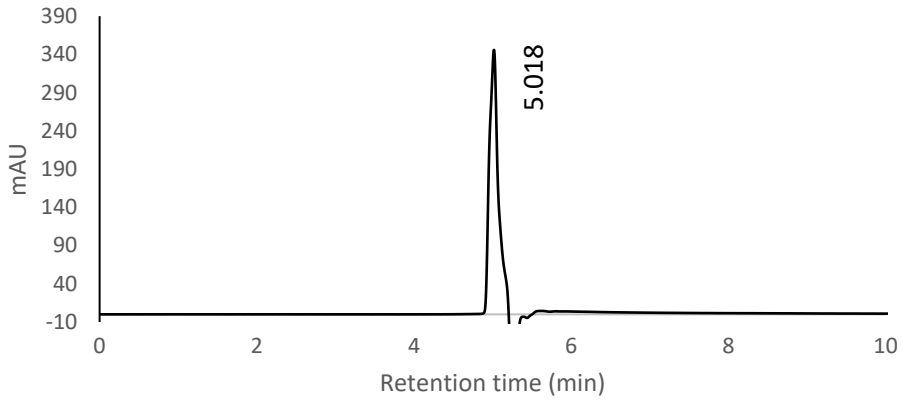

b.

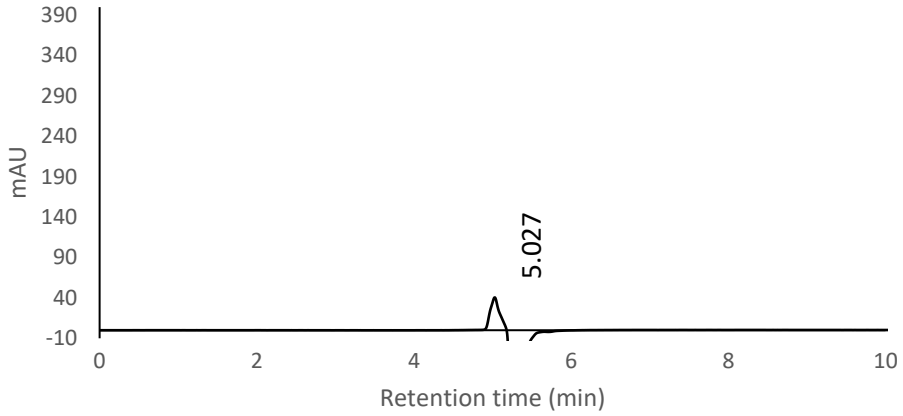

Figure 3.34: Detection of changes in cyanidin concentration with time using HPLC. Cyanidin at a concentration of 100 µM was incubated at room temperature in PBS, pH 7.4, and measured by HPLC with UV-vis detection at 525 nm (with reference wavelength 360 nm). **a)** The detection of cyanidin shortly (about 1 min) after addition to PBS 7.4. **b)** The detection of cyanidin 30 min after adding it to PBS 7.4.

An increase in PGA 1 min after addition of cyanidin to PBS was evident (**Figure 3.35a and 3.37)**. In addition, **Figure 3.35b** shows that the peak for PGA in the cyanidin solution after 2 h of incubation at room temperature increased significantly. This increase in peak area for PGA reached a maximum within 2 h of incubating cyanidin in PBS, as the PGA levels in the cyanidin solution after 4 and 8 h were similar (**Figure 3.35c and 3.35d, respectively).**

a.

5.278

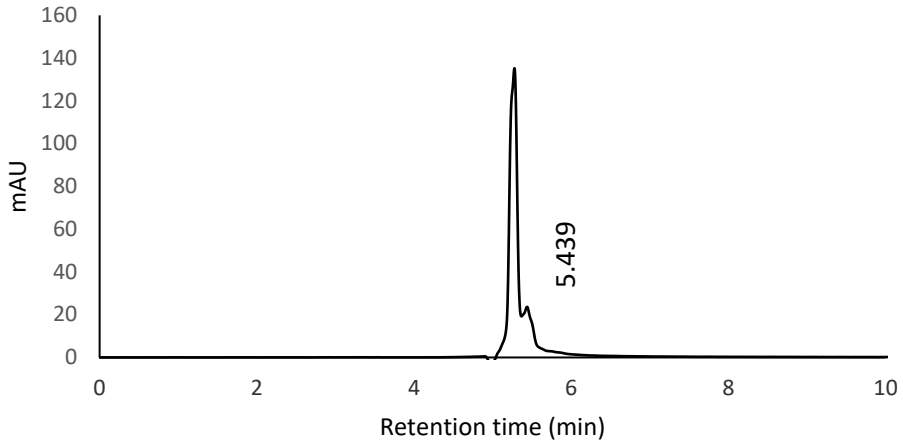
160
140
120
100
80
60
40
20
0
mAU
5.439
0
2
4
6
8
10
Retention time (min)

b.

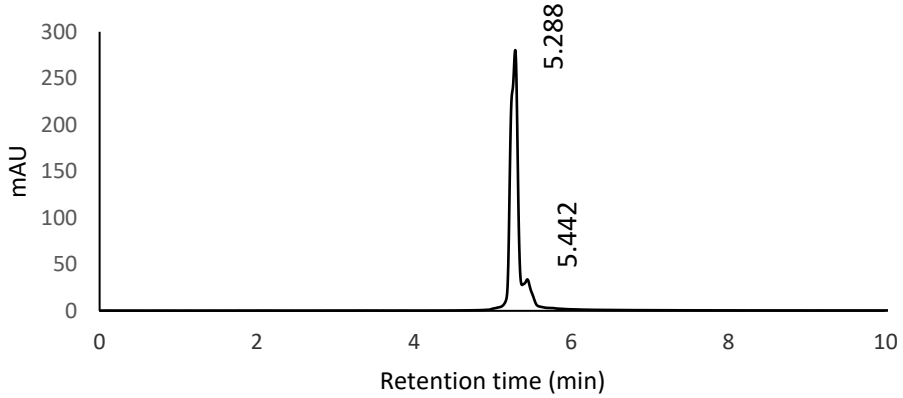
300
250
200
150
100
50
0
mAU
5.288
5.442
0
2
4
6
8
10
Retention time (min)

c.

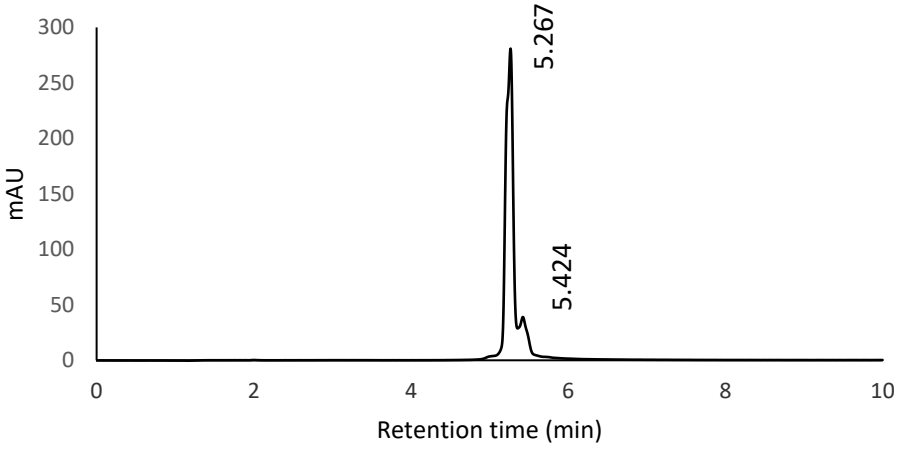
300
250
200
150
100
50
0
mAU
5.267
5.424
0
2
4
6
8
10
Retention time (min)

d.

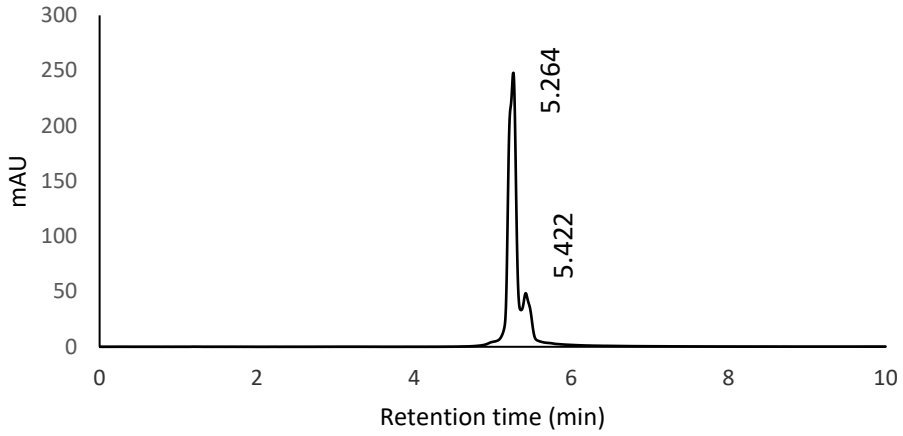

Figure 3.35: Detection of changes in the concentration of PGA with time in a cyanidin solution using HPLC. Cyanidin was added to PBS at a concentration of 100 µM followed by incubation at room temperature and the measurement of PGA at different intervals using HPLC. PGA was detected at 315 nm and a retention time of ~5.28 min: **a)** soon after adding cyanidin to PBS (pH 7.4), **b)** after 2hr incubation, **c)** after 4h incubation, and **d)** after 8h incubation.

In order to quantify PGA peaks found in cyanidin solutions, a standard curve was established for PGA using a pure standard chemical. The standard curve for PGA in PBS (pH 7.4) is shown in **Figure 3.36**. The peaks were detected at a wavelength of 315 nm and a retention time of 5.288 min.

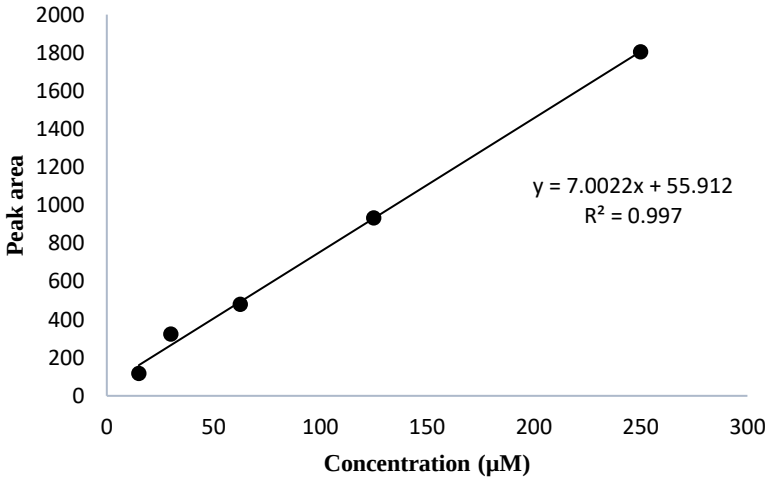

Figure 3.36: Phloroglucinaldehye (PGA) standard curve. PGA was dissolved in PBS at different concentrations. Each sample was then run through the column following the same HPLC procedure and mobile phases. The mobile solvents were water (A) and acetonitrile (B). The mobile

phase started with 10% B from 0 to 2 min. The percentage of B was at 70% from 2 to 20 min. Flow rate was 1 mL min^{-1} and temperature was 22.0±1°C. The equation which resulted from plotting the concentration (µM) vs peak area was used to calculate the concentrations in cyanidin solutions.

After calculating the concentration of PGA in a 250 µM cyanidin solution at the different incubation periods, a concentration of 140 µM was evident in the first measurement after addition of cyanidin to PBS (4-5 min), and a maximum concentration of PGA of 250 µM was reached after 2 h (**Figure 3.37**). This maximum concentration was equivalent to the initial concentration of cyanidin (250 µM).

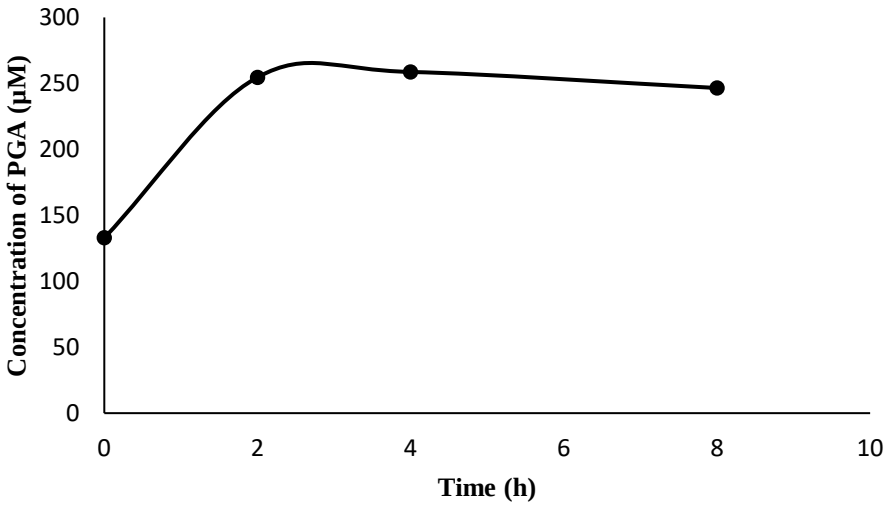

Figure 3.37: The change in the concentration of phloroglucinaldehye (PGA) with time in a PBS solution of cyanidin. Cyanidin was added at 250 µM to PBS and incubated at room temperature, and the PGA levels were determined over time using HPLC with UV-vis detection at 315 nm. The concentrations were calculated using a standard curve which plotted the change in concentration against the increase in absorbance (Figure 5.35) (in a single measurement at each time point).

3.5.3. Mass spectrometry (MS) analyses of cyanidin degradation and degradation product formation

To further understand the degradation/transformation of cyanidin, MS was employed to detect the molecular weights of products found in the degradation process. MS results show that a product with an m/z value of 154, which corresponds to PCA and PGA, was detected immediately after adding cyanidin to neutral 10% methanol in water and remained for at least 6 h (**Appendix C)**. **Figure 3.38 s**hows the change in peak intensity at 153 m/z with time. To verify the presence of PCA, product ions were generated for the peak at 153 Da (representative of PGA and PCA with a molecular weight of 154 Da) using the tandem MS (negative mode) (MS/MS) (**Appendix D**). The peaks generated were then compared to those produced when a PCA standard was subjected to similar MS/MS parameters (**Appendix E**).

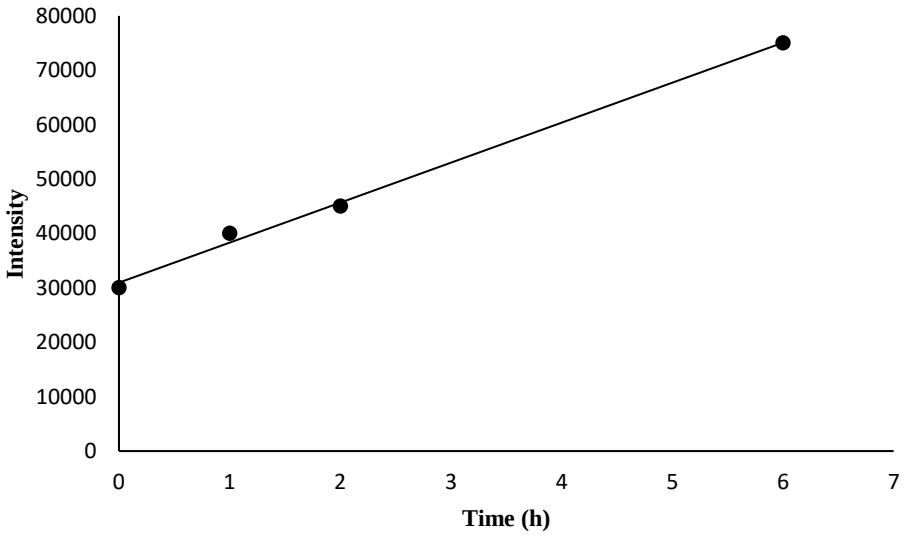

Figure 3.38: The change in peak intensity at 153 m/z with time. Cyanidin was added at 10 µM to MS grade water with 10% methanol and incubated at room temperature. The peaks at 153 m/z were determined over time using MS. A correlation was then established between the peak intensity and the time (in a single measurement at each time point).

The general purpose of this method was to detect any compound that has a mass/charge within an m/z range of 303 and 287. Flavylium ion (expected to appear at 285 m/z) was not detected immediately after adding cyanidin to the same solvent (10% MS-grade methanol in MS-grade water) using Q1 (negative mode). However, the peak (at m/z of 285) was detected using enhanced full scan. Interestingly, peaks with m/z of 303 corresponding to chalcone and hemiketal (302 Da) intermediates were detected at times zero, 2 h and 6 h (**Figure 3.39** and **Appendix F)**. Unfortunately, no standards were available for chalcone and hemiketal. Therefore, Peakview® software was used to predict the product ions of hemiketal and chalcone. MS/MS was used to generate product ions for the peak 303. All peaks that appear as product ions were shown plausible using the Software (**Appendix G**). In addition, the structure of the observed product ions were rationalized as shown in **Figure 3.40**. This shows, although not definitive, that the compound detected at m/z peak of 303 is most likely either chalcone or hemiketal.

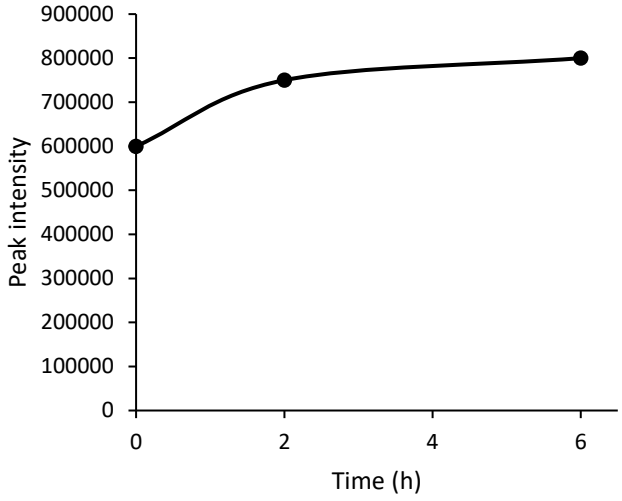

Figure 3.39: **The change in peak intensity at 302 m/z with time.** Cyanidin was added at 10 µM to MS grade water with 10% methanol and incubated at room temperature. The peaks at 302 m/z were determined over time using mass spectrometry. A correlation was then established between the peak intensity and the time (in a single measurement at each time point).

a.

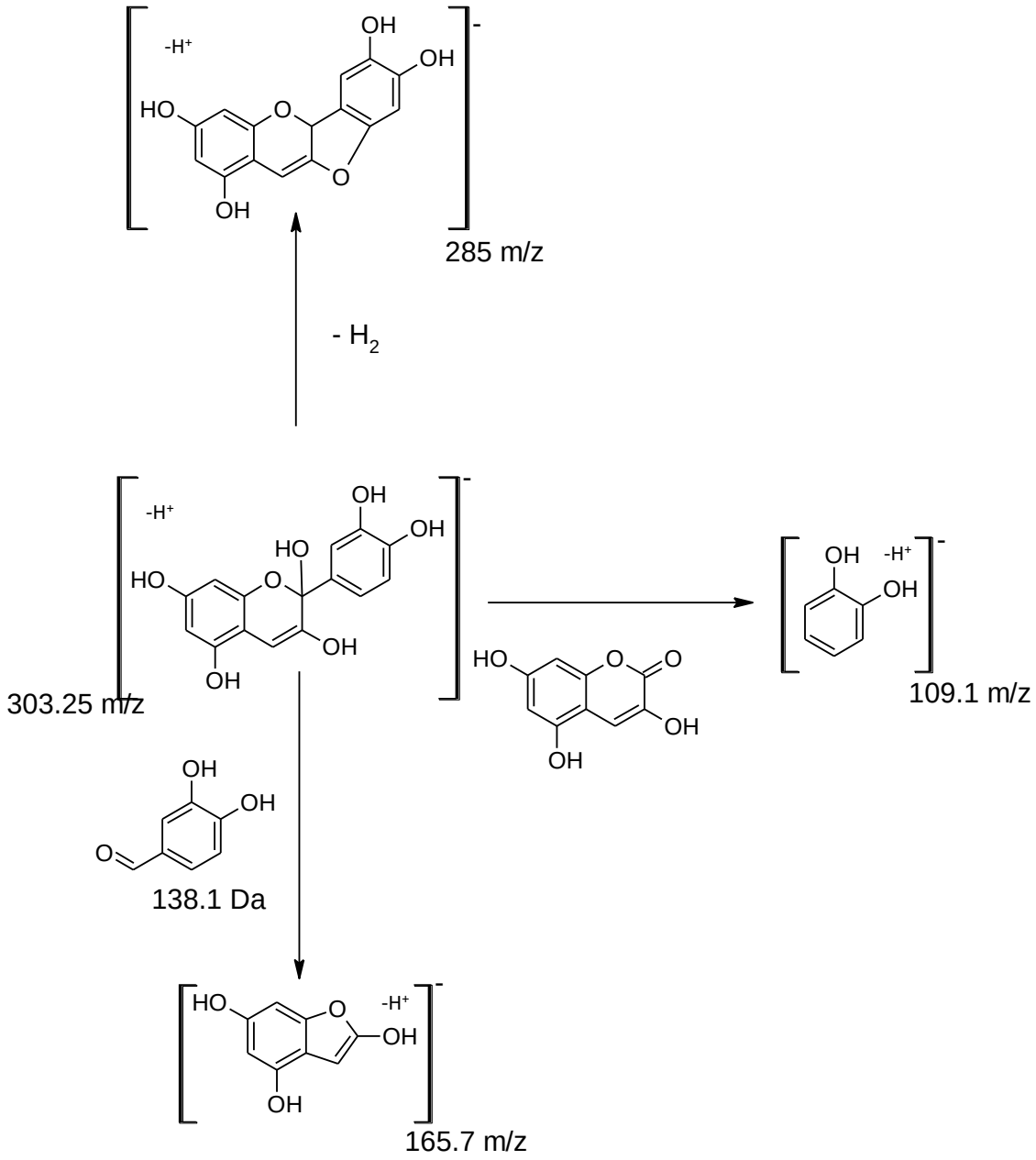

b.

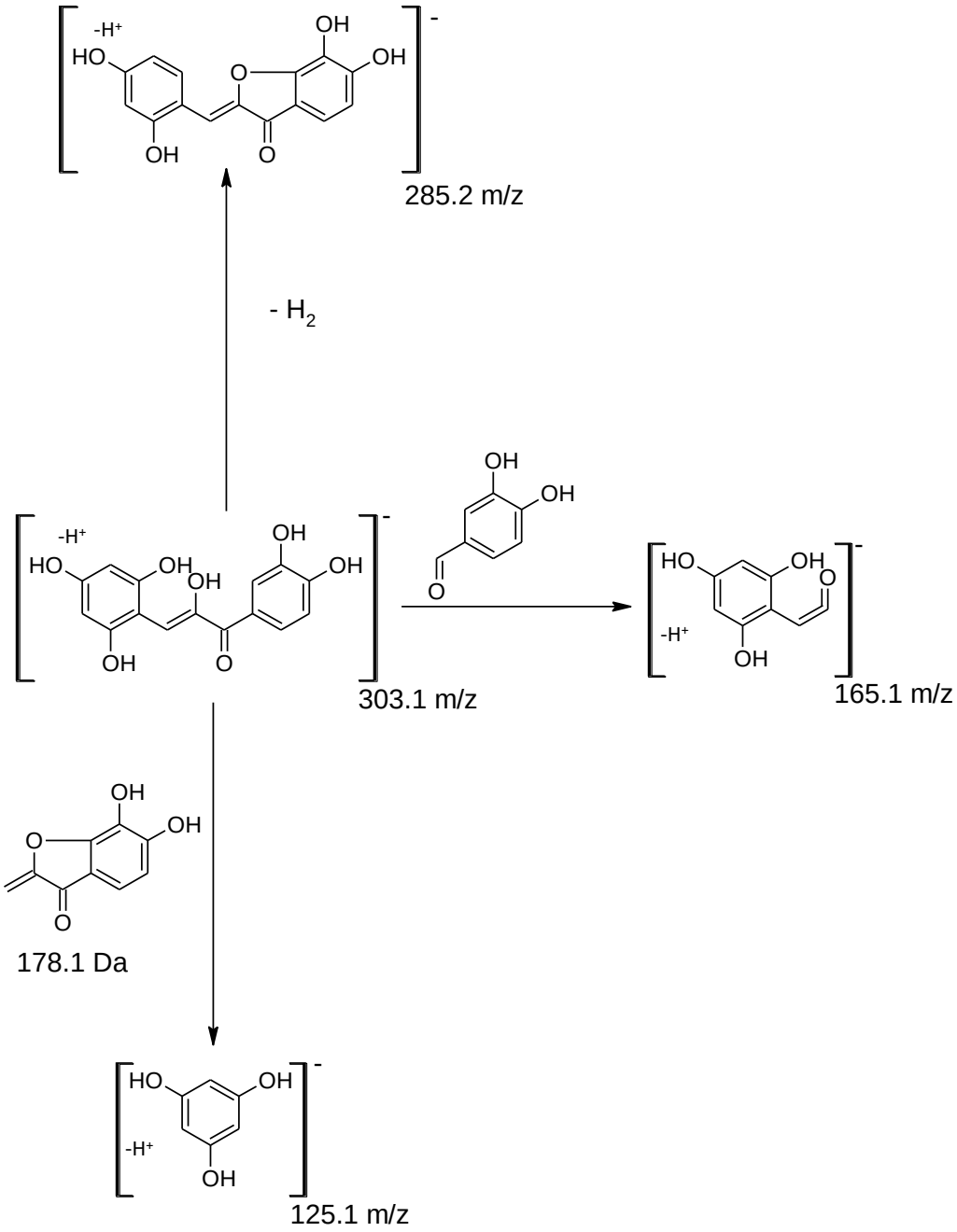

Figure 3.40: The rationalization of ion products produced by hemiketal and chalcone in MS/MS (negative mode). Product ions generated in MS/MS for a) hemiketal and b) chalcone.

CHAPTER FOUR: DISCUSSION, CONCLUSION AND FUTURE DIRECTIONS

4.1. DISCUSSION

The human health benefits of anthocyanidins have been well recognized (Khoo *et al*, 2017). In addition to their potent antioxidant activity, we hypothesized that the mitochondriotropic ability of anthocyanidins can enhance their bioactivity over other flavonoid subclasses that lack these characteristics. Comparative studies between anthocyanidins and other subclasses of flavonoids are needed to understand the significance of structural characteristics in exerting a bioactivity. Despite their favourable potent bioactivity, anthocyanidins are presumed to degrade rapidly to PCA and PGA. Their lack of stability is supported by degradation studies showing the rapid disappearance of the flavylium ion. Nevertheless, these studies dismiss the possibility of intermediary compounds (such as hemiketal and chalcone) appearance and sustainability.

Consequently, we set forward a novel series of experiments to show that cyanidin is stable for sufficient periods in different media to exert a bioactivity that may surpass that of its metabolites (PCA and PGA) and other flavonoids (quercetin, catechin and C3G) in protecting differentiated H9c2 cells from mitochondrial ROS-mediated cytotoxicity of doxorubicin. Due to its mitochondriotropic characteristics, the hypothesis was that cyanidin would accumulate in the mitochondria and exert a better cytoprotective ability compared to flavonoids from different subclasses.

4.1.1. Cytotoxicity of doxorubicin

Few studies have attempted to investigate in detail the acute effects of doxorubicin on mitochondrial ROS generation that may lead to decreases in cardiomyocyte viability and

mitochondrial function. Such information is essential for understanding the mechanism in which antioxidants protect cardiomyocytes from doxorubicin's insult. Furthermore, most previous studies have used undifferentiated H9c2 cells, which as dividing cells may have a different mechanism of doxorubicin cytotoxicity to the *in vivo* mature differentiated cardiomyocytes (Branco *et al*, 2012; 2015). This difference may lead to inaccuracy in understanding the mechanisms of the *in vivo* cardiotoxicity. Therefore, the time course and mechanisms of doxorubicin-induced cytotoxicity in differentiated cardiomyocytes was evaluated in this work. Using differentiated H9c2 cells, high concentrations of doxorubicin (5 μM) caused a significant reduction in cell survival with short (3 or 6 h) incubation periods when followed by a drug free period (24 h). These results indicate doxorubicin's rapid effect on the cells, which manifests into cell death after an extended drug free period. These observations differ from previous reports that only showed extensive cell death when doxorubicin was incubated with the cardiomyocytes for extended periods (12-48 h) (Branco *et al*, 2012; Choi *et al*, 2007).

Importantly, our *in vitro* treatment pattern involving short exposure to high doxorubicin concentrations mimics the pattern which the heart experiences after intravenous bolus administration of doxorubicin in clinical practice (Adriamycin, 2014; Johansen, 1981; Rahman *et al*, 1986). These results imply that doxorubicin can trigger rapid changes in cardiomyocytes which by initiating the process of apoptosis manifests into cell death after an extended period, as discussed below. These findings are important considering the clinical use of doxorubicin which is administered as intravenous bolus injection peripherally once every 7-10 days. With a distribution half-life of 12 minutes, the heart will experience very high concentrations of doxorubicin for a short period of time before a distribution equilibrium is reached with the rest of the tissues and organs of the body (Speth *et al*, 1988). Furthermore, rapid elimination kinetics

(where half-life is only 1-3 h) indicates a relatively short duration of exposure to doxorubicin, which is cleared from the body within hours of intravenous administration. Our study with short term exposure of differentiated cardiomyoctyes to doxorubicin better reflects the clinical usage of doxorubicin as compared with published studies which use longer exposure periods and undifferentiated cardiomyocyte cell lines.

Interestingly, cell density assessments following 3 or 6 h exposure of differentiated H9c2 cells to 1 µM doxorubicin showed no acute effects on cell survival. This observation possibly rules out the pathological process of cellular necrosis as a mechanism of doxorubicin-induced cell death in this model. The observation that cell death becomes significant at 12 and 24 h incubation with doxorubicin suggested that a more protracted process, such as apoptosis, was the cell death mechanism (Fink and Cookson, 2005).

Since cell viability (MTT) assessments following 3 or 6 h exposure to doxorubicin showed no effects on cell viability, cellular necrosis as a mechanism of doxorubicin-induced cell death is likely ruled out. Instead, a more organised process, such as apoptosis, is the potential cell death mechanism. Apoptosis is less likely to cause leakage of cellular contents and does not involve inflammatory-mediated tissue damage (Fink and Cookson, 2005). Studies involving cytotoxicity evaluations with doxorubicin report that apoptosis is the principal mechanism of cell death (Tan *et al*, 2010) supporting the assertion that doxorubicin-mediated toxicity of cardiomyocytes likely involves apoptotic mechanisms.

The delayed cytotoxicity possibly caused by rapid effects, prompted our determination of accute effects of doxorubicin on mitochondrial and cellular ROS. At 5 µM, doxorubicin caused an elevation in mitochondrial superoxide within 30 min of incubation with the cardiomyocytes **(Figure 3.5)**. These results are similar to those of Mukhopadhyay *et al* (2007), who showed an

increase in mitochondrial superoxide within 60 min by 10-50 µM doxorubicin in undifferentiated H9c2 cells. Differentiated H9c2 cells are reported to have increased cellular respiration rates as compared with undifferentiated H9c2 cells (Patten *et al*, 2017). Hence, an insult to mitochondria (such as that caused by doxorubicin) would have more profound effects in differentiated cells. This explains the lower concentration (5 µM) and shorter incubation period (30 min) required in our assays to observe an increase in mitochondrial ROS generation. In addition, the increase in ROS observed in most *in vitro* studies after prolonged periods of doxorubicin exposure (eg Bernuzzi *et al,* 2009; Branco *et al*, 2012; Berthiaume and Wallace, 2007; Cheung *et al,* 2015; Doroshow and Davies, 1986; Hosseinzadah *et al*, 2011; Kim *et al*, 2006; Mukhopadhyay *et al*, 2009; 2007; Octavia *et al*, 2012; Singal and Iliskovic, 1998; Tan *et al*, 2010; Tsang *et al*, 2003; Wei *et al*, 2015) likely relates to cellular apoptosis. However, such prolonged exposures with doxorubicin suggests apoptosis as a mechanism for ROS increase (Akopova *et al*, 2012, Chen *et al*, 2003) rather than a direct redox-cycling activity in the heart.

In contrast, our observations provide evidence for the occurrence of a redox-cycling effect as a major cause of doxorubicin-induced mitochondrial superoxide in the differentiated H9c2 cells. This rapidly induced effect supports the observation of increased free radical levels caused by redox-cycling in isolated mitochondria (Doroshow and Davies, 1986) as a possible mechanism in intact cardiomyocytes. Such superoxide production is expected to occur rapidly after the interaction of doxorubicin with complex I (Gilliam *et al*, 2012; Keizer *et al* 1990; Monsuez *et al*, 2010). Since cardiomyocytes rely mainly on aerobic respiration (Stanley, 2004), complex I has a crucial role in mitochondrial energy metabolism. Therefore, exposure of cardiomyocytes to doxorubicin will likely result in similar redox-cycling and superoxide production. Therefore, our

results align with these reports and support the redox-cycling activity in cardiomyocytes as a mechanism of cardiotoxicity.

An increase in mitochondrial superoxide and other ROS may damage mitochondrial integrity (decrease the MMP) and energy metabolism (measured by MTT) (Guo *et al*, 2013; Murphy, 2009). However, our results show that the rapid increase in mitochondrial superoxide was not correlated with an early (30 or 60 min) increase in intracellular ROS, change in MMP, or decrease in energy metabolism (**Figures 3.6, 3.7, 3.8**), despite the use of high doxorubicin concentrations (5 or 20 μM). Instead, extended periods (6-12 h) were required to affect these parameters. Upon generation, superoxide molecules can rapidly and spontaneously form other derived oxygen reactive species (Powers and Jackson, 2008), react with highly efficient endogenous antioxidants that suppress their reactivity, or react with mitochondrial macromolecules to cause extensive damage to mitochondrial integrity and function (Forman *et al*, 2009; Halliwell, 1994; Halliwell and Gutteridge, 1990; Molina-Heredia *et al*, 2006; Vranova *et al*, 2008). Therefore, the delayed effects on mitochondrial function is most likely due to the extended periods required for mitochondrial superoxide and other ROS to reach levels that deplete endogenous antioxidants and overwhelm the antioxidant enzymes present, which then allows their reaction with mitochondrial macromolecules.

These overall observations establish that the toxicity of doxorubicin is most likely caused by redox-cycling activity which results in a rapid elevation in free radicals. This is manifested in cell death and changes to mitochondrial function after extended periods. These new insights into the mechanism of doxorubicin-mediated cardiomyocyte toxicity enables investigations into the cytoprotective behaviour of antioxidants such as cyanidin.

4.1.2. Cytoprotective effects of flavonoids in doxorubicin-induced cardiomyocyte cytotoxicity

The establishment of the mechanism of doxorubicin's cytotoxicity (namely elevation in mitochondrial free radical levels) suggested that co-administration with a mitochondrial antioxidant may mitigate the cytotoxicity observed with its exposure. Therefore, we investigated protection by cyanidin compared to other flavonoids.

Similar to observations from Choi *et al* (2007), our results showed that cyanidin was able to protect H9c2 cells when added after the incubation with doxorubicin. We then coducted experiments using differentiated H9c2 cells with the same treatment patterns (**Figure 3.9**). The protection observed when doxorubicin and cyanidin were added consecutively, indicated that cells 'affected' by the insult initially, were subsequently 'rescued' by the antioxidant (cyanidin). Although encouraging, these results are only evident to the protection of cyanidin against apoptosis-mediated cell death. However, since doxorubicin is also suggested to cause a rapid redox-cycle mediated ROS elevation in myocytes (Gilliam *et al*, 2012; Monsuez *et al*, 2010) an approach that inhibits such activity is highly crucial. Our novel treatment pattern of cyanidin together with doxorubicin followed by a free drug period (co-treatment and delayed assessment, Section 4.3.3.) provided strong evidence of the early protective effects against redox-cycle induced ROS. Interestingly, cytoprotection was not observed following co-administration of doxorubicin with cyanidin (with single or multiple additions) for 24 h and assessment of cell survival at the end of the exposure period (**Figure 3.10**). The requirement of a drug free period implies that a "limited" protection maybe insignificant, hence undetectable initially in the first 24 h, but prevents a decrease in cell viability after a further period of time. Thus, cyanidin may have the potential to protect cardiomyocytes from the well known cardiotoxicity of doxorubicin when administered together, suggesting a possible significant role in clinical practice.

The significance of mitochondria-targeted antioxidants, such as synthetic TPP compounds, in some conditions of mitochondrial oxidative stress has been well established (Oyewole and Birch-Machin, 2015). However, although the intracellular antioxidant activity of the different flavonoids has been previously evaluated using different cellular models (Bornsek *et al*, 2012; Galleano *et al*, 2010; Kellett *et al*, 2018), the importance of the mitochondriotropic ability of these compounds has not been addressed. To understand the importance of structural characteristics in determining the antioxidant and mitochondriotrophic activity of anthocyanins, the cytoprotective ability of cyanidin was compared to its glucoside (C3G) and to flavonoids with different charge (specifically quercetin and catechin) (**Figures 3.11, 3.12, 3.13**). Although all flavonoids were capable of increasing cell survival in doxorubicin-exposed cardiomyocytes, cyanidin had overall higher effectiveness. These enhanced effects were most likely due to the favourable structural characteristics of cyanidin which include its more positive charge at physiological pH (compared to quercetin and catechin) and suitable lipophilicity (compared to C3G) (Peng, 2012).

Our results showed that a short (3 h) co-incubation with cyanidin or C3G suppressed the doxorubicin-induced early increase in mitochondrial superoxide (**Figure 3.14**), which mechanistically may help maintain cell viability. The requirement of at least 6 h co-incubation for quercetin and catechin implies that they are not as efficient as mitochondrial antioxidants. However, the equal ability of quercetin and cyanidin to decrease mitochondrial superoxide generation after 30 min exposure to 5 µM doxorubicin shows that they are both effective initially, but the protection by cyanidin is retained to a greater extent over time (**Figure 3.14**). This extended protection suggests that the accumulation of cyanidin in the mitochondria for periods longer than other flavonoids.

In addition, cyanidin and quercetin significantly lowered intracellular ROS generation with extended (12 h) doxorubicin exposure, while only cyanidin decreased intracellular ROS at 6 h (**Figure 3.15**). The earlier effect observed with cyanidin suggests a rapid accumulation in the mitochondria and ability to preempt later ROS generation. Despite the increase in superoxide and ROS generation caused by the extended incubation periods with doxorubicin (12 h), cyanidin and quercetin retained their protective effects. The observation is evidence for their initial antioxidant activity which lasted for extended periods, and may be related to an ability to prevent apoptosis and associated ROS-induced ROS release.

Effects of doxorubicin and flavonoids on mitochondrial integrity and function were evaluated using EM, and measurements of MMP and MTT reduction. EM images 24 h after exposure to doxorubicin for 24 h showed that cyanidin was able to prevent changes in mitochondrial morphology in this treatment pattern (**Figure 3.17**). In measurements of MMP after 12 h doxorubicin exposure however, cyanidin nor other flavonoids tested were able to significantly protect mitochondrial integrity. One explanation for the lack of protective activity despite significantly lowering ROS at this time point, might be a mechanism independent of ROS that affects the MMP when targeted by doxorubicin. For example, doxorubicin can inhibit complex I (Gilliam *et al*, 2013) which affects its ability to move protons to the intermembrane space thus reducing MMP. Nevertheless, protection by flavonoids against decreased reduction of MTT, which involves complex I, argues against this mechanism. Another explanation might be that doxorubicin causes opening of the mitochondrial permeability transition pore (mPTP), which allows the free movement of ions and small molecules across the membrane leading to the dissipation of the MMP (Gorini *et al*, 2018). The opening of the mPTP can be reversible at early stages or if the stress doesn't lead to apoptosis (Ly *et al*, 2003; Crompton, 1999) which could allow

restoration at a later time point. In this way, the protection may become evident at a later time point (i.e. after a drug free period).

Consistent with their effects on mitochondrial superoxide after 6 h exposure to doxorubicin (**Figure 3.7**), cyanidin, quercetin and catechin were able to effectively protect against a decrease in mitochondrial energy metabolism, as measured by the MTT assay, at this time point (**Figure 3.16**). The MTT assay involves reduction of MTT by complex I of mitochondria, which becomes impaired in conditions of oxidative stress and lipid peroxidation (Ahmed Alamoudi *et al,* 2018) through reaction of critical protein thiols with reactive aldehydes and other oxidants (Lin *et al,* 2002). Therefore, the protective ability can be a result of protection of thiol groups in complex I from lipid peroxides and aldehyde adduct formation. The suitable lipophilicity of these flavonoids is highly crucial to protect against lipid peroxidation and inactivation of thiol groups located deep in complex I. This may also explain the enhanced MTT protective effects of catechin over C3G despite their similar effects on mitochondrial superoxide and ROS levels. The hydrophilicity of C3G hinders its spread to lipophilic sites in and around complex I, and hence may limit its protective ability and MTT restoration.

Cyanidin is thought to degrade rapidly to PCA and PGA in physiologically relevant environments (Fang, 2014) and it is commonly believed that the degradation products exert the majority of the bioactivity. Yet addition of PCA or PGA to cardiomyocytes had limited cytoprotective behaviour as compared with cyanidin (**Figure 3.11, 3.12**). Perhaps cyanidin itself (quinoid form or flavylium ion), or intermediates during the degradation to PCA and PGA, such as the hemiketal and/or chalcone were responsible for the cytoprotection observed with cyanidin administration. The assumption that the chalcone can exert an antioxidant activity is justified by previous reports that showed such behaviour (Bukhari *et al,* 2012; Lahsasni *et al,* 2014; Sokmen

and Khan, 2016). Supported by previous experiments which detected cyanidin in the heart 30 min after its injection to rats (Peng, 2012), our results indicated the survival of the parent compound and/or intermediate compound(s) for sufficient periods to exert an activity (**Figures 3.29, 3.35, 3.37** and **3.39**). Our results may also explain the discrepancies in the activities between cyanidin and other flavonoids that also degrade to PCA and PGA-like compounds (Rodriguez-Mateos *et al,* 2014; Stevens and Maier, 2016). That is, compounds other than the mutual degradation products PGA and PCA (Braune *et al,* 2001) most likely cause the discrepancies in their bioactivities (Meyer *et al,* 1998).

In addition to their antioxidant activity, different flavonoids were shown to have an important effect on different cellular pathways. For example, different flavonoids including anthocyanidins were reported to bind with iron metal which may assist in lowing ROS formation (Kaiserova et al, 2007; Afanasev *et al*, 1989). Different flavonoids were also reported to induce endogenous enzymes such as glutathione-S-transferase which may further lower ROS levels (Elliott *et al,* 1992; Filipe *et al,* 2002). Another meahcinsm in which anthocyanins can protect the cells is protecting the DNA from ROS by forming a DNA triplex complex (Sarma and Sharma, 1999; Mas *et al*, 2000).

4.1.3. Accumulation of cyanidin intracellularly

Our results showed that cyanidin gave better cytoprotection, despite having similar antioxidant potency compared to other ortho-dihydroxy flavonoids, such as quercetin and catechin, in many antioxidant assays (Meyer *et al*, 1998, Rice-Evans *et al*, 1996). Therefore, a difference in the intracellular and mitochondrial accumulation of these compounds would explain the enhanced cytoprotective activity of cyanidin despite its reduced stability compared to quercetin, catechin and C3G. This explanation stems from the reported ability of cyanidin to accumulate in heart cells after an IV injection to rats (Peng, 2011). However, no attempt has been made to detect its

intracellular levels in cultured cells. Hence, we set forward experiments to determine the difference in the intracellular accumulation of the flavonoids using differentiated H9c2 cells.

UV-vis data showed no success in detecting intracellular cyanidin in H9c2 cells based on absorption spectrum (200-800 nm) measurment and the use of a high number of pelleted H9c2 cells. Measuring of the entire spectrum was an attempt to detect any change in the structure of cyanidin caused by metabolism or degradation.

Furthermore, the failure of the highly sensitive HPLC and MS analytical tools in the detection of intracellular cyanidin might be caused by the multiple steps involved in the sample preparation despite the use of acidified ACN. In addition, liquid chromatography was used with MS (LC-MS) to eliminate the potential effect of electrolytes on detection capabilities. Despite these efforts, cyanidin was undetectable intracellularly. Fortunately, the fluorescence characteristics of cyanidin enabled its intracellular detection. The wavelengths used matched that of cyanidin when dissolved in ACN (0.1% FA) (**Appendix G**). This further showed that the detected fluorescence from intracellular extracts was most likely due to cyanidin. However, due to the low sensitivity/specificity compared to fluorescence of control cells, the method would need substantial development but could be useful in future studies. Unfortunately, catechin and C3G had no detectable fluorescence characteristics which preempted our attempt to detect them intracellularly.

4.1.4. Effect of cyanidin on HepG2 and K562 cells

To explore whether cyanidin may enhance or mitigate effects of doxorubicin on cancer cells, HepG2 liver and K562 lymphocyte cancer cell lines were employed in our studies since doxorubicin is often used in liver cancer and leukemia (American Cancer Society, 2016; National Cancer Institute, 2018). The potential ability of antioxidants to protect cancer cells from the

treatments by lowering ROS is a growing concern. High ROS in cancer cells encourages further mutations, which lead to enhancement in cellular proliferation, and cell migration (Liou and Storz, 2010). Therefore, a reduction in ROS may halt tumor growth and progression (Olsson *et al,* 2006; Tsuda *et al,* 2013; Wang and Lewers, 2007). Some chemotherapeutics, though, rely on induction of ROS to cause cancer death (Teppo *et al,* 2017). Reduction in ROS levels in conjunction with such drugs might mitigate their cytotoxic effects. Despite its antioxidant activity, cyanidin had no significant effect on the HepG2 or K562 cell survival or doxorubicin-mediated cytotoxicity and alteration in their mitochondrial function (**Figures 3.21, 3.22**). This provides preliminary evidence to a lack of inhibitory effects for this antioxidant when used with doxorubicin.

In agreement with published reports (Mutlu Altundağ *et al*, 2018; Zhou *et al*, 2017), quercetin showed potentiating and cytotoxic effects when treated with or without doxorubicin against both cancer cell lines (**Figures 3.21, 3.22**). However, its effects were previously shown to be due to its ability to inhibit P-glycoprotein (Limtrakul *et al*, 2005) and downregulate Bcl-xl (Wang *et al*, 2012) rather than its antioxidant ability. These mechanisms may explain the superior potency of quercetin over cyanidin in cancer cells. Consequently, in addition to its cardiomyocyte protective ability, quercetin can potentiate doxorubicin's cytotoxicity. Despite its greater cardioprotectant antioxidant activity, cyanidin may not be as ideal as quercetin in cancer therapy.

4.1.5. Degradation of cyanidin and other flavonoids in cell culture media

The lack of stability of some flavonoids in different media has been documented in a few studies (Hu *et al,* 2007). However, these studies did not involve comparisons between the different flavonoid subclasses. To explore if the bioactivities of the different flavonoids were influenced by stability in physiological media, we compared their stability in PBS and cell culture media (with or without 10% FBS). Such information is crucial to allow a better understanding of their relative

bioactivities, and the chemical species that may be involved. Our results showed a faster disappearance of cyanidin than quercetin, catechin and C3G when dissolved in PBS and DMEM (**Figure 3.29, 3.31, 3.32, 3.33**). In agreement with literature (Albuquerque *et al*, 2017; Kay *et al*, 2009), catechin and C3G had relatively enhanced stability in the different media compared to cyanidin and quercetin.

Similar to the literature (Maini *et al,* 2012), our results showed a degradation of quercetin in DMEM (without FBS) with a t½ of 63 min at room temperature (22±1°C), compared to a t½ of ~ 1 h at 25°C observed by Maini *et al* (2012). In contrast to the results of Maini et al (2012), who found a much slower degradation of quercetin in Dulbecco's PBS (t½ of ~ 6 h) compared to DMEM, we found a lower stability in PBS (t½ of 30 min). Apart from a slight difference in pH (7.2, vs 7.4 herein), other explanations for the different results may be less phosphate and the possible presence of calcium and magnesium in Dulbecco's PBS (the paper by Maini *et al,* 2012, didn't identify the product number or formulation used). Since hydrolysis can be catalyzed by phosphate ions (El-Seoud *et al*, 2002), the presence of these ions might have caused the difference in the degradation rate observed between our results.

The effect of FBS addition to DMEM on the degradation of quercetin has not been previously reported. This further emphasises the importance of our finding which showed no effect on the degradation of cyanidin, but a substantial improvement on the stability of quercetin in DMEM with 10% FBS (t½ > 12 h). A possible explanation for the different effect of FBS on the stability of cyanidin and quercetin is the binding ability of each compound to albumin. We anticipate a low binding ability of cyanidin to bovine serum albumin compared to a relatively strong binding constant between the protein and quercetin (binding constant of 2.8×10^{8} M^{-1}) (Wang *et al*, 2006).

In addition, our results highlight the effect of media on the degradation patterns of different flavonoids. Hence, careful attention must be made to the difference in the rate of degradation of different flavonoids when their bioactivity is studied in cell culture experiments.

The superior bioactivity of cyanidin despite its rapid disappearance (compared to other flavonoids tested in this thesis) suggests different explanations. One explanation may be the formation of intermediate(s) (with potent activity) instead of its immediate degradation to the less bioactive PCA and PGA. Alternatively, the flavylium ion may enter the cell before its degradation in the media. Once in the cells, a stabilizing environment might enhance the stability of cyanidin hence allow it to exert a potent activity. One stabilizing factor may be the binding of cyanidin to the different proteins or lipids in the cell (particularly in the mitochondria). In addition, since anthocyanidins are more stable in an acidic environment, the mitochondrion's acidic surrounding environment can possibly enhance the survival and mitochondrial uptake of cyanidin to allow its protective effects against mitochondrial ROS. These factors may offer an explanation to the enhanced bioactivity of cyanidin against a mitochondrial stressor such as doxorubicin compared to the other flavonoids.

The rapid degradation of cyanidin to PCA and PGA is hypothesized to occur through the formation of hemiketal and chalcone intermediate compounds (Kay *et al*, 2009). However, no attempt was reported to detect these intermediate compounds. Although cyanidin rapidly disappears when present in PBS as detected by UV-vis spectrometry, a relatively slow increase in the concentration of PCA and PGA was observed with HPLC. These results provide evidence that cyanidin does not degrade immediately to PCA and PGA. Instead, relatively stable intermediates (hemiketal and chalcone) are formed and survive for a certain time period (~ 6 h). Interestingly, a sharp (within 5 min) increase in PCA was detected after the addition of cyanidin to PBS followed

by a slower increase with time. This biphasic phenomenon was observed within the first 5 min using UV-vis spectrometry. The observed phenomenon is an indication of the rapid degradation of cyanidin to an intermediate compound followed by a relatively slow disappearance of the intermediates. Furthermore, the observation of such behaviors in PBS but not other media (DMEM with or without FBS) is evidence to the variation in the degradation behaviour with different media.

The effect of different media on the degradation of cyanidin has been overlooked in the literature. The stability of cyanidin in cell culture medium with or without 10% FBS was slightly, but not significantly different ($t_{1/2}$ 21.6 min and 18.7 min, respectively). The results surprisingly show that 10% FBS had no significant effect on the stability of cyanidin suggesting a minimal binding or stabilizing ability, at the experimental conditions employed (with 10% FBS as the amount of serum). Differences in the structures of bovine and human albumin (Steinhardt *et al,* 1971) may explain the absence of binding ability with FBS compared to human albumin binding capacity (cyanidin binding constant of 2.72×10^5 M^{-1}) (Cahyana and Gordon, 2013).

Components (mainly salts) present in the media or buffers showed a significant effect on the degradation process of cyanidin. For example, its degradation was very fast in PBS ($t_{1/2}$ of 10.2 min). Hydrolysis is known to be catalyzed by phosphate ions through general acid-base catalysis (El-Seoud *et al,* 2002). We showed that adding cyanidin to HEPES buffer (which has no phosphate ions) improved its stability ($t_{1/2}$ of 32.6 min). Therefore, the enhancement of cyanidin degradation by phosphate (in PBS) suggests hydrolysis as a possible mechanism. In summary, these results highlight the importance of understanding the effects of the medium on the stability of cyanidin in degradation studies. In addition, our results provide evidence that the degradation of cyanidin to PCA and PGA may not be a rapid as previously proposed.

4.1.6. Stability of cyanidin in human serum

The ultimate relevance of these *in vitro* studies is the use of cyanidin in dietetic or pharmaceutical practice. Importantly, its stability in human serum has not been evaluated previously. In addition, knowing that cyanidin degradation depends on the medium, determining its stability in human serum is crucial. Our experimental results in human serum suggest that cyanidin has adequate stability, with a $t_{1/2}$ of 43.2 min, for distribution to tissues and clinical effectiveness. The increased stability of cyanidin in human serum compared to other media tested is most likely due to its binding ability to human serum albumin (Cahyana and Gordon, 2013). Moreover, the high concentration of serum proteins, such as albumin (which is ~ 55% of serum proteins) in the pure human serum used in our experiments, is 10 fold higher that the concentration of serum proteins in DMEM with 10% serum (FBS). The stability of cyanidin in human serum supports our initial *in vivo* observations with cyanidin-injected rats, showing that cyanidin was detectable in tissues 30 min after injection (Peng, 2012). These results provide crucial significance to the medium used when evaluating the degradation of cyanidin. With a $t_{1/2}$ of 43.2 min in human serum, cyanidin stability is probably suitable for usage in clinical practice.

4.1.7. Mechanism of cyanidin degradation and formation of products

The rapid degradation of cyanidin to PCA and PGA was speculated to occur through the formation of intermediate compounds (Kay *et al*, 2009). Although a rapid (within 5 min) disappearance of cyanidin was detected using UV-vis spectrometry when present in PBS (**Figure 3.29**), a 2 h period was required for PGA to increase to levels that equaled the initial concentration of cyanidin (**Figure 3.37**). These results agree with published data that showed a rapid decrease in cyanidin's concentration and a slow increase in PCA and PGA (13 h) (Kay *et al*, 2009). The difference in the time required to reach a plateau in PGA levels is most likely caused by a change

in the experimental protocol. Instead of injecting the cyanidin sample into the HPLC while retaining the neutral pH, Kay's group mixed it with an acidic mobile phase during injection. This may cause a significant change in the equilibrium between the flavylium ion and the intermediate compounds leading to a change in the composition of cyanidin's solution. To avoid this, we used similar mobile phases (water and ACN) but kept the pH at 7.4. Despite these differences, both data suggest that relatively stable intermediates (hemiketal and chalcone) may have formed and survived for a certain period of time. In previous studies, no attempts were reported to detect the hemiketal and chalcone intermediate compounds.

In a novel addition, we also reported a sharp increase in PGA detected soon (within 5 min) after the addition of cyanidin to PBS using HPLC. This result suggests an initial rapid degradation of cyanidin followed by a slow degradation phase. This biphasic phenomenon was also observed in the first withing the first 3 min using UV-vis spectrometry. These observations suggest a rapid degradation of cyanidin to PGA (within minutes) passing though the intermediates (phase one). Once the concentrations of PGA and PCA reach a specific value, a backward reaction can occur between the aldehyde of PGA and the acid of PCA forming a chalcone. This backward reaction then slows down the formation of PGA (phase two). The continuation of the spontaneous degradation of the flavylium ion will result in the formation of chalcone thus shifting the equilibrium towards the formation of PCA and PGA. The process will proceed until the flavylium ion is finished. Furthermore, the observation of such behaviors in PBS is anticipated to be caused by the phosphate ions found in this medium. A lower concentration or lack of phosphate in other media might have slowed the hydrolytic degradation reactions to levels where PCA and PGA are slowly formed at a similar pace to the formation of the chalcone. Hence, we hypothesis that only one phase of degradation was observed in these media.

To observe the presence of the intermediates we followed our HPLC results with MS experiments. The results from HPLC were supported by observations from MS that showed the immediate disappearance of flavylium ion but the detection of peaks at 302 m/z (representing hemiketal and/or chalcone) for at least 6 hours after adding cyanidin to LC/MS grade water (with 10% methanol). The need for the enhanced full scan employment to detect flavylium ion implies its presence at minute concentration or its reduced potential to ionize in the MS instrument. Since the flavylium ion was detected when cyanidin was dissolved in acidified 10% methanol in water (LC-MS grade) (**Appendix F**), the ionization of the compound is not presented as an obstacle for its detection. Unfortunately, the determination of the concentration of hemiketal and/or chalcone was not feasible for the lack of both standard and internal standard compounds. Interestingly, these results were obtained when cyanidin was added to water with 10% methanol to increase its ionization with MS. Despite its rapid degradation in such solvent (**Appendix H**), the hemiketal/chalcone was detectable for at least 6 hrs.

In summary, our experimental results show that cyanidin does not degrade immediately to PGA and PCA once added to a physiological medium. Instead, depending on the medium used, cyanidin (or the intermediary compounds) may survive for extended periods (with a $t_{1/2}$ of about 43.2 min). These results agree with previous reports that showed a rapid degradation of cyanidin but a slow formation of PGA and PCA (Kay *et al*, 2009). Without acknowledging the possible presence of intermediate compounds (hemiketal and chalcone), an assumption was formed indicating that both end products (PCA and PGA) cause the bioactivity. However, our results may provide a stronger scientific explanation to the variation in the bioactivities of cyanidin and the other flavonoids (Meyer *et al*, 1998) despite the similar degradation products (Stevens and Maier, 2016; Rodriguez-Mateos *et at*, 2014; Braune *et al*, 2001). We showed that the rapid decrease in

cyanidin causes the formation of hemiketal and chalcone which are able to survive for an extended period thus explaining the lengthy duration required to increase PCA and PGA to a plateau level.

4.2. CONCLUSIONS

Our results provide evidence of the stability of cyanidin for sufficient periods to exert bioactivity that exceeds that of its degradation products (PCA and PGA). Our results also show doxorubicin's ability to induce a rapid increase in mitochondrial superoxide generation in differentiated H9c2 cardiomyocytes that resulted in delayed cell death. Importantly, doxorubicin-mediated cytotoxicity and mitochondrial damage was mitigated by the four tested flavonoids, cyanidin, quercetin, catechin and C3G. However, results showed that cyanidin had the highest bioactivity compared to the other flavonoids. We speculate that cyanidin's favourable structural characteristics, which can allow a higher accumulation of cyanidin intracellularly and in the mitochondria, contributed to its greater bioactivity relative to the other tested flavonoids. However, our attempts to provide evidence of intracellular accumulation (and in mitochondria) were not successful. Interestingly, cyanidin also had no undesired effects on the cytotoxicity of doxorubicin against the cancer cell lines HepG2 and K562. These results present the widely available cyanidin as a potentially useful cardioprotector against mitochondrial ROS inducers, including doxorubicin.

4.3. CHALLENGES AND LIMITATIONS

Stability is a major challenge when working with flavonoids in general, particularly with anthocyanidins. For this, cyanidin was dissolved initially in DMSO (the most stabilizing solvent) and stored at -80^{o}C in small aliquots until needed. Another issue is the effect of pH on its stability. Careful attention to the pH of media was always taken when dealing with cyanidin. Another limitation to this study is the requirement of high concentrations to observe an effect. Although these concentrations may not be relevant nutritionally, they may be achievable pharmaceutically.

In addition, apoptosis as a mechanism of cell death induced by doxorubicin in cardiomyocytes was not evaluated in this work. Evaluating such mechanism would be significant to propose apoptosis as a mechanism of cell death as opposed to necrosis. However, future investigations can involve such assay.

4.4. FUTURE DIRECTIONS

The presented research highlights the significance of anthocyanidins in protecting the heart from mitochondrial oxidative stress inducers such as doxorubicin despite their presumed high degradation rate. It also identifies new opportunities and future research directions.

Cyanidin was shown to degrade rapidly in different media. However, due to the lack of standard compounds, the detection and isolation of the different intermediates was not accomplished. A possible approach would be the incorporation of a carbon isotope (^{13}C) atom at sites in the structure of cyanidin. MS can then be used to determine the kinetics for the disappearance/formation of the different compounds in the degradation pathway. This method will further highlight the survival ability of cyanidin parent compound and/or its degradation intermediates in different physiological and MS-compatible media. In addition, this method might enable the determination of the stabilizing conditions of each compound in the degradation pathway to allow its purification. One condition that has a significant role in stabilizing the different forms of cyanidin is the acitiy of the vehecle. Therefore, determining the acitiy at which certain a structure is stabilized would then allow an attempt to introduce chemical modifications. This would positively prevent/lower the degradation of the compound of interest.

The incorporation of ^{13}C (Zhang *et al*, 2011) would also facilitate the detection of different compounds (flavylium, hemiketal, chalcone) intracellularly using MS in *in vitro* and *in vivo* studies. Similar to C3G (Ferrars *et al*, 2014; Czank *et al*, 2013), a comprehensive understanding

of the *in vivo* pharmacokinetic behaviour of cyanidin and its metabolites would also be achievable with the introduction of ^{13}C atom. This method may allow the determination of the bioactive components and their accumulation in different tissues and organs of the body. We also propose the detection of a labeled cyanidin and its degradation compounds over time in mitochondria *in vitro*. Thus, the formation of the bioactive compounds during the degradation of cyanidin after its accumulation in the mitochondria may be an advantageous characteristic. Should cyanidin utilize its favourable structural characteristics to accumulate in the mitochondria then degrade to a more bioactive compound (eg. chalcone) (Gacche *et al,* 2008; Lahasasni *et al,* 2014, Belsare *et al,* 2010) such behaviour would present it as a prodrug. Because synthesizing prodrugs is an accepted technique to improve the pharmacokinetics of many medications (Teagarden and Nema, 2007; Granero and Amidon, 2006; Ohwada *et al*, 2002), introducing cyanidin with such behaviour could be advantageous. Once established, the introduction of chemical modifications to the structure of cyanidin may permit the stabilization of these bioactive compounds.

Another approach to improve its stability, cyanidin can be incorporated into a nanoparticle carrier. Such an approach has been shown effective in improving the stability and potency of different compounds when incorporated with heart-targeted nanoparticles (Liu *et al,* 2014a). However, this approach has not been evaluated in the cardioprotective ability of cyanidin. Because of their wide availability, nanoparticles with compatible physicochemical characteristics with cyanidin must be selected. Initially, stabilisation studies must be conducted to ensure the stability of cyanidin-nanoparticle complex. These will also be followed by evaluations to ensure the improvement of the stability of cyanidin. *In vitro* evaluations would then be conducted to determine the effect of such incorporation on the protective ability of cyanidin against the chemotherapeutic toxicity with cancer cells. Following this, the cytoprotective activity of

cyanidin-nanoparticle complex would be evaluated using doxorubicin-mediated cytotoxicity in differentiated H9c2 cells.

Our initial results which showed cyanidin's inability to affect doxorubicin toxicity to HepG2 and K562 cells were encouraging. However, these results should be followed by large-scale experiments involving several chemotherapeutic agents (with different mechanisms of action) and many antioxidant compounds (from different groups). In addition, cell lines from 10-15 different cancer types would be utilized for such a screen. Such comprehensive evaluation would allow a better understanding of antioxidant use in cancer therapy. Should cancer protection behaviour for antioxidants be minimal, the use of these agents would enhance the survival rate by protecting different tissues and organs.

In addition to its ROS-induction in cardiomyocytes, doxorubicin (and possibly other chemotherapeutics) are associated with atrial and ventricular fibrillation, QT-prolongation, ST-elevation and arrhythmias which leads to cardiotoxicity (Guglin *et al*, 2009; Nousiainen *et al*, 1999). Although many mechanisms have been proposed for such changes in the electrocardiogram (ECG), ROS is not yet known to have a role in these changes. However, antioxidants such as dexrazoxane (Junjing *et al*, 2010) and proanthocyanidins (Ammar *et al*, 2013) have shown good potency in preventing acute QT prolongation caused by doxorubicin potentially by scavenging different ROS (Junjing *et al*, 2010; Ducroq *et al*, 2010; Hasinoff *et al*, 2003). Therefore, as antioxidants, flavonoids may prevent doxorubicin-induced ECG changes. Interestingly, *in vitro* assays have been established to predict the effect of compounds on ECG (Hammond and Pollard, 2005). Inhibition of the alpha subunit of a potassium ion channel in the heart cells is one major cause for QT-prolongation and ECG changes (Hammond and Pollard, 2005). Human embryonic kidney 293 (HEK293) cells stably expressing hERG have been used as a model to evaluate the

effect of drugs on this channel that underlies QT and ECG changes (Ducroq *et al*, 2010; Fanoe et al, 2009). Therefore, we propose using such simple *in vitro* system to evaluate the effect of doxorubicin and flavonoids on this channel.

Our *in vitro* bioactivity and degradation experiments with cyanidin would persuade future *in vivo* work. Doxorubicin with or without cyanidin would be administered intravenously to mice followed by recording the ECG to determine the heart protective ability caused by the flavonoid. The the protective ability of cyanidin would then be compared to that of other flavonoids (from different subgroups). These proposed *in vivo* experiments would evaluate the relative protective effects against the toxicity of doxorubicin on the heart functionality.

REFERENCES

Albuquerque BR, Prieto MA, Barros L, Ferreira I. Assessment of the stability of catechin-enriched extracts obtained from *Arbutus unedo* L. fruits: Kinetic mathematical modeling of pH and temperature properties on powder and solution systems. *Ind Crop Prod.* (2017) **99**, 150-162.

Abourashed EA. Bioavailability of plant-derived antioxidants. *Antioxidants*. (2013) **2**, 309-332. Adhikari DV, Francis JA, Schutzki RE, Chandra A, Nair MG. Quantification and characterisation of cyclo-oxygenase and lipid peroxidation inhibitory anthocyanins in fruits of Amelanchier. *Phytochem Anal.* (2005) **16**, 175-180.

Adriamycin, Data Sheet, 2014, accessed on Jan, 04, 2019. https://www.medsafe.govt.nz/profs/Datasheet/a/adriamycininj.pdf

Afanasev IB, Dorozhko AI, Brodskii AV, Kostyuk VA, Potapovitch AI. Chelating and free radical scavenging mechanisms of inhibitory action of rutin and quercetin in lipid peroxidation. *Biochem Pharmacol.* (1989) **38**, 1763-1769.

Agapova LS, Chernyak BV, Domnina LV, Dugina VB, Efimenko AY, Fetisova EK, Ivanova OY, Kalinina NI, Khromova NV, Kopnin BP, Kopnin PB, Korotetskaya MV, Lichinitser MR, Lukashev AL, Pletjushkina OY, Popova EN, Skulachev MV, Shagieva GS, Stepanova EV, Titova EV, Tkachuk VA, Vasiliev JM, Skulachev VP. Mitochondria-targeted plastoquinone derivatives as tools to interrupt execution of the aging program. 3. Inhibitory effect of SkQ1 on tumor development from p53-deficient cells. *Biochemistry (Mosc)*. (2008) **73**,1300-1316.

Ahmed Alamoudi W, Ahmad F, Acharya S, Haque S, Alsamman K, K Herzallah H, T Al-Otaibi S. A simplified colorimetric method for rapid detection of cell viability and toxicity in adherent cell culture systems. *J BUON*. (2018) **23**, 1505-1513.

Ahotupa M, Bussacchini-Griot V, Béréziat JC, Camus AM, Bartsch H. Rapid oxidative stress induced by N-nitrosamines. *Biochem Biophys Res Commun.* (1987) **146**, 1047-1054.

Akopova OV, Kolchinskaya LI, Nosar VI, Bouryi VA, Mankovska IN, Sagach VF. Cytochrome C as an amplifier of ROS release in mitochondria. *Fiziol Zh.* (2012) **58**, 3-12.

Al-Awwadi NA, Araiz C, Bornet A, Delbosc S, Cristol JP, Linck N, Azay J, Teissedre PL, Cros G. Extracts enriched in different polyphenolic families normalize increased cardiac NADPH oxidase expression while having differential effects on insulin resistance, hypertension, and cardiac hypertrophy in high-fructose-fed rats. *J Agric Food Chem.* (2005) **53**, 151-157.

Alexandre J, Batteux F, Nicco C, Chéreau C, Laurent A, Guillevin L, Weill B, Goldwasser F. Accumulation of hydrogen peroxide is an early and crucial step for paclitaxel-induced cancer cell death both in vitro and in vivo. *Int J Cancer.* (2006) **119**, 41-48.

Aliev G, Liu J, Shenk JC, Fischbach K, Pacheco GJ, Chen SG, Obrenovich ME, Ward WF, Richardson AG, Smith MA, Gasimov E, Perry G, Ames BN. Neuronal mitochondrial amelioration by feeding acetyl-L-carnitine and lipoic acid to aged rats. *J Cell Mol Med.* (2009) **13**, 320-333.

Alvarez V, Corao AI, Sánchez-Ferrero E, De Mena L, Alonso-Montes C, Huerta C, Blázquez M, Ribacoba R, Guisasola LM, Salvador C, García-Castro M, Coto E. Mitochondrial transcription factor A (TFAM) gene variation in Parkinson's disease. *Neurosci Lett.* (2008) **432**, 79-82.

American Cancer Society, Chemotherapy for Liver Cancer, accessed Dec, 21st, 2018. https://www.cancer.org/cancer/liver-cancer/treating/chemotherapy.html

Ames BN, Liu J. Delaying the mitochondrial decay of aging with acetylcarnitine. *Ann N Y Acad Sci.* (2004) **1033**, 108-116.

Ammar el-SM, Said SA, El-Damarawy SL, Suddek GM. Cardioprotective effect of grape-seed proanthocyanidins on doxorubicin-induced cardiac toxicity in rats. *Pharm Biol.* (2013) **51**, 339-344.

Andres-Lacueva C, Shukitt-Hale B, Galli RL, Jauregui O, Lamuela-Raventos RM, Joseph JA. Anthocyanins in aged blueberry-fed rats are found centrally and may enhance memory. *Nutr Neurosci.* (2005) **8**, 111-120.

Anisimov VN, Bakeeva LE, Egormin PA, Filenko OF, Isakova EF, Manskikh VN, Mikhelson VM, Panteleeva AA, Pasyukova EG, Pilipenko DI, Piskunova TS, Popovich IG, Roshchina NV, Rybina OY, Saprunova VB, Samoylova TA, Semenchenko AV, Skulachev MV, Spivak IM, Tsybul'ko EA, Tyndyk ML, Vyssokikh MY, Yurova MN, Zabezhinsky MA, Skulachev VP. Mitochondria-targeted plastoquinone derivatives as tools to interrupt execution of the aging program. 5. SkQ1 prolongs lifespan and prevents development of traits of senescence. *Biochemistry (Mosc).* (2008) **73**, 1329-1342.

Antonenko YN, Avetisyan AV, Bakeeva LE, Chernyak BV, Chertkov VA, Domnina LV, Ivanova OY, Izyumov DS, Khailova LS, Klishin SS, Korshunova GA, Lyamzaev KG, Muntyan MS, Nepryakhina OK, Pashkovskaya AA, Pletjushkina OY, Pustovidko AV, Roginsky VA, Rokitskaya TI, Ruuge EK, Saprunova VB, Severina II, Simonyan RA, Skulachev IV, Skulachev MV, Sumbatyan NV, Sviryaeva IV, Tashlitsky VN, Vassiliev JM, Vyssokikh MY, Yaguzhinsky LS, Zamyatnin AA Jr, Skulachev VP. Mitochondria-targeted plastoquinone derivatives as tools to interrupt execution of the aging program. 1. Cationic plastoquinone derivatives: synthesis and in vitro studies. *Biochemistry (Mosc).* (2008) **73**, 1273-1287.Aruoma OI. Methodological considerations for characterizing potential antioxidant actions of bioactive components in plant foods. *Mutat Res.* (2003) **523-524**, 9-20.

Ashour OM, Elberry AA, Alahdal A, Al Mohamadi AM, Nagy AA, Abdel-Naim AB, Abdel-Sattar EA, Mohamadin AM. Protective effect of bilberry (VacciniμM myrtillus) against doxorubicin-induced oxidative cardiotoxicity in rats. *Med Sci Monit*. (2011) **17**, 110-115.

Bakeeva LE, Barskov IV, Egorov MV, Isaev NK, Kapelko VI, Kazachenko AV, Kirpatovsky VI, Kozlovsky SV, Lakomkin VL, Levina SB, Pisarenko OI, Plotnikov EY, Saprunova VB, Serebryakova LI, Skulachev MV, Stelmashook EV, Studneva IM, Tskitishvili OV, Vasilyeva AK, Victorov IV, Zorov DB, Skulachev VP. Mitochondria-targeted plastoquinone derivatives as tools to interrupt execution of the aging program .2. Treatement of some ROS- and age-related diseases (heart arrhythmia, heart infarctions, kidney ischemia and stroke. *Biochem (Mosc).* (2008) **73**, 1288-1299.

Ballinger SW. Mitochondrial dysfunction in cardiovascular disease. *Free Radic Biol Med.* (2005) **38**, 1278-1295.

Bandy B, Bechara EJ. Bioflavonoid rescue of ascorbate at a membrane interface. *J Bioenerg Biomembr.* (2001) **33**, 269-277.

Barbieri E, Sestili P. Reactive oxygen species in skeletal muscle signaling. *J Signal Transduct.* (2012) **2012**, 982794-982811.

Barclay LR, Vinqvist MR. Do spin traps also act as classical chain-breaking antioxidants? A quantitative kinetic study of phenyl tert-butylnitrone (PBN) in solution and in liposomes. *Free Radic Biol Med.* (2000) **28**, 1079-1090.

Baur JA, Pearson KJ, Price NL, Jamieson HA, Lerin C, Kalra A, Prabhu VV, Allard JS, LopezLluch G, Lewis K. Resveratrol improves health and survival of mice on a high-calorie diet. *Nature.* (2006) **444**, 337-342.

Baynes JW, Thorpe SR. Role of oxidative stress in diabetic complications: A new perspective on an old paradigm. *Diabetes.* (1999) **48**, 1-9.

Baynes JW. Role of oxidative stress in development of complications in diabetes. *Diabetes*. (1991) **40**, 405-412.

Bazzano LA, Serdula Beecher GR. Overview of dietary flavonoids: nomenclature, occurrence and intake. *J Nutr*. (2003) **133**, 3248S-3254S.

Beal MF. Mitochondria take center stage in aging and neurodegeneration. *Ann. Neurol.* (2005) **58**, 495-505.

Beecher GR. Overview of dietary flavonoids: nomenclature, occurrence and intake. *J Nutr*. (2003) **133**, 3248-3254.

Belin AC, Bjork BF, Westerlund M, Galter D, Sydow O, Lind C, Pernold K, Rosvall L, Håkansson A, Winblad B, Nissbrandt H, Graff C, Olson L. Association study of two genetic variants in mitochondrial transcription factor A (TFAM) in Alzheimer's and Parkinson's disease. *Neurosci Lett.* (2007) **420**, 257-262.

Belsare DP, Pal SC, Kazi AA, Kankate R. Evaluation of antioxidant activity of chalcones and flavonoids. *Int J ChemTech Res.* (2010) **2**, 1080-1089.

Berlett BS, Stadtman ER. Protein oxidation in aging, disease and oxidative stress. *J Biol Chem.* (1997) **272**, 20313-20316.

Bernuzzi F, Recalcati S, Alberghini A, Cairo G. Reactive oxygen species-independent apoptosis in doxorubicin-treated H9c2 cardiomyocytes: role for heme oxygenase-1 down-modulation. *Chem Biol Interact.* (2009) **177**, 12-20.

Berthiaume, JM. and Wallace, KB. Adriamycin-induced oxidative mitochondrial cardiotoxicity. *Cell Biol. Toxicol.* (2007) **23**, 15-23.

Birben E, Sahiner UM, Sackesen C, Erzurum S, Kalayci O. Oxidative stress and antioxidant defense. *World Allergy Organ J*. (2012) **5**, 9-19.

Borkowski T, Szymusiak H, Gliszczynska-Rwiglo A, Rietjens IM, Tyrakowska B. Radical scavenging capacity of wine anthocyanins is strongly pH-dependent. *J Agric Food Chem.* (2005) **53**, 5526-5534.

Branco AF, Sampaio SF, Moreira AC, Holy J, Wallace KB, Baldeiras I, Oliveira PJ, Sardão VA. Differentiation-dependent doxorubicin toxicity on H9c2 cardiomyoblasts. *Cardiovasc Toxicol.* (2012) **12**, 326-340.

Branco AF, Pereira SP, Gonzalez S, Gusev O, Rizvanov AA, Oliveira PJ. Gene Expression Profiling of H9c2 Myoblast Differentiation towards a Cardiac-Like Phenotype. *PLoS One.* (2015) **10**, e0129303.

Braune A. Gütschow M, Engst W, Blaut M. Degradation of quercetin and luteolin by Eubacterium ramulus. *Appl Environ Microbiol.* (2001) **67**, 5558-5567.

Bub A, Watzl B, Heeb D, Rechkemmer G, Briviba K. Malvidin-3-glucoside bioavailability in humans after ingestion of red wine, dealcoholized red wine and red grape juice. *Eur J Nutr.* (2001) **40**, 113-120.

Bukhari SN, Jasamai M, Jantan I. Synthesis and biological evaluation of chalcone derivatives (mini review). *Mini Rev Med Chem.* (2012) **12**, 1394-1403.

Cadenas E, Davies KJ. Mitochondrial free radical generation, oxidative stress, and aging. *Free Radic Biol Med.* (2000) **29**, 222-230.

Cahyana Y, Gordon MH. Interaction of anthocyanins with human serum albumin: influence of pH and chemical structure on binding. *Food Chem.* (2013) **141**, 2278-2285.

Carvour M, Song C, Kaul S, Anantharam V, Kanthasamy A. Chronic low-dose oxidative stress induces caspase-3-dependent PKCdelta proteolytic activation and apoptosis in a cell culture model of dopaminergic neurodegeneration. *Ann NY Acad Sci.* (2008) **1139**, 197-205.

Cavallini L, Bindoli A, Siliprandi N. Comparative evaluation of antiperoxidative action of silymarin and other flavonoids. *Pharmacol Res Comm.* (1978) **10**, 133-136.

Chacko SM, Nevin KJ, Dhanyakrishnan R, Kumar P. Protective effect of *p*-coumaric acid against doxorubicin induced toxicity in H9c2 cardiomyoblast cell lines. *Toxicol Rep.* (2015) **2**, 1213-1221.

Chang KC, Chung SY, Chong WS, Suh JS, Kim SH, Noh HK, Seong BW, Ko HJ, Chun KW. Possible superoxide radical-induced alteration of vascular reactivity in aortas from streptozotocin-treated rats. *J Pharmacol Exp Ther.* (1993) **266**, 992-1000.

Chatterjee K, Zhang J, Honbo N, Karliner JS. Doxorubicin Cardiomyopathy. *Cardiology*. (2010) **115**, 155–162.

Chebotarev AN. Snigur, DV. Study of the acid-base properties of quercetin in aqueous solutions by color measurements. *J Anal Chem.* (2015) **70**, 55-59.

Chen JY, Hu RY, Chou HC. Quercetin-induced cardioprotection against doxorubicin cytotoxicity. *J Biomed Sci.* (2013) **20**, 95-105.

Chen Q, Chai YC, Mazumder S, Jiang C, Macklis RM, Chisolm GM, Almasan A. The late increase in intracellular free radical oxygen species during apoptosis is associated with cytochrome c release, caspase activation, and mitochondrial dysfunction. *Cell Death Differ.* (2003) **10**, 323-334.

Cheung KG, Cole LK, Xiang B, Chen K, Ma X, Myal Y, Hatch GM, Tong Q, Dolinsky VW. Sirtuin-3 (SIRT3) protein attenuates doxorubicin-induced oxidative stress and improves mitochondrial respiration in H9c2 cardiomyocytes. *J Biol Chem.* (2015) **290**, 10981-10993.

Cho YE, Basu A, Dai A, Heldak M, Makino A. Coronary endothelial dysfunction and mitochondrial reactive oxygen species in type 2 diabetic mice. *Am J Physiol Cell Physiol.* (2013) **305**, 1033-1040.

Choi EH, Chang HJ, Cho JY, Chun HS. Cytoprotective effect of anthocyanins against doxorubicin-induced toxicity in H9c2 cardiomyocytes in relation to their antioxidant activities. *Food Chem Toxicol.* (2007) **45**, 1873-1881.

Choi EH, Park JH, Kim MI, Chun HS. Alleviation of doxorubicin-induced toxicities by anthocyanin-rich bilberry (Vaccinium myrtillus l.) extract in rats and mice. *Biofactors* (2010) **36**, 319-327.

Chularojmontri L, Gerdprasert O, Wattanapitayakul SK. Pummelo protects doxorubicin-induced cardiac cell death by reducing oxidative stress, modifying glutathione transferase expression, and preventing cellular senescence. *Evid Based Complement Alternat Med.* (2013) **2013**, 254835

Chun OK, Kim D, Lee CY. Superoxide radical scavenging activity of the major polyphenols in fresh plums. *J Agric Food Chem.* (2003) **51**, 8067–8072.

Circu ML, Aw TY. Reactive oxygen species, cellular redox systems, and apoptosis. *Free Radic Biol Med*. (2010) **48**, 749-762.

Conti V, Izzo V, Corbi G, Russomanno G, Manzo V, De Lise F, Di Donato A, Filippelli A. Antioxidant supplementation in the treatment of aging-associated diseases. *Front Pharmacol*. (2016) **7**, 24-35.

Covey MV, Murphy MP, Hobbs CE, Smith RA, Oorschot DE. Effect of the mitochondrial antioxidant, Mito Vitamin E, on hypoxic-ischemic striatal injury in neonatal rats: a dose-response and stereological study. *Exp. Neurol.* (2006) **199**, 513–519.

Crozier A, Del Rio D, Clifford MN. Bioavailability of dietary flavonoids and phenolic compounds. *Mol Aspects Med.* (2010) **31**, 446-467.

Czank C, Cassidy A, Zhang Q, Morrison DJ, Preston T, Kroon PA, Botting NP, Kay CD. HμMan metabolism and elimination of the anthocyanin, cyanidin-3-glucoside: a (13)C-tracer study. *Am J Clin Nutr*. (2013) **97**, 995-1003.

Dai J, Gupte A, Gates L, Mumper RJ. A comprehensive study of anthocyanin-containing extracts from selected blackberry cultivars: extraction methods, stability, anticancer properties and mechanisms. *Food Chem Toxicol.* (2009) **47**, 837-847.

Dalle-Donne I, Aldini G, Carini M, Colombo R, Rossi R, Milzani A. Protein carbonylation, cellular dysfunction and disease progression. *J Cell Mol Med.* (2006) **10**, 389-406.

Darvesh AS, Carroll RT, Bishayee A, Geldenhuys WJ, Van der Schyf CJ. Oxidative stress and Alzheimer's disease: dietary polyphenols as potential therapeutic agents. *Expert Rev Neurother.* (2010) **10**, 729-745.

Dauchet L, Dallongeville J. Fruit and vegetables and cardiovascular disease: epidemiological evidence from the non-Western world. *Br J Nutr.* (2008) **99**, 219-220.

Davies KJ, Doroshow JH. Redox cycling of anthracyclines by cardiac mitochondria. I. Anthracycline radical formation by NADH dehydrogenase. *J Biol Chem.* (1986) **261**, 3060-3067.

de Ferrars RM, Czank C, Zhang Q, Botting NP, Kroon PA, Cassidy A, Kay CD. The pharmacokinetics of anthocyanins and their metabolites in hμMans. *Br J Pharmacol*. (2014) **171**, 3268-3282.

de Moura MB, dos Santos LS, Van Houten B. Mitochondrial dysfunction in neurodegenerative diseases and cancer. *Environ Mol Mutagen.* (2010) **51**, 391-405.

Dennery PA. Effects of oxidative stress on embryonic development. *Birth Defects Res C Embryo Today.* (2007) 81, 155-162.

de Oliveira MR, Nabavi SM, Braidy N, Setzer WN, Ahmed T, Nabavi SF. Quercetin and the mitochondria: a mechanistic view. *Biotechnol Adv.* (2016) **34**, 532-549.

de Whalley CV, Rankin SM, Hoult JR, Jessup W, Leake DS. Flavonoids inhibit the oxidative modification of low density lipoproteins by macrophages. *Biochem Pharmacol.* (1990) **39**,1743-1750.Devasagayam TP, Tilak JC, Boloor KK, Sane KS, Ghaskadbi SS, Lele RD. Free radicals and antioxidants in human health: current status and future prospects. *J Assoc Physicians India.* (2004) **52**, 794-804.

Dhalla NS, Elmoselhi AB, Hata T, Makino N. Status of myocardial antioxidants in ischemiareperfusion injury. *Cardiovasc Res.* (2000) **47**, 446-456.

Diamanti J, Mezzetti B, Giampieri F, Alvarez-Suarez JM, Quiles JL, Gonzalez-Alonso A, Ramirez-Tortosa Mdel C, Granados-Principal S, Gonzáles-Paramás AM, Santos-Buelga C, Battino M. Doxorubicin-induced oxidative stress in rats is efficiently counteracted by dietary anthocyanin differently enriched strawberry (Fragaria × ananassa Duch.). *J Agric Food Chem.* (2014) **62**, 3935-3943.

Diaz-Hung ML, Gonzalez Fraguela ME. Oxidative stress in neurological diseases: Cause or effect? *Neurologia*. (2014) **29**, 451-452.

Dong J, Liu, Zhu R. Targeting ROS for cancer therapy. *Chemo Open Access.* (2016) **5**, 1000199-1000208.

Dong Q, Chen L, Lu Q, Sharma S, Li L, Morimoto S, Wang G. Quercetin attenuates doxorubicin cardiotoxicity by modulating Bmi-1 expression. *Br J Pharmacol.* (2014) **171**, 4440-4454.

Doroshow JH, Davies KJ. Redox cycling of anthracyclines by cardiac mitochondria. II. Formation of superoxide anion, hydrogen peroxide, and hydroxyl radical. *J Biol Chem.* (1986) **261**, 3068-3074.

Doroshow JH. Anthracycline antibiotic-stimulated superoxide, hydrogen peroxide, and hydroxyl radical production by NADH dehydrogenase. *Cancer Res*. (1983) **43**, 4543-4551.

Dragicevic N, Smith A, Lin X, Yuan F, Copes N, Delic V, Tan J, Cao C, Shytle RD, Bradshaw, PC. Green tea epigallocatechin-3-gallate (EGCG) and other flavonoids reduce Alzheimer's amyloid-induced mitochondrial dysfunction. *J Alzheimers Dis.* (2011) **26**, 507-521.

Ducroq J, Moha ou Maati H, Guilbot S, Dilly S, Laemmel E, Pons-Himbert C, Faivre JF, Bois P, Stücker O, Le Grand M. Dexrazoxane protects the heart from acute doxorubicin-induced QT prolongation: a key role for I(Ks). *Br J Pharmacol*. (2010) **159**, 93-101.

Eichholzer M, Luthy J, Gutzwiller F, Stahelin HB. The role of folate, antioxidant vitamins and other constituents in fruit and vegetables in the prevention of cardiovascular disease: the epidemiological evidence. *Int J Vitam Nutr Res.* (2001) **71**, 5-17.

Elingold I, Isollabella MP, Casanova MB, Celentano AM, Perez C, Cabrera JL, Diez RA, Dubin M. Mitochondrial toxicity and antioxidant activity of a prenylated flavonoid isolated from Dalea elegans. *Chem Biol Interact.* (2008) **171**, 294-305.

Elliott AJ, Scheiber SA, Thomas C, Pardini RS. Inhibition of glutathione reductase by flavonoids. A structure-activity study. *Biochem Pharmacol.* (1992) **44**, 1603-1608.

El-Seoud OA, Ruasse MF, Rodrigues WA. Kinetics and mechanism of phosphate-catalyzed hydrolysis of benzoate esters: comparison with nucleophilic catalysis by imidazole and o-iodosobenzoate. *J Chem Soc, Perkin Trans 2.* (2002) **2,** 1053-1058.

Escandar GM, Sala LF. Complexing behavior of rutin and quercetin. *Can J Chem.* (1991) **69**, 1994-2001.

Etminan M, Gill SS, Samii A. Intake of vitamin E, vitamin C, and carotenoids and the risk of Parkinson's disease: a meta-analysis. *Lancet Neurol.* (2005) **4**, 362-365.

Fahn S. A pilot trial of high-dose alpha-tocopherol and ascorbate in early Parkinson's disease. *Ann Neurol*. (1992) **32**, 128-132.

Fang J. Bioavailability of anthocyanins. *Drug Metab Rev.* (2014) **46**, 508-520.

Fang YZ, Yang S, Wu G. Free radicals, antioxidants, and nutrition. *Nutrition*. (2002) **18**, 872-879.

Fanoe S, Jensen GB, Sjøgren P, Korsgaard MP, Grunnet M. Oxycodone is associated with dose-dependent QTc prolongation in patients and low-affinity inhibiting of hERG activity in vitro. *Br J Clin Pharmacol.* (2009) **67**, 172-179.Fetisova EK, Avetisyan AV, Izyumov DS, Korotetskaya MV, Chernyak BV, Skulachev VP. Mitochondria-targeted antioxidant SkQR1 selectively protects MDR (Pgp 170)-negative cells against oxidative stress. *FEBS Lett.* (2010) **584**, 562-566.

Filipe P, Morliere P, Patterson LK, Hug GL, Maziere JC, Maziere C, Freitas JP, Fernandes A, Santus R. Mechanisms of flavonoid repair reactions with amino acid radicals in models of biological systems: a pulse radiolysis study in micelles and human serum albumin. *Biochim Biophys Acta.* (2002) **1572**, 150-162.

Fink SL, Cookson BT. Apoptosis, pyroptosis, and necrosis: mechanistic description of dead and dying eukaryotic cells. *Infect Immun*. (2005) **73**, 1907-1916.

Fiorani M, Guidarelli A, Blasa M, Azzolini C, Candiracci M, Piatti E, Cantoni O. Mitochondria accµMulate large amounts of quercetin: prevention of mitochondrial damage and release upon oxidation of the extramitochondrial fraction of the flavonoid. *J Nutr Biochem.* (2010) **21**, 397-404.

Fleschhut J, Kratzer F, Rechkemmer G, Kulling SE. Stability and biotransformation of various dietary anthocyanins in vitro. *Eur J Nutr.* (2006) **45**, 7-18.

Focaccetti C, Bruno A, Magnani E, Bartolini D, Principi E, Dallaglio K, Bucci EO, Finzi G, Sessa F, Noonan DM, Albini A. Effects of 5-fluorouracil on morphology, cell cycle, proliferation, apoptosis, autophagy and ROS production in endothelial cells and cardiomyocytes. *PLoS One.* (2015), **10**, e0115686-0115701.

Forman HJ, Zhang H, Rinna A. Glutathione: overview of its protective roles, measurement, and biosynthesis. *Mol Aspects Med.* (2009) **30**, 1-12.

Popa-Freidovich I. Fundamental aspects of reactive oxygen species, or what's the matter with oxygen? *NY Acad Sci.* (1999) **893**,13-18.

Fridovich I. Superoxide dismutases. *Adv Enzymol Relat Areas Mol Biol.* (1986) **58**, 61-97.

Fuchs-Tarlovsky V. Role of antioxidants in cancer therapy. *Nutrition.* (2013) **29**, 15-21.

Gabbita SP, Lovell MA, Markesbery WR. Increased nuclear DNA oxidation in the brain in Alzheimer's disease. *J Neurochem.* (1998) **71**, 2034-2040.

Gacche RN, Dhole NA, Kamble SG, Bandgar BP. In-vitro evaluation of selected chalcones for antioxidant activity. *J Enzyme Inhib Med Chem.* (2008) **23**, 28-31.

Galleano M, Verstraeten SV, Oteiza PI, Fraga CG. Antioxidant actions of flavonoids: thermodynamic and kinetic analysis. *Arch Biochem Biophys.* (2010) **501**, 23-30.

Gao L, Laude K, Cai H. Mitochondrial pathophysiology, reactive oxygen species, and cardiovascular diseases. *Vet Clin North Am Small Anim Pract.* (2008) **38**, 137-155,

Garcia-Closas R, Gonzalez CA, Agudo A, Riboli E. Intake of specific carotenoids and flavonoids and the risk of gastric cancer in Spain. *Cancer Causes Control*. (1999) **10**, 71-75.

Gaweda-Walerych K, Zekanowski C. The impact of mitochondrial DNA and nuclear genes related to mitochondrial functioning on the risk of Parkinson's disease. *Curr Genomics*. (2013) **14**, 543-559.

Gella A, Durany N. Oxidative stress in Alzheimer disease. *Cell Adh Migr.* (2009) **3**, 88-93.

Gewirtz DA. A critical evaluation of the mechanisms of action proposed for the antitµMor effects of the anthracycline antibiotics adriamycin and daunorubicin. *Biochem Pharmacol*. (1999) **57**, 727-741.

Ghosh A, Langley MR, Harischandra D, Neal ML, Jin H, Anantharam V, Joseph J, Brenza T, Narasimhan B, Kanthasamy A, Kalyanaraman B, Kanthasamy AG. Mitoapocynin treatment protects against neuroinflammation and dopaminergic neurodegeneration in a preclinical animal model of Parkinson's disease. *J Neuroimmune Pharmacol.* (2016) **11**, 259-278.

Ghosh R, Alajbegovic A, Gomes AV. NSAIDs and Cardiovascular Diseases: Role of Reactive Oxygen Species. *Oxid Med Cell Longev.* (2015) **2015**, 536962.

Gilliam LAA, Fisher-Wellman KH, Lin CT, Maples JM, Cathey BL, Neufer PD. The anticancer agent doxorubicin disrupts mitochondrial energy metabolism and redox balance in skeletal muscle. *Free Radic Biol Med.* (2013) **65**, 988-996.

Gorini S, De Angelis A, Berrino L, Malara N, Rosano G, Ferraro E. Chemotherapeutic Drugs and mitochondrial dysfunction: focus on doxorubicin, trastuzumab, and sunitinib. *Oxid Med Cell Longev.* (2018) **18**, 7582730-7582745.

Grabacka MM, Gawin M, Pierzchalska M. Phytochemical modulators of mitochondria: the search for chemopreventive agents and supportive therapeutics. *Pharmaceuticals (Basel).* (2014) **7**, 913-942.

Graham D, Huynh NN, Hamilton CA, Beattie E, Smith RA, Cocheme HM, Murphy MP, Dominiczak AF. Mitochondria-targeted antioxidant MitoQ10 improves endothelial function and attenuates cardiac hypertrophy. *Hypertension*. (2009) **54**, 322-328.

Granero GE, Amidon GL. Stability of valacyclovir: implications for its oral bioavailability. *Int J Pharm.* (2006) **317**, 14-18. Gregersen S, Samocha-Bonet D, Heilbronn LK, Campbell LV. Inflammatory and Oxidative Stress Responses to High-Carbohydrate and High-Fat Meals in Healthy Humans. *J Nutr Metab.* (2012) **2012**, 1-8.

Guglin M, Aljayeh M, Saiyad S, Ali R, Curtis AB. Introducing a new entity: chemotherapy-induced arrhythmia. *Europace*. (2009) **11**, 1579-1586.

Guo C, Sun L, Chen X, Zhang D. Oxidative stress, mitochondrial damage and neurodegenerative diseases. *Neural Regen Res.* (2013) **8**, 2003-2014.

Haenen GR, Bast A. Scavenging of hypochlorous acid by lipoic acid. *Biochem Pharmacol.* (1991) **42**, 2244-2246.

Hagiwara A, Miyashita K, Nakanishi T, Sano M, Tamano S, Kadota T, Koda T, Nakamura M, Imaida K, Ito N, Shirai T. Pronounced inhibition by a natural anthocyanin, purple corn color, of 2-amino-1-methyl-6-phenylimidazo[4,5-b]pyridine (PhIP)-associated colorectal carcinogenesis in male F344 rats pretreated with 1,2-dimethylhydrazine. *Cancer Lett.* (2001) **171**, 17-25.

Hajhashemi V, Vaseghi G, Pourfarzam M, Abdollahi A. Are antioxidants helpful for disease prevention? *Res Pharm Sci.* (2010) **5**, 1-8.

Halliwell B, Gutteridge JM. Role of free radicals and catalytic metal ions in human disease: An overview. *Meth Enzymol.* (1990) **186**, 1-85.

Halliwell B. Free radicals and antioxidants: a personal view. *Nutr Rev.* (1994) **52**, 253-265.

Hammond TG, Pollard CE. Use of in vitro methods to predict QT prolongation. *Toxicol Appl Pharmacol.* (2005) **207**, 446-450.

Han XZ, Gao S, Cheng YN, Sun YZ, Liu W, Tang LL, Ren DM. Protective effect of naringenin-7-O-glucoside against oxidative stress induced by doxorubicin in H9c2 cardiomyocytes. *Biosci Trends.* (2012) **6**, 19-25.

Handy DE, Loscalzo J. Redox regulation of mitochondrial function. *Antioxid Redox Signal.* (2012) **16**, 1323–1367.

Haraguchi H, Mochida Y, Sakai S, Masuda H, Tamura Y, Mizutani K, Tanaka O, Chou W H. Protection against oxidative damage by dihydroflavonols in Engelhardtia chrysolepis. *Biosci Biotechnol Biochem.* (1996) **60**, 945-948.

Harman D. Aging: a theory based on free radical and radiation chemistry. *J Gerontol.* (1956) **2**, 298-300.

Harman, D. The biologic clock: the mitochondria? *J Am Geriatr Soc.* (1972) **20**, 145-147.

Hasinoff BB, Schroeder PE, Patel D. The metabolites of the cardioprotective drug dexrazoxane do not protect myocytes from doxorubicin-induced cytotoxicity. *Mol Pharmacol.* (2003) **64**, 670-678.

Hassanpour FM, Ghule AE, Bodhankar SL, Dikshit M. Cardioprotective effect of whole fruit extract of pomegranate on doxorubicin-induced toxicity in rat. *Pharm Biol.* (2011) **49**, 377-382.

Hassimotto N M, Genovese M I, Lajolo F M. Absorption and metabolism of cyanidin-3-glucoside and cyanidin-3-rutinoside extracted from wild mulberry (Morus nigra L.) in rats. *Nutr Res.* (2008) **28**, 198-207.

Havsteen BH. The biochemistry and medical significance of the flavonoids. *Pharmacol. Ther.* (2002) **96**, 67-202.

Heim KE, Tagliaferro AR, Bobilya DJ. Flavonoid antioxidants: chemistry, metabolism and structure-activity relationships. *J Nutr Biochem.* (2002) **13**, 572-584.

Hertog MG, Feskens EJ, Kromhout D. Antioxidant flavonols and coronary heart disease risk. *Lancet.* (1997) **349**, 699.

Hertog MG, Feskens EJ, Hollman PC, Katan MB, Kromhout D. Dietary antioxidant flavonoids and risk of coronary heart disease: the Zutphen elderly study. *Lancet*. (1993) **342**, 1007-1011.

Hertog MG, Kromhout D, Aravanis C, Blackburn H, Buzina R, Fidanza F, Giampaoli S, Jansen A, Menotti A, Nedeljkovic S. Flavonoid intake and long-term risk of coronary heart disease and cancer in the seven countries study. *Arch Intern Med.* (1995) **155**, 381-386.

Hobbs CE, Oorschot DE. Neonatal rat hypoxia-ischemia: long-term rescue of striatal neurons and motor skills by combined antioxidant-hypothermia treatment. *Brain Pathol.* (2008) **18**, 443-454.

Hodnick WF, Duval DL, Pardini, R. Inhibition of mitochondrial respiration and cyanide-stimulated generation of reactive oxygen species by selected flavonoids. *Biochem Pharmacol*. (1994). **47**, 573-580.

Hollman PCH. Absorption, bioavailability, and metabolism of flavonoids. *Pharm Biol.* (2004) **42**, 74-83.

Hosseini A, Bakhtiari E, Mousavi SH. Protective Effect of *Hibiscus Sabdariffa* on doxorubicin-induced cytotoxicity in H9c2 cardiomyoblast cells. *Iran J Pharm Res.* (2017) **16**, 708-713.

Hosseinzadeh L, Behravan J, Mosaffa F, Bahrami G, Bahrami A, Karimi G. Curcumin potentiates doxorubicin-induced apoptosis in H9c2 cardiac muscle cells through generation of reactive oxygen species. *Food Chem Toxicol*. (2011) **49**, 1102-1109.

Houtkooper RH, Vaz FM. Cardiolipin, the heart of mitochondrial metabolism. *Cell Mol Life Sci.* (2008) **65**, 2493-2506.

Hsu HY, Wen MH. Lipopolysaccharide-mediated reactive oxygen species and signal transduction in the regulation of interleukin-1 gene expression. *J Biol Chem.* (2002) **277**, 22131-22139.

Hu M. Commentary: bioavailability of flavonoids and polyphenols: call to arms. *Mol Pharm*. (2007) **4**, 803-806.

Huang P-G, Kuo W-W, Shen C-Y, Chen Y-F, Lin Y-M, Ho T-J, Padma V-V, Lo J-F, Huang C-Y, Huang C-Y. Anthocyanin attenuates doxorubicin-induced cardiomyotoxicity via estrogen receptor-α/β and stabilizes HSF1 to inhibit the IGF-IIR apoptotic pathway. *Int J Mol Sci.* (2016) **17**, 1588-1604.

Huh SW, Bae SM, Kim YW, Lee JM, Namkoong SE, Lee IP, Kim SH, Kim CK, Ahn WS. Anticancer effects of (-)-epigallocatechin-3-gallate on ovarian carcinoma cell lines. *Gynecol Oncol.* (2004) **94**, 760-768.

Injac R, Strukelj B. Recent advances in protection against doxorubicin-induced toxicity. *Technol Cancer Res Treat.* (2008) **7**, 497-516.

Iyyaswamy A, Rathinasamy S. Effect of chronic exposure to aspartame on oxidative stress in the brain of albino rats. *J Biosci.* (2012) **37**, 679-688.

Jakobs S, Stoldt S, NeµMann D. Light microscopic analysis of mitochondrial heterogeneity in cell populations and within single cells. *Adv Biochem Engin/Biotechnol* (2011) **124**, 1-19.

Jang YP, Zhou J, Nakanishi K, Sparrow JR. Anthocyanins protect against A2E photooxidation and membrane permeabilization in retinal pigment epithelial cells. *Photochem Photobiol*. (2005) **81**, 529-536.

Jauslin ML, Meier T, Smith RA, Murphy MP. Mitochondria-targeted antioxidants protect Friedreich Ataxia fibroblasts from endogenous oxidative stress more effectively than untargeted antioxidants. *FASEB J.* (2003) **17**, 1972-1974.

Jiang J, Briede JJ, Jennen DG, Van Summeren A, Saritas-Brauers K, Schaart G, Kleinjans JC, de Kok TM. Increased mitochondrial ROS formation by acetaminophen in human hepatic cells is associated with gene expression changes suggesting disruption of the mitochondrial electron transport chain. *Toxicol Lett*. (2015) **234**, 139-150.

Jin H, Kanthasamy A, Ghosh A, Anantharam V, Kalyanaraman B, Kanthasamy AG. Mitochondria-targeted antioxidants for treatment of Parkinson's disease: Preclinical and clinical outcomes. *Biochim Biophys Acta Mol Basis Dis.* (2014) **1842**, 1282-1294.

Johansen PB. Doxorubicin pharmacokinetics after intravenous and intraperitoneal administration in the nude mouse. *Cancer Chemother Pharmacol.* (1981) **5**, 267-270.

Jovanovic SV, Steenken S, Tosic M, Marjanovic B, Simic MG. Flavonoids as antioxidants. *J Am Chem Soc.* (1994) **116**, 4846-4851.

Junjing Z, Yan Z, Baolu Z. Scavenging effects of dexrazoxane on free radicals. *J Clin Biochem Nutr*. (2010) **47**, 238-245.

Kahkonen MP, Heinonen M. Antioxidant activity of anthocyanins and their aglycons. *J Agric Food Chem*. (2003) **51**, 628-633.

Kaiserova H, Simůnek T, van der Vijgh WJ, Bast A, Kvasnicková E. Flavonoids as protectors against doxorubicin cardiotoxicity: role of iron chelation, antioxidant activity and inhibition of carbonyl reductase. *Biochim Biophys Acta.* (2007) **1772**, 1065-1074.

Kalt W, Blumberg JB, McDonald J E, Vinqvist-Tymchuk MR, Fillmore SA, Graf BA, O'Leary, JM, Milbury PE. Identification of anthocyanins in the liver, eye, and brain of blueberry-fed pigs. *J Agric Food Chem.* (2008) **56**, 705-712.

Kay CD, Kroon PA, Cassidy A. The bioactivity of dietary anthocyanins is likely to be mediated by their degradation products. *Mol Nutr Food Res.* (2009) **53** 92-101.

Keizer HG, Pinedo HM, Schuurhuis GJ, Joenje H. Doxorubicin (adriamycin): a critical review of free radical-dependent mechanisms of cytotoxicity. *Pharmacol Ther.* (1990) **47**, 219-231.

Keller JN, Pang Z, Geddes JW, Begley JG, Germeyer A, Waeg G, et al. Impairment of glucose and glutamate transport and induction of mitochondrial oxidative stress and dysfunction in synaptosomes by amyloid beta-peptide—role of the lipid peroxidation product hydroxynonenal. *J Neurochem.* (1997) **69**, 273-284

Kellett ME, Greenspan P, Pegg RB. Modification of the cellular antioxidant activity (CAA) assay to study phenolic antioxidants in a Caco-2 cell line. *Food Chem.* (2018) **244**, 359-363.

Kelsey, N., Hulick, W., Winter, A., Ross, E., and Linseman, D. Neuroprotective effects of anthocyanins on apoptosis induced by mitochondrial oxidative stress. *Nutr Neurosci*. (2011) **14**, 249-259.

Kern M, Fridrich D, Reichert J, Skrbek S, Nussher A, Hofem S, Vatter S, Pahlke G, Rüfer C, Marko D. Limited stability in cell culture mediμM medium and hydrogen peroxide formation affect the growth inhibitory properties of delphinidin and its degradation product gallic acid. *Mol Nutr Food Res*. (2007) **51**, 1163-1172.

Khanduja KL, Bhardwaj A, Kaushik G. Resveratrol inhibits N-nitrosodiethylamine-induced ornithine decarboxylase and cyclooxygenase in mice. *J Nutr Sci Vitaminol.* (Tokyo) (2004) *50,* 61-65.

Khoo HE, Azlan A, Tang ST, Lim SM. Anthocyanidins and anthocyanins: colored pigments as food, pharmaceutical ingredients, and the potential health benefits. *Food Nutr Res*. (2017) **61**, 1361779-1361799.

Kim SY, Kim SJ, Kim BJ, Rah SY, Chung SM, Im MJ, Kim UH. Doxorubicin-induced reactive oxygen species generation and intracellular Ca2+ increase are reciprocally modulated in rat cardiomyocytes. *Exp Mol Med.* (2006) **38**, 535-545.

Kimes B, Brandt B. Properties of a clonal muscle cell line from rat heart. *Exp Cell Res.* (1976) **98**, 367-381.

Kirkinezos IG, Moraes CT. Reactive oxygen species and mitochondrial diseases. *Semin Cell Dev Boil*. (2001) **12**, 449-457.

Kitazawa M, Anantharam V, Kanthasamy AG. Dieldrin-induced oxidative stress and neurochemical changes contribute to apoptopic cell death in dopaminergic cells. *Free Radic Biol Med.* (2001) **31**, 1473-1485.

Kitazawa M, Wagner JR, Kirby ML, Anantharam V, Kanthasamy AG. Oxidative stress and mitochondrial-mediated apoptosis in dopaminergic cells exposed to methylcyclopentadienyl manganese tricarbonyl. *J Pharmacol Exp Ther.* (2002) **302**, 26-35.

Kizhakekuttu TJ, Wang J, Dharmashankar K, Ying R, Gutterman DD, Vita JA, Widlansky ME. Adverse alterations in mitochondrial function contribute to type 2 diabetes mellitus-related endothelial dysfunction in humans. *Arterscler Thromb Vasc Biol.* (2012) **32**, 2531-2539.

Kode A, Rajendrasozhan S, Caito S, Yang SR, Megson IL, Rahman I. Resveratrol induces glutathione synthesis by activation of Nrf2 and protects against cigarette smoke-mediated oxidative stress in human lung epithelial cells. *Am J Physiol Lung Cell Mol Physiol.* (2008) **294**, 478-488.

Kong JM, Chia LS, Goh N K, Chia TF, Brouillard R. Analysis and biological activities of anthocyanins. *Phytochemistry.* (2003). **64**, 923-933.

Kowalczyk E, Kopff A, Fijałkowski P, Kopff M, Niedworok J, Błaszczyk J, Kedziora J, Tyslerowicz P. Effect of anthocyanins on selected biochemical parameters in rats exposed to cadmium. *Acta. Biochim. Pol.* (2003) **50**, 543-548.

Kumar S, Pandey AK. Chemistry and biological activities of flavonoids: an overview. *Scientific World Journal.* (2013) **2013**, 162750-162766.

Kumari S, Badana AK, G MM, G S, Malla R. Reactive oxygen species: a key constituent in cancer survival. *Biomark Insights*. (2018) **13**, 1-9.

Ladiges W, Wanagat J, Preston B, Loeb L, Rabinovitch P. A mitochondrial view of aging, reactive oxygen species and metastatic cancer. *Aging Cell*. (2010) **9**, 462-465.

Lahsasni SA, Al Korbi FH, Aljaber NA. Synthesis, characterization and evaluation of antioxidant activities of some novel chalcones analogues. *Chem Cent J.* (2014) **8**, 32-42.

Lamberti M, Porto S, Marra M, Zappavigna S, Grimaldi A, Feola D, Pesce D, Naviglio S, Spina A, Sannolo N, Caraglia M. 5-Fluorouracil induces apoptosis in rat cardiocytes through intracellular oxidative stress. *J Exp Clin Cancer Res*. (2012) **31**, 60-68.

Lan J, Jiang DH. Desferrioxamine and vitamin E protect against iron and MPTP-induced neurodegeneration in mice. *J Neural Transm.* (1997) **104**, 469-481.

Lazze MC, Pizzala R, Savio M, Stivala LA, Prosperi E, Bianchi L. Anthocyanins protect against DNA damage induced by tert-butyl-hydroperoxide in rat smooth muscle and hepatoma cells. *Mutat Res.* (2003) **535**, 103-115.

Kamiloglu S, Capanoglu E, Grootaert C, Camp JV Anthocyanin absorption and metabolism by human intestinal Caco-2 cells-a review. *Int J Mol Sci.* (2015) **16**, 21555-21574.

Lemanska K, Szymusiak H, Tyrakowska B, Zieliński R, Soffers AE, Rietjens IM. The influence of pH on antioxidant properties and the mechanism of antioxidant action of hydroxyflavones. *Free Radic Biol Med.* (2001) **31**, 869-881.Liberman EA, Topaly VP, Tsofina LM, Jasaitis AA, Skulachev VP. Mechanism of coupling of oxidative phosphorylation and the membrane potential of mitochondria. *Nature*. **222** (1969) 1076-1078.

Lila MA, Burton-Freeman B, Grace M, Kalt W. Unraveling Anthocyanin Bioavailability for Human Health. *Annu Rev Food Sci Technol.* (2016) **7,** 375-393.

Pung YF, Rocic P, Murphy MP, Smith RA, Hafemeister J, Ohanyan V, Guarini G, Yin L, Chilian WM. Resolution of mitochondrial oxidative stress rescues coronary collateral growth in Zucker obese fatty rats. *Arter Thromb Vasc Biol.* (2012) **32**, 325-334.

Lila MA. Anthocyanins and human health: an in vitro investigative approach. *J Biomed Biotechnol. (2004)* **2004**, 306-313.

Lim S, Rashid MA, Jang M, Kim Y, Won H, Lee J, Woo JT, Kim YS, Murphy MP, Ali L, Ha J, Kim SS. Mitochondria-targeted antioxidants protect pancreatic beta-cells against oxidative stress and improve insulin secretion in glucotoxicity and glucolipotoxicity. *Cell Physiol Biochem*. (2011) **28**, 873-886.

Limtrakul P, Khantamat O, Pintha K. Inhibition of P-glycoprotein function and expression by kaempferol and quercetin. *J Chemother.* (2005) **17**, 86-95.

Lin TK, Hughes G, Muratovska A, Blaikie FH, Brookes PS, Darley-Usmar V, Smith RA, Murphy MP. Specific modification of mitochondrial protein thiols in response to oxidative stress: a proteomics approach. *J Biol Chem.* (2002) **277**, 17048-17056.

Liou GY, Storz P. Reactive oxygen species in cancer. *Free Radic Res*. (2010) **44**, 479-496.

Liu M, Li M, Wang G, Liu X, Liu D, Peng H, Wang Q. Heart-targeted nanoscale drug delivery systems. *J Biomed Nanotechnol.* (2014a) **10**, 2038-2062.

Liu Y, Zhang D, Wu Y, Wang D, Wei Y, Wu J, Ji B. Stability and absorption of anthocyanins from blueberries subjected to a simulated digestion process. *Int J Food Sci Nutr.* (2014b) **65**, 440-

Llobet D, Eritja N, Encinas M, Sorolla A, Yeramian A, Schoenenberger JA, Llombart-Cussac A, Marti RM, Matias-Guiu X, Dolcet X. Antioxidants block proteasome inhibitor function in endometrial carcinoma cells. *Anticancer Drugs.* (2008) **19**, 115-24.

Long J, Gao F, Tong L, Cotman CW, Ames BN, Liu J. Mitochondrial decay in the brains of old rats: ameliorating effect of alpha-lipoic acid and acetyl-Lcarnitine. *Neurochem Res*. (2009) **34**, 755-763.

Lovell MA, Markesbery WR. Oxidative DNA damage in mild cognitive impairment and late-stage Alzheimer's disease. *Nucleic Acids Res.* (2007) **35**, 7497-7504.

Lozano I, Van der Werf R, Bietiger W, Seyfritz E, Peronet C, Pinget M, Jeandidier N, Maillard E, Marchioni E, Sigrist S, Dal S. High-fructose and high-fat diet-induced disorders in rats: impact on diabetes risk, hepatic and vascular complications. *Nutr Metab (Lond).* (2016) **13**, 15-28.

Maczurek A, Hager K, Kenklies M, Sharman M, Martins R, Engel J, Carlson DA, Münch G. Lipoic acid as an anti-inflammatory and neuroprotective treatment for Alzheimer's disease. *Adv Drug Deliv Rev.* (2008) **60**, 1463-1470.

Madamanchi NR, Runge MS. Mitochondrial dysfunction in atherosclerosis. *Circ Res.* (2007) **100**, 460-473.

Maini S, Hodgson HL, Krol ES. The UVA and aqueous stability of flavonoids is dependent on B-ring substitution. *J Agric Food Chem.* (2012) **60**, 6966-6976.

Malaguti M, Angeloni C, Hrelia S. Polyphenols in exercise performance and prevention of exercise-induced muscle damage. *Oxid Med Cell Longev.* (2013) **2013**, 1-9.

Mandziuk S, Baj T, Sieniawska E, Dudka J, Gieroba R, Iwan M, Glowniak K. Protective effect of Mutellina purpurea polyphenolic compounds in doxorubicin-induced toxicity in H9c2 cardiomyocytes. *Drug Chem Toxicol.* (2015a) **38**, 1-8.

Mandziuk S, Gieroba R, Korga A, Matysiak W, Jodlowska-Jedrych B, Burdan F, Poleszak E, Kowalczyk M, Grzycka-Kowalczyk L, Korobowicz E, Jozefczyk A, Dudka J. The differential effects of green tea on dose-dependent doxorubicin toxicity. *Food Nutr Res*. (2015b) **59**, 29754-29765.

Marin L, Miguélez EM, Villar CJ, Lombó F. Bioavailability of dietary polyphenols and gut microbiota metabolism: antimicrobial properties. *Biomed Res Int.* (2015) **2015**, 905215-905233.

Mas T, Susperregui J, Berke B, Cheze C, Moreau S, Nuhrich A, Vercauteren J. DNA triplex stabilization property of natural anthocyanins. *Phytochemistry*. (2000) **53**, 679-687.

Matsushima S, Ide T, Yamato M, Matsusaka H, Hattori F, Ikeuchi M, Kubota T, Sunagawa K, Hasegawa Y, Kurihara T, Oikawa S, Kinugawa S, Tsutsui H. Overexpression of mitochondrial peroxiredoxin-3 prevents left ventricular remodeling and failure after myocardial infarction in mice. *Circulation.* (2006) **113**, 1779-1786.

Mattson MP, Chan SL. Neuronal and glial calcium signaling in Alzheimer's disease. *Cell Calcium.* (2003) **34**, 385-397.

May JM. Is ascorbic acid an antioxidant for the plasma membrane? *FASEB J.* (1999) **13**, 995-1006.

Mazza G, Kay CD, Cottrell T, Holub BJ. Absorption of anthocyanins from blueberries and serum antioxidant status in human subjects. *J Agric Food Chem*. (2002) **50**, 7731-7737.

Meyer A S, Heinonen M, Frankel EN. Antioxidant interactions of catechin, cyanidin, caffeic acid, quercetin, and ellagic acid on human LDL oxidation. *Food Chem.* (1998) **61**, 71-75.

Middleton E Jr, Kandaswami C. Effects of flavonoids on immune and inflammatory cell functions. *Biochem Pharmacol.* (1992) **43**, 1167-1179.

Middleton E, Kandaswami C, Theoharides TC. The effects of plant flavonoids on mammalian cells: implications for inflammation, heart disease, and cancer. *Pharmacol. Rev.* (2000) **52**, 673-751.

Milani P, Gagliardi S, Cova E, Cereda C. SOD1 Transcriptional and Posttranscriptional Regulation and Its Potential Implications in ALS. *Neurol Res Int.* (2011) **2011**, 458427-458436

Mink PJ, Scrafford CG, Barraj LM, Harnack L, Hong CP, Nettleton JA, Jacobs DR. Flavonoid intake and cardiovascular disease mortality: a prospective study in postmenopausal women. *Am J Clin Nutr. (*2007) **85**, 895-909.

Minotti G, Menna P, Salvatorelli E, Cairo G, Gianni L. Anthracyclines: molecular advances and pharmacologic developments in antitumor activity and cardiotoxicity. *Pharmacol Rev.* (2004) **56**, 185-229.

Miquel J, Economos AC, Fleming J, Johnson JE, Jr. Mitochondrial role in cell aging. *Exp Gerontol*. (1980) **15**, 575-591

Mitscher LA. Telikepalli natural antimutagenic agents. *Mutat Res.* (1996) **350**, 142-143.

Mojzisova G, Sarissky M, Mirossay L, Martinka P, Mojzis J. Effect of flavonoids on daunorubicin-induced toxicity in H9c2 Cardiomyoblasts. *Phytother Res.* (2009) **23**, 136-139.

Molina-Heredia FP, Houée-Levin C, Berthomieu C, Touati D, Tremey E, Favaudon V, Adam V, Nivière V. Detoxification of superoxide without production of H2O2: antioxidant activity of superoxide reductase complexed with ferrocyanide. *Proc Natl Acad Sci U S A.* (2006) **103**, 14750-14755.

Monsuez JJ, Charniot JC, Vignat N, Artigou JY. Cardiac side-effects of cancer chemotherapy. *Int J Cardiol.* (2010) **144**, 3-15. Mosmann T. Rapid colorimetric assay for cellular growth and survival: application to proliferation and cytotoxicity assays. *J Immunol Methods.* (1983) **65**, 55-63.

Mugesh G, du Mont WW, Sies H. Chemistry of biologically important. Synthetic organoselenium compounds. *Chem Rev.* (2001) **101**, 2125-2179.

Mukhopadhyay P, Rajesh M, Sándor Bátkai S, Kashiwaya Y, György Haskó G, Liaudet L, Szabó C, Pacher P. Role of superoxide, nitric oxide, and peroxynitrite in doxorubicin-induced cell death in vivo and in vitro. *Am J Physiol Heart Circ Physiol.* (2009) **296**, H1466-H1483.

Mukhopadhyay P, Rajesh M, Yoshihiro K, Haskó G, Pachera P. Simple quantitative detection of mitochondrial superoxide production in live cells. *Biochem Biophys Res Commun.* (2007) **358**, 203-208.

Murphy MP Targeting lipophilic cations to mitochondria. *Biochim Biophys Acta*. (2008) **1777**, 1028-1031.

Murphy MP, Smith RA. Targeting antioxidants to mitochondria by conjugation to lipophilic cations. *Annu Rev Pharmacol Toxicol.* (2007) **47**, 629-656.

Murphy MP. How mitochondria produce reactive oxygen species. *Biochem J.* (2009) **417**, 1-13.

Mutlu Altundağ E, Yılmaz AM, Koçtürk S, Taga Y, Yalçın AS. Synergistic Induction of Apoptosis by Quercetin and Curcumin in Chronic Myeloid Leukemia (K562) Cells. *Nutr Cancer*. (2018) **70**, 97-108.

Nasri S. Roghani M. Baluchnejadmojarad T. Rabani T. Balvardi M. Vascular mechanisms of cyanidin-3-glucoside response in streptozotocin-diabetic rats. *Pathophysiology* (2011) **18**, 273-278.

National Cancer Institution, drug approved for leukemia, 2018, accessed on Dec, 21st, 2018. https://www.cancer.gov/about-cancer/treatment/drugs/leukemia

Neroev VV, Archipova MM, Bakeeva LE, Fursova AZh, Grigorian EN, Grishanova AY, Iomdina EN, Ivashchenko ZhN, Katargina LA, Khoroshilova-Maslova IP, Kilina OV, Kolosova NG, Kopenkin EP, Korshunov SS, Kovaleva NA, Novikova YP, Philippov PP, Pilipenko DI, Robustova OV, Saprunova VB, Senin II, Skulachev MV, Sotnikova LF, Stefanova NA, Tikhomirova NK, Tsapenko IV, Shchipanova AI, Zinovkin RA, Skulachev VP. Mitochondria-targeted plastoquinone derivatives as tools to interrupt execution of the aging program. 4. Age-related eye disease. SkQ1 returns vision to blind animals. *Biochemistry (Mosc).* (2008) **73**, 1317-1328.

Neto C. Cranberry and blueberry: evidence for protective effects against cancer and vascular diseases. *Mol Nutr Food Res.* **51**, 652-664.

Nijveldt RJ, van Nood E, van Hoorn DE, Boelens PG, van Norren K, van Leeuwen PA. Flavonoids: a review of probable mechanisms of action and potential applications. *Am J Clin Nutr.* (2001) **74**, 418-425.

Nousiainen T, Vanninen E, Rantala A, Jantunen E, Hartikainen J. QT dispersion and late potentials during doxorubicin therapy for non-Hodgkin's lymphoma. *J Intern Med.* (1999) **245**, 359-364.

Obrenovich ME, Nair NG, Beyaz A, Aliev G, Reddy VP. The role of polyphenolic antioxidants in health, disease, and aging. *Rejuvenation Res*. (2010) **13**, 631-643.

Octavia Y. Tocchetti CG, Gabrielson KL, Janssens S, Crijns HJ, Moens AL. Doxorubicin-induced cardiomyopathy: from molecular mechanisms to therapeutic strategies. *J Mol Cell Cardiol.* (2012) **52**, 1213-1225.

Odunze IN, Klaidman LK, Adams JD., Jr MPTP toxicity in the mouse brain and vitamin E. *Neurosci Lett.* (1990) **108**, 346-349.

Ohwada J, Murasaki C, Yamazaki T, Ichihara S, Umeda I, Shimma N. Synthesis of novel water soluble benzylazolium prodrugs of lipophilic azole antifungals. *Bioorg Med Chem Lett.* (2002) **12**, 2775-2780.

Olive PL, Banáth JP. The comet assay: a method to measure DNA damage in individual cells. Nat Protoc. (2006) **1**, 23-29.

Olsson ME, Gustavsson KE, Andersson S, Nilsson A, Duan RD. Inhibition of cancer cell proliferation in vitro by fruit and berry extracts and correlations with antioxidant levels. *J Agric Food Chem.* (2004) **52**, 7264-7271.

Olsson ME, Andersson CS, Oredsson S, Berglund RH, Gustavsson KE. Antioxidant levels and inhibition of cancer cell proliferation in vitro by extracts from organically and conventionally cultivated strawberries. *J Agric Food Chem*. (2006) **54**, 1248-1255.

Orellana EA, Kasinski AL. Sulforhodamine B (SRB) Assay in cell culture to investigate cell proliferation. *Bio Protoc.* (2016) **6**, e1984-e1993.

Osellame LD, Blacker TS, Duchen MR. Cellular and molecular mechanisms of mitochondrial function. *Best Pract Res Clin Endocrinol Metab.* (2012) **26**, 711-723.

Ott M, Gogvadze V, Orrenius S, Zhivotovsky B. Mitochondria, oxidative stress and cell death. *Apoptosis* (2007) **12**, 913-922.

Owada T, Yamauchi H, Saitoh SI, Miura S, Machii H, Takeishi Y. Resolution of mitochondrial oxidant stress improves aged-cardiovascular performance. *Coron Artery Dis.* (2017) **28**, 33-43.

Oyewole AO, Birch-Machin MA. Mitochondria-targeted antioxidants. *FASEB J.* (2015) **29**, 4766-4771.

Padayatty SJ, Katz A, Wang Y, Eck P, Kwon O, Lee JH, Chen S, Corpe C, Dutta A, Dutta SK, Levine M. Vitamin C as an antioxidant: evaluation of its role in disease prevention. *J Am Coll Nutr.* (2003) **22**, 18-35.

Panday A, Sahoo MK, Osorio D, Batra S. NADPH oxidases: an overview from structure to innate immunity-associated pathologies. *Cellular & Mol Immunol.* (2015) **12**, 5-23.

Paradies G, Paradies V, De Benedictis V, Ruggiero FM, Petrosillo G. Functional role of cardiolipin in mitochondrial bioenergetics. *Biochim Biophys Acta.* (2014) **1837**, 408-417.

Parkinson Study Group. Effects of tocopherol and deprenyl on the progression of disability in early Parkinson's disease. *N Engl J Med*. (1993) **328**, 176-183.

Patten V, Chabaesele I, Sishi B, Van Vuuren D. Cardiomyocyte differentiation: Experience and observations from 2 laboratories. *Journal of the South African heart association*. (2012) **14**, 96-107.

Peng, F. Mitochondrial uptake of anthocyanidins and protection from oxidative stress. (2012). University of Saskachewan.

Pereira SL, Ramalho-Santos J, Branco AF, Sardão VA, Oliveira PJ, Carvalho RA. Metabolic remodeling during H9c2 myoblast differentiation: Relevance for in vitro toxicity studies. *Cardiovasc Toxicol.* (2011) **11**, 180-190.

Peres W, Tunon MJ, Collado PS, Herrmann S, Marroni N, Gonzalez-Gallego J. The flavonoid quercetin ameliorates liver damage in rats with biliary obstruction. *J Hepatol.* (2000) **33**, 742-750.

Pham-Huy LI, He H, Pham-Huy C. Free radicals, antioxidants in disease and health. *Int J Biomed Sci.* (2008) **4**, 89-96.

Pisonero-Vaquero S, González-Gallego J, Sánchez-Campos S, García-Mediavilla MV. Flavonoids and related compounds in non-alcoholic fatty liver disease therapy. *Curr Med Chem.* (2015) **22**, 2991-3012.

Pojer E, Mattivi F, Johnson D, Stockley CS. The case for anthocyanin consumption to promote human health: a review. *Compr Rev Food Sci F.* (2013) **12**, 483-508.

Popa-Wagner A, Mitran S, Sivanesan S, Chang E, Buga AM. ROS and brain diseases: the good, the bad, and the ugly. *Oxid Med Cell Longev.* (2013), **2013**, 1-14.

Powers SK, Jackson MJ. Exercise-induced oxidative stress: cellular mechanisms and impact on muscle force production. *Physiol Rev.* (2008) **88**, 1243-1276.

Prior RL, Lazarus SA, Cao G, Muccitelli H, Hammerstone JF. Identification of procyanidins and anthocyanins in blueberries and cranberries (VacciniμM spp.) using high-performance liquid chromatography/mass spectrometry. *J Agric Food Chem.* (2001) **49**, 1270-1276

Prior RL, Rogers TR, Khanal RC, Wilkes SE, Wu X, Howard LR. Urinary excretion of phenolic acids in rats fed cranberry. *J Agric Food Chem.* (2010) **58**, 3940-3949.

Qanungo S, Das M, Haldar S, Basu A. Epigallocatechin-3-gallate induces mitochondrial membrane depolarization and caspase-dependent apoptosis in pancreatic cancer cells. *Carcinogenesis*. (2005) **26**, 958-967.

Qian P, Yan LJ, Li YQ, Yang HT, Duan HY, Wu JT, Fan XW. Wang SL. Cyanidin ameliorates cisplatin-induced cardiotoxicity via inhibition of ROS-mediated apoptosis. *Exp Ther Med.* (2018) **15**, 1959-1965

Rahman A, Carmichael D, Harris M, Roh JK. Comparative pharmacokinetics of free doxorubicin and doxorubicin entrapped in cardiolipin liposomes. *Cancer Res.* (1986) **46**, 2295-2299.

Ramesova S, Sokolova R, Degano I, Bulickova J, Zabka J, Gal M. On the stability of the bioactive flavonoids quercetin and luteolin under oxygen-free conditions. *Anal Bioanal Chem*. (2012) **402**, 975-982.

Reddy PH. Mitochondrial oxidative damage in aging and Alzheimer's disease: implications for mitochondrially targeted antioxidant therapeutics. *J Biomed Biotechnol.* (2006) **2006**, 31372-31385.

Reichard JF, Dalton TP, Shertzer HG, Puga A. Induction of oxidative stress responses by dioxin and other ligands of the aryl hydrocarbon receptor. *Dose Response*. (2006) **3**, 306-331.

Rein D, Lotito S, Holt RR, Keen CL, Schmitz HH, Fraga CG. Epicatechin in human plasmahuman serum: in vivo determination and effect of chocolate consumption on plasma oxidation status. *J Nutr.* (2000) **130**, 2109-2114.

Rice-Evans CA, Miller NJ, Paganga G. Structure-antioxidant activity relationships of flavonoids and phenolic acids. *Free Radic Biol Med*. (1996) **20**, 933-956.

Robb EL, Winkelmolen L, Visanji N, Brotchie J, Stuart JA. Dietary resveratrol administration increases MnSOD expression and activity in mouse brain. *Biochem Biophys Res Commun.* (2008) **372**, 254-259.

Rodriguez-Mateos A, Vauzour D, Krueger CG, Shanmuganayagam D, Reed J, Calani L, Mena P, Del Rio D, Crozier A. Bioavailability, bioactivity and impact on health of dietary flavonoids and related compounds: an update. *Arch Toxicol.* (2014) **88**, 1803-1853.

Roghani M, Behzadi G. Neuroprotective effect of vitamin E on the early model of Parkinson's disease in rat: behavioral and histochemical evidence. *Brain Res.* (2001) **892**, 211-217.

Ross MF, Kelso GF, Blaikie FH, James AM, Cocheme HM, Filipovska A, Ros TD, Hurd TR, Smith RA, Murphy MP. Lipophilic triphenylphosphonium cations as tools in mitochondrial bioenergetics and free radical biology. *Biochemistry (Mosc).* (2005) **70**, 222-223.

Wells BG, Dipiro JT, Schwinghammer T, Dipiro CV. (2009). Oncological disorders. In: *Pharmacotherapy handbook (7th edition).* McGraw-Hill Professional, Page 679-719.

Sadzuka Y, Sugiyama T, Shimoi K, Kinae N, Hirota S. Protective effect of flavonoids on doxorubicin-induced cardiotoxicity. *Toxicol Lett.* (1997) **92**, 1-7.

Sala A, Recio MD, Giner RM, Manez S, Tournier H, Schinella G, Rios JL. Anti-inflammatory and antioxidant properties of Helichrysum italicum. *J. Pharm. Pharmacol.* (2002) **54**, 365-371.

Sancho RA, Pastore GM. Evaluation of the effects of anthocyanins in type 2 diabetes. *Food Res Int.* (2012) **46**, 378-386.

Sandalio LM, Rodríguez-Serrano M, Romero-Puertas MC, del Río LA. Role of peroxisomes as a source of reactive oxygen species (ROS) signaling molecules. *Subcell. Biochem.* (2013) **69**, 231-255.

Sano M, Ernesto C, Thomas RG, Klauber MR, Schafer K, Grundman M, Woodbury P, Growdon J, Cotman CW, Pfeiffer E, Schneider LS, Thal LJ. A controlled trial of selegiline, alphatocopherol, or both as treatment for Alzheimer's disease. The Alzheimer's disease cooperative study. *N. Engl. J Med.* (1997) **336**, 1216-1222.

Santos AC, Uyemura SA, Lopes JL, Bazon JN, Mingatto FE, Curti C. Effect of naturally occurring flavonoids on lipid peroxidation and membrane permeability transition in mitochondria. *Free Radic Biol Med.* (1998) **24**, 1455-1461.

Sarma AD, Sharma R. Anthocyanin-DNA copigmentation complex: mutual protection against oxidative damage. *Phytochemistry.* (1999) **52**, 1313-1318.

Sasaki R, Nishimura N, Hoshino H, Isa Y, Kadowaki M, Ichi T, Tanaka A, Nishiumi S, Fukuda I, Ashida H, Horio F, Tsuda T. Cyanidin 3-glucoside ameliorates hyperglycemia and insulin sensitivity due to downregulation of retinol binding protein 4 expression in diabetic mice. *Biochem. Pharmacol.* (2007) **74**, 1619-1627.

Scheider WL, Hershey LA, Vena JE, Holmlund T, Marshall JR. Freudenheim, Dietary antioxidants and other dietary factors in the etiology of Parkinson's disease. *Mov. Disord.* (1997) **12**, 190-196.

Schieber M, Chandel NS. ROS function in redox signaling and oxidative stress. *Curr Biol.* (2014) **24**, 453-462.

Seeram NP, Bourquin LD, Nair MG. Degradation products of cyanidin glycosides from tart cherries and their bioactivities. *J Agric Food Chem* (2001) **49**, 4924

Seeram NP, Adams LS, Zhang Y, Lee R, Sand D, Scheuller HS, Heber D. Blackberry, black raspberry, blueberry, cranberry, red raspberry, and strawberry extracts inhibit growth and stimulate apoptosis of human cancer cells in vitro. *J Agric Food Chem.* (2006) **54**, 9329-9339.

Seidl SE, Potashkin JA. The promise of neuroprotective agents in Parkinson's disease. *Front Neurol*. (2011) **2**, 68-87.

Serraino I, Dugo L, Dugo P, Mondello L, Mazzon E, Dugo G, Caputi AP, Cuzzocrea S. Protective effects of cyanidin-3-O-glucoside from blackberry extract against peroxynitrite-induced endothelial dysfunction and vascular failure. *Life Sci.* (2003) **73**, 1097-1114.

Shankar S, Ganapathy S, Hingorani SR, Srivastava RK. EGCG inhibits growth, invasion, angiogenesis and metastasis of pancreatic cancer. *Front Biosci.* (2008) **13**, 440-452.

Shankar S, Suthakar G, Srivastava RK. Epigallocatechin-3-gallate inhibits cell cycle and induces apoptosis in pancreatic cancer. *Front Biosci.* (2007) **12**, 5039-5051.

Sheu SS, Nauduri D, Anders MW. Targeting antioxidants to mitochondria: a new therapeutic direction. *Biochimica Biophysica Acta.* (2006) **1762**, 256-265.

Sies H, Stahl W. Vitamins E and C, beta-carotene, and other carotenoids as antioxidants. *Am J Clin Nutr*. (1995) **62**, 1315-1321.

Simone CB, Simone NL, Simone V, Simone CB. Antioxidants and other nutrients do not interfere with chemotherapy or radiation therapy and can increase kill and increase survival, part 1. *Altern Ther Health Med.* (2007) **13**, 22-28.

Singal PK, Iliskovic N. Doxorubicin-induced cardiomyopathy. *N Engl J Med.* (1998) **339**, 900-905.

Singh K, Bhori M, Kasu YA, Bhat G, Marar T. Antioxidants as precision weapons in war against cancer chemotherapy induced toxicity - Exploring the armoury of obscurity. *Saudi Pharm J*. (2017) **26**, 177-190.

Singh K, Bhori M, Kasu YA, Bhat G, Marar T. Antioxidants as precision weapons in war against cancer chemotherapy induced toxicity - Exploring the armoury of obscurity. *Saudi Pharm J.* (2018) **26**, 177-190.

Skulachev MV, Antonenko YN, Anisimov VN, Chernyak BV, Cherepanov DA, Chistyakov VA, Egorov MV, Kolosova NG, Korshunova GA, Lyamzaev KG, Plotnikov EY, Roginsky VA, Savchenko AY, Severia, Severin FF, Shkurat TP, Tashlitsky VN, Shidlovsky KM, Vyssokikh MY, Zamyatnin AA, Jr, Zorov DB, Skulachev VP. Mitochondrial-targeted plastoquinone derivatives. Effect on senescence and acute age-related pathologies. *Curr Drug targets*. (2011) **12**, 800-826.

Smith RA, Murphy MP. Animal and human studies with the mitochondria-targeted antioxidant MitoQ. *Ann NY Acad Sci.* (2010) **1201**, 96-103.

Smith RA, Murphy MP. Mitochondria-targeted antioxidants as therapies. *Discov. Med.* (2011) **11**, 106-114.

Smith RA, Porteous CM, Gane AM, Murphy MP. Delivery of bioactive molecules to mitochondria in vivo. *Proc Natl Acad Sci U. S. A.* (2003) **100**, 5407-5412.

Smith RA, Porteous CM, Coulter CV, Murphy MP. Selective targeting of an antioxidant to mitochondria. *Eur J Biochem.* (1999) **263**, 709-716.

Sokmen M, Akram Khan M. The antioxidant activity of some curcuminoids and chalcones. *Inflammopharmacology.* (2016) **24**, 81-86.

Speth PA, van Hoesel QG, Haanen C. Clinical pharmacokinetics of doxorubicin. *Clin Pharmacokinet.* (1988) **15**, 15-31.

Stanley WC. Myocardial energy metabolism during ischemia and the mechanisms of metabolic therapies. *J Cardiovasc Pharmacol Ther*. (2004) **9**, S31-45.

Steinbacher P, Eckl P. Impact of oxidative stress on exercising skeletal muscle. *Biomolecules.* (2015) **5**, 356-377.

Stevens JF, Maier CS. The chemistry of gut microbial metabolism of polyphenols. *Phytochemistry Reviews Phytochem Rev.* (2016) **15**, 4250-444.

Sun J, Chu YF, Wu XZ, Liu RH. Antioxidant and antiproliferative activities of common fruits. *J. Agri. Food Chem.* (2002) **50**, 7449-7454.

Szeto HH. Mitochondria-targeted cytoprotective peptides for ischemia-reperfusion injury. *Antioxid Redox Signal.* (2008) **10**, 601-619.

Talavera S, Felgines C, Texier O, Besson C, Gil-Izquierdo A, Lamaison JL., Rmsy C. Anthocyanin metabolism in rats and their distribution to digestive area, kidney, and brain. *J Agric Food Chem.* (2005) **53**, 3902-3908.

Tan X, Wang DB, Lu X, Wei H, Zhu R, Zhu SS, Jiang H, Yang ZJ. Doxorubicin induces apoptosis in H9c2 cardiomyocytes: role of overexpressed eukaryotic translation initiation factor 5A. *Biol Pharm Bull.* (2010) **33**, 1666-1672.

Tangpong J, Miriyala S, Noel T, Sinthupibulyakit C, Jungsuwadee P, St Clair DK. Doxorubicin-induced central nervous system toxicity and protection by xanthone derivative ofgarcinia mangostana. *Neuroscience*. (2011) **175**, 292-299.

Tapiero H, Tew KD, Ba GN, Mathe G. Polyphenols: do they play a role in the prevention of human pathologies? *Biomed. Pharmacother.* (2002) **56**, 200-207.

Teagarden DL, Nema S. (2007). Case study: Parecexib: A prodrug of valdecoxib. In: *Prodrugs.* Springer. Page 1335-1346.

Tenore GC, Manfra M, Stiuso P, Coppola L, Russo M, Ritieni A, Campiglia P. Polyphenolic pattern and in vitro cardioprotective properties of typical red wines from vineyards cultivated in Scafati (Salerno, Italy). *Food Chem.* (2013) **140**, 803-809.

Teppo HR, Soini Y, Karihtala P. Reactive oxygen species-mediated mechanisms of action of targeted cancer therapy. *Oxid Med Cell Longev*. (2017) **2017**, 1485283-1485294.

Terrill JR, Radley-Crabb HG, Iwasaki T, Lemckert FA, Arthur PG, Grounds MD. Oxidative stress and pathology in muscular dystrophies: focus on protein thiol oxidation and dysferlinopathies. *FEBS J.* (2013) **280**, 4149-4164.

Tewey KM, Rowe TC, Yang L, Halligan BD, Liu LF. Adriamycin-induced DNA damage mediated by mammalian DNA topoisomerase II. *Science.* (1984) **226**, 466-468.

Thannickal VJ, Fanburg BL. Reactive oxygen species in cell signaling. *Am J Physiol Lung Cell Mol Physiol.* (2000) **279**, 1005-1028.

Thilakarathna SH, Rupasinghe VHP., Flavonoid bioavailability and attempts for bioavailability enhancement. *Nutrients*. (2013) **5**, 3367-3387.

Thomasset S, Teller N, Cai H, Marko D, Berry DP, Steward, WP, Gescher AJ. Do anthocyanins and anthocyanidins, cancer chemopreventive pigments in the diet, merit development as potential drugs? *Cancer Chemother. Pharmacol.* (2009) **64**, 201-211.

Thorn CF, Oshiro C, Marsh S, Hernandez-Boussard T, McLeod H, Klein TE, Altman RB. Doxorubicin pathways: pharmacodynamics and adverse effects. *Pharmacogenet Genomics* (2011) **21**, 440-446.

Tokarska-Schlattner M, Zaugg M, Zuppinger C, Wallimann T, Schlattner U. New insights into doxorubicin-induced cardiotoxicity: the critical role of cellular energetics. *J Mol Cell Cardiol.* (2006) **41**, 389-405.

Tomita T, Sadakata H, Tamura M, Matsui H. Indomethacin-induced generation of reactive oxygen species leads to epithelial cell injury before the formation of intestinal lesions in mice. *J. Physiol. Pharmacol.* (2014) **65**, 435-440

Trnka J, Elkalaf M, Andel M. Lipophilic triphenylphosphonium cations inhibit mitochondrial electron transport chain and induce mitochondrial proton leak. *PLoS One.* (2015) **10**, 0121837-0121851.

Trumbeckaite S, Bernatoniene J, Majiene D, Jakstas V, Savickas A, Toleikis A. The effect of flavonoids on rat heart mitochondrial function. *Biomed Pharmacother.* (2006) **60**, 245-248.

Tsang WP, Chau SP, Kong SK, Fung KP, Kwok TT. Reactive oxygen species mediate doxorubicin induced p53-independent apoptosis. *Life Sci*. (2003) **73**, 2047-2058.

Tsuda H, Kunitake H, Kawasaki-Takaki R, Nishiyama K, Yamasaki M, Komatsu H, Yukizaki C. Antioxidant activities and anti-cancer cell proliferation properties of Natsuhaze (Vaccinium oldhamii Miq.), Shashanbo (V. bracteatum Thunb.) and blueberry cultivars. *Plants (Basel).* (2013) **2**, 57-71.

Tsuda T, Horio F, Kitoh J, Osawa T. Protective effects of dietary cyanidin 3-O-beta-D-glucoside on liver ischemia-reperfusion injury in rats. *Arch. Biochem. Biophys.* (1999) **368**, 361-366.

Tsuda T, Horio F, Osawa T. The role of anthocyanins as an antioxidant under oxidative stress in rats. *Biofactors.* (2000) **13**, 133-139.

Tsuda T. Dietary anthocyanin-rich plants: biochemical basis and recent progress in health benefits studies. *Mol Nutr Food Res.* (2012) **56**, 159-170.

Tsuda T, Horio F, Uchida K, Aoki H, Osawa T. Dietary cyanidin 3-O-beta-D-glucoside-rich purple corn color prevents obesity and ameliorates hyperglycemia in mice. *J Nutr*. (2003) **133**, 2125-2130.

Tsutsui H, Ide T, Kinugawa S. Mitochondrial oxidative stress, DNA damage, and heart failure. *Antioxid Redox Signal.* (2006) **8**, 1737-1744.

Turrens JF. Mitochondrial formation of reactive oxygen species. *J Physiol.* (2003) **552**, 335-344 van Acker FA, Hulshof JW, Haenen GR, Menge WM, van der Vijgh WJ, Bast A. New synthetic flavonoids as potent protectors against doxorubicin-induced cardiotoxicity. *Free Radic Biol. Med.* (2001) **31**, 31-37.

Vanzo A, Vrhovsek U, Tramer F, Mattivi F, Passamonti S. Exceptionally fast uptake and metabolism of cyanidin 3-glucoside by rat kidneys and liver. *J Nat.Prod.* (2011) **74**, 1049-1054.

Vauzour D, Vafeiadou K, Rodriguez-Mateos A, Rendeiro C, Spencer JPE. The neuroprotective potential of flavonoids: a multiplicity of effects. *Genes Nutr.* (2008) **3**, 115-126.

Vichai V, Kirtikara K. Sulforhodamine B colorimetric assay for cytotoxicity screening. *Nat Protoc.* (2006) **1**, 1112-1116.

Vitaglione P, Donnarumma G, Napolitano A, Galvano F, Gallo A, Scalfi L, Fogliano V. Protocatechuic acid is the major human metabolite of cyanidin-glucosides. *J Nutr.* (2007) **137**, 2043-2048.

Vranova E, Inze D, Van Breusegem F. Signal transduction during oxidative stress. *J Exp Bot.* (2002) **53**, 1227-1236

Wadsworth TL, Bishop JA, Pappu AS, Woltjer RL, Quinn JF. Evaluation of coenzyme Q as an antioxidant strategy for Alzheimer's disease. *J Alzheimers Dis.* (2008) **14**, 225-234.

Wallace TC, Giusti MM (2013). Bioavailability and Bioabsorption of Anthocyanins. In: *Anthocyanins in health and disease. McGhie TK, Stevenson DE. (Eds).* CRC Press, Page 91-94.

Walle T. Absorption and metabolism of flavonoids. *Free Radic Biol Med.* (2004) **36**, 829-837.

Wang G, Zhang J, Liu L, Sharma S, Dong Q. Quercetin potentiates doxorubicin mediated antitumor effects against liver cancer through p53/Bcl-xl. *PLoS One.* (2012) **7**, 51764.

Wang H, Nair MG, Strasburg GM, Chang YC, Booren AM, Gray JI, DeWitt DL. Antioxidant and antiinflammatory activities of anthocyanins and their aglycon, cyanidin, from tart cherries. *J Nat Prod*. (1999) **62**, 294-296.

Wang S, Lewers KS. Antioxidant activities and anticancer cell proliferation properties of wild strawberries. *JASHS*. (2007) **132**, 647-658.

Wang C, Wu QH, Wang Z, Chen DG. Interaction of quercetin and bovine serum albumin. *Guang Pu Xue Yu Guang Pu Fen Xi.* (2006) **26**, 1672-1675.

Wang SQ, Zhu XF, Wang XN, Shen T, Xiang F, Lou HX. Flavonoids from Malus hupehensis and their cardioprotective effects against doxorubicin-induced toxicity in H9c2 cells. *Phytochemistry*. (2013) **87**, 119-125.

Wang W, Quinn PJ. The location and function of vitamin E in membranes (Review). *Molec Membrane Biol.* (2000) **17**, 143-156.

Weber CA, Ernst ME. Antioxidants, supplements, and Parkinson's disease. *Ann Pharmacother.* (2006) **40**, 935-938.

Wei L, Surma M, Gough G, Shi S, Lambert-Cheatham N, Chang J, Shi J. Dissecting the mechanisms of doxorubicin and oxidative stress-induced cytotoxicity: The involvement of actin cytoskeleton and ROCK1. *PLoS One.* (2015) **10**, e0131763-e0131781.

Witte ME, Geurts JJ, de Vries HE, van der Valk P, van Horssen J. Mitochondrial dysfunction: a potential link between neuroinflammation and neurodegeneration? *Mitochondrion.* (2010) **10**, 411-418.

Xiao ZP, Peng ZY, Peng MJ, Yan WB, Ouyang YZ, Zhu HL. Flavonoids health benefits and their molecular mechanism. *Mini Rev Med Chem*. (2011) **11**, 169-177.

Yang CS, Landau JM, Huang MT, Newmark HL. Inhibition of carcinogenesis by dietary polyphenolic compounds. *Annu Rev Nutr*. (2001) **21**, 381-406

Yang GY, Liao J, Kim K, Yurkow EJ, Yang CS. Inhibition of growth and induction of apoptosis in human cancer cell lines by tea polyphenols. *Carcinogenesis*. (1998) **19**, 611-616.

Yang L, Zhao K, Calingasan NY, Luo G, Szeto HH, Beal MF. Mitochondria targeted peptides protect against 1-methyl-4-phenyl-1,2,3,6-tetrahydropyridine neurotoxicity. *Antioxid. Redox Signal*. (2009) **11,** 2095-2104.

Yang P, Yuan C, Wang H, Han F, Liu Y, Wang L, Liu Y. Stability of anthocyanins and their degradation products from Cabernet Sauvignon red wine under gastrointestinal pH and temperature conditions. *Molecules*. (2018) **23**, 354-374.

Yao LH, Jiang YM, Shi J, Tomas-Barberan FA, Datta N, Singanusong R, Chen SS. Flavonoids in food and their health benefits. *Plant Foods Hum Nutr*. (2004) **59**, 113-22.

Yokoyama C, Sueyoshi Y, Ema M, Mori Y, Takaishi K, Hisatomi H. Induction of oxidative stress by anticancer drugs in the presence and absence of cells. *Oncol Lett.* (2017) **14**, 6066-6070.

Young IS, Tate S, Lightbody JH, McMaster D, Trimble ER. The effects of desferrioxamine and ascorbate on oxidative stress in the streptozotocin diabetic rat. *Free Radic Biol Med.* (1995) **18**, 833-840.

Zang QS, Sadek H, Maass DL, Martinez B, Ma L, Kilgore JA, Williams NS, Frantz DE, Wigginton JG, Nwariaku FE, Wolf SE, Minei JP. Specific inhibition of mitochondrial oxidative stress suppresses inflammation and improves cardiac function in a rat pneumonia-related sepsis model. *Am J Physiol Heart Circ Physiol.* (2012) **302**, 1847-1859

Zeeshan HMA, Lee GH, Kim HR, Chae HJ. Endoplasmic reticulum stress and associated ROS. *Int J Mol Sci.* (2016) **17**, 327-347.

Zhang DX, Gutterman DD. Mitochondrial reactive oxygen species-mediated signaling in endothelial cells. *Am J Physiol Heart Circ Physiol.* (2007) **292**, 2023-2031.

Zhang L, Li J, Zong L, Chen X, Chen K, Jiang Z, Nan L, Li X, Li W, Shan T, Ma Q, Ma Z. Reactive oxygen species and targeted therapy for pancreatic cancer. *Oxid Med Cell Longev*. (2016) **2016**, 1616781-1616790.

Zhang P, Yi LH, Meng GY, Zhang HY, Sun HH, Cui LQ. Apelin-13 attenuates cisplatin-induced cardiotoxicity through inhibition of ROS-mediated DNA damage and regulation of MAPKs and AKT pathways. *Free Radic Res.* (2017) **51**, 449-459.

Zhang Q, Botting NP, Kay C. A gram scale synthesis of a multi-13C-labelled anthocyanin, [6,8,10,3',5'-13C5]cyanidin-3-glucoside, for use in oral tracer studies in humans. *Chem Commun (Camb).* (2011) **47**, 10596-10598.

Zhang S, Liu X, Bawa-Khalfe T, Lu LS, Lyu YL, Liu LF, Yeh ET. Identification of the molecular basis of doxorubicin-induced cardiotoxicity. *Nat Med.* (2012) **18**, 1639-1642.

Zhang SM, Hernan MA, Chen H, Spiegelman D, Willett WC, Ascherio A. Intakes of vitamins E and C, carotenoids, vitamin supplements, and PD risk. *Neurology*. (2002) **59**, 1161-1169.

Zhang Y, Ikeno Y, Qi W, Chaudhuri A, Li Y, Bokov A, Thorpe SR, Baynes JW, Epstein C, Richardson A, Van Remmen H. Mice deficient in both Mn superoxide dismutase and glutathione peroxidase-1 have increased oxidative damage and a greater incidence of pathology but no reduction in longevity. *J Gerontol A Biol Sci Med Sci.* (2009a) **64**, 1212-1220.

Zhang YW, Shi J, Li YJ, Wei L. Cardiomyocyte death in doxorubicin-induced cardiotoxicity. *Arch Immunol Ther Exp (Warsz).* (2009b) **57**, 435-445.

Zhao K, Luo G, Zhao GM, Schiller PW, Szeto HH. Transcellular transport of a highly polar 3+ net charge opioid tetrapeptide. *J Pharm Exp Ther.* (2003) **304**, 425-432.

Zhao K, Zhao GM, Wu D, Soong Y, Birk AV, Schiller PW, Szeto HH. Cell-permeable peptide antioxidants targeted to inner mitochondrial membrane inhibit mitochondrial swelling, oxidative cell death, and reperfusion injury. *J Biol Chem.* (2004) **279**, 34682-34690.

Zhao K1, Luo G, Giannelli S, Szeto HH.Mitochondria-targeted peptide prevents mitochondrial depolarization and apoptosis induced by tert-butyl hydroperoxide in neuronal cell lines. *Biochem Pharmacol.* (2005) **70**, 1796-1806.

Zhao JG, Yan QQ, Lu LZ, Zhang YQ. In vivo antioxidant, hypoglycemic, and anti-tumor activities of anthocyanin extracts from purple sweet potato. *Nutr Res Pract*. (2013) **7**, 359-365.

Zheng W, Wang SY. Oxygen radical absorbing capacity of phenolics in blueberries, cranberries, chokeberries, and lingonberries. *J Agric Food Chem.* (2003) **51**, 502-509.

Zhou J, Fang L, Liao J, Li L, Yao W, Xiong Z, Zhou X. Investigation of the anti-cancer effect of quercetin on HepG2 cells in vivo. *PLoS One.* (2017) **12**, e0172838-e0172848.

Zunino S. Type 2 diabetes and glycemic response to grapes or grape products. *J Nutr*. (2009) **139**, 1794-800.

Zuo L, Zhou T, Pannell BK, Ziegler AC, Best TM. Biological and physiological role of reactive oxygen species – the good, the bad and the ugly. *Acta Physiol (Oxf).* (2015) **214**, 329-348.

Appendix

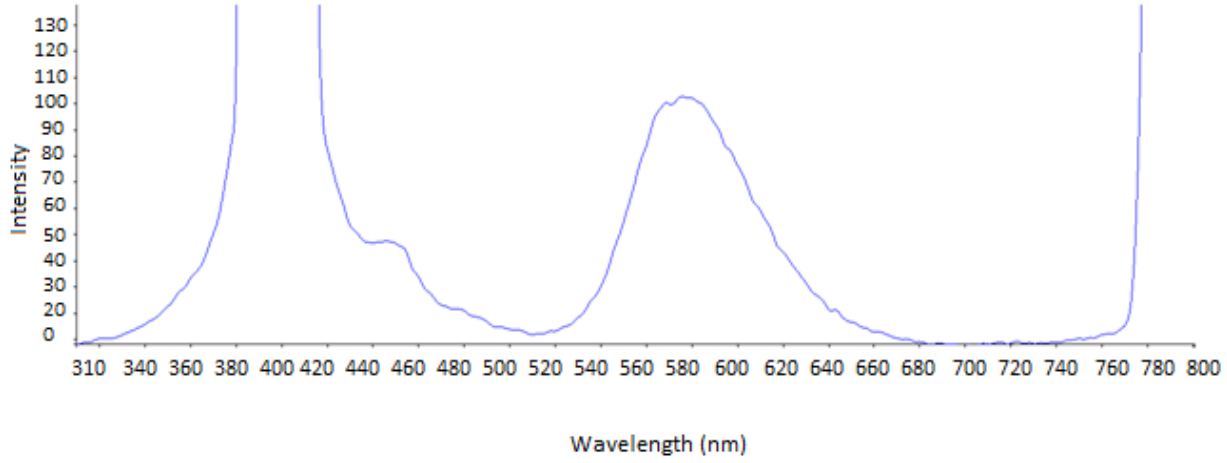

Appendix A: Emission fluorescence scan (Ex: 400 nm) of cyanidin in ACN (0.1% FA). Emission intensity scan was measured after adding cyanidin to ACN (0.1% FA), the excitation at 400 nm.

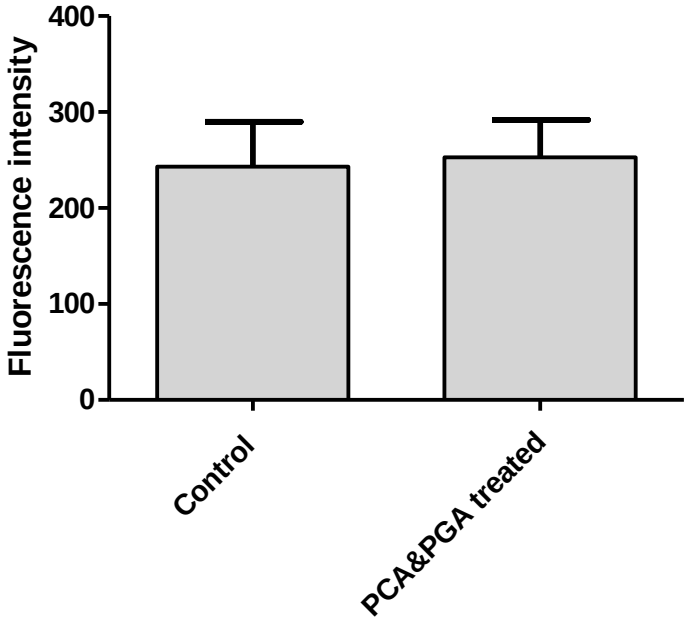

Appendix B: Mean±SD of fluorescence measurement of intracellular protocatechuic acid (PCA) and phloroglucinaldehye (PGA). Fluorescence was not detected in lysates of differentiated H9c2 cells treated with PCA and PGA. Excitation and emission wavelength were 400 and 590 nm, respectively.

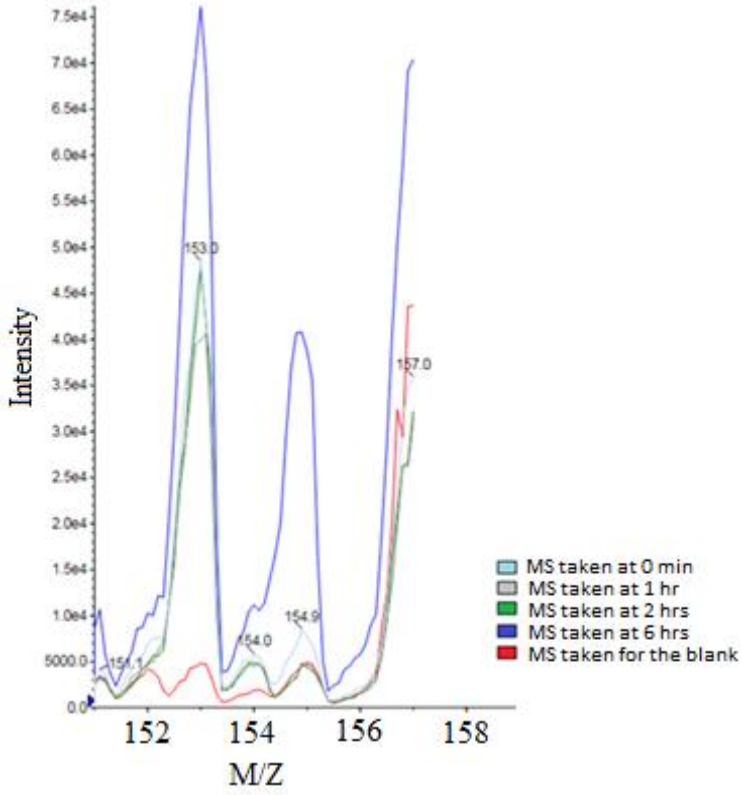

Appendix C: Degradation of cyanidin in %10 methanol water detected by mass spectrometry (MS). Cyanidin (10 µM) was added to 10% methanol/water. Applied biosystems MDS SCIEX 4000 QTRAP MS instrument. Results show the detection of a peak at 153 m/z corresponding to 154 Da which is the molecular weight for both protocatechuic acid (PCA) and phloroglucinaldehye (PGA). Results show that PCA and/or PGA were detected after 0, 1, 2 and 6 h of dissolving cyanidin in 10% methanol/water.

a.

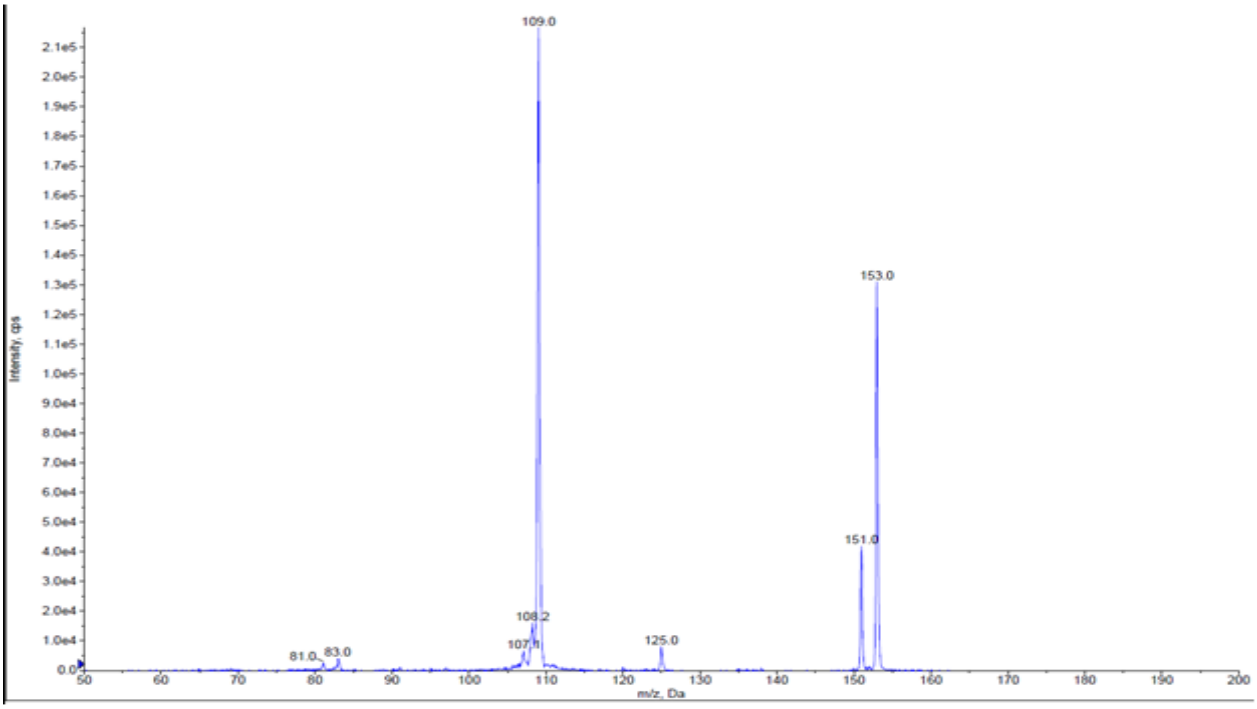

b.

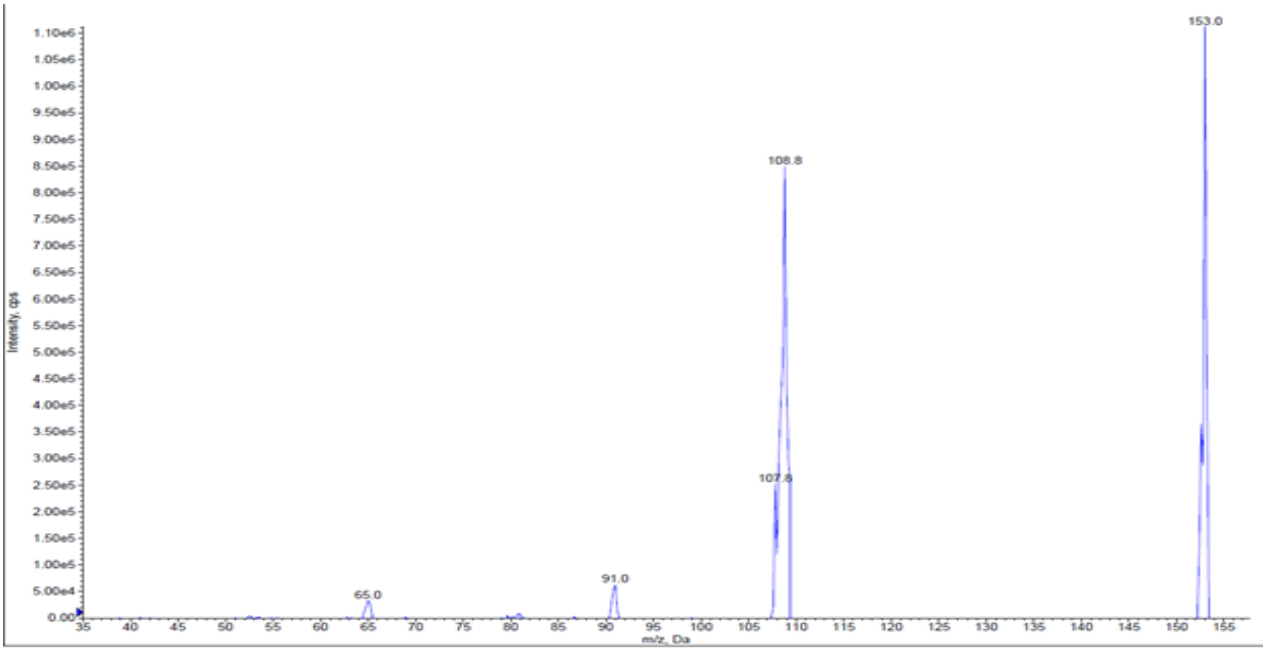

Appendix D.a and D.b: Mass spectrometry (MS) detection of protocatechuic acid (PCA) and phloroglucinaldehye (PGA) in cyanidin (10 µM) dissolved in 10% methanol in water (v/v). Cyanidin was added at 10 µM to %10 methanol in water, and incubated at 25°C followed by the

detection of PCA/PGA by MS. The detected peak (153 Da) was then subjected to MS/MS and the product ions produced were recorded **a)** at time zero and **b)** at 6 h.

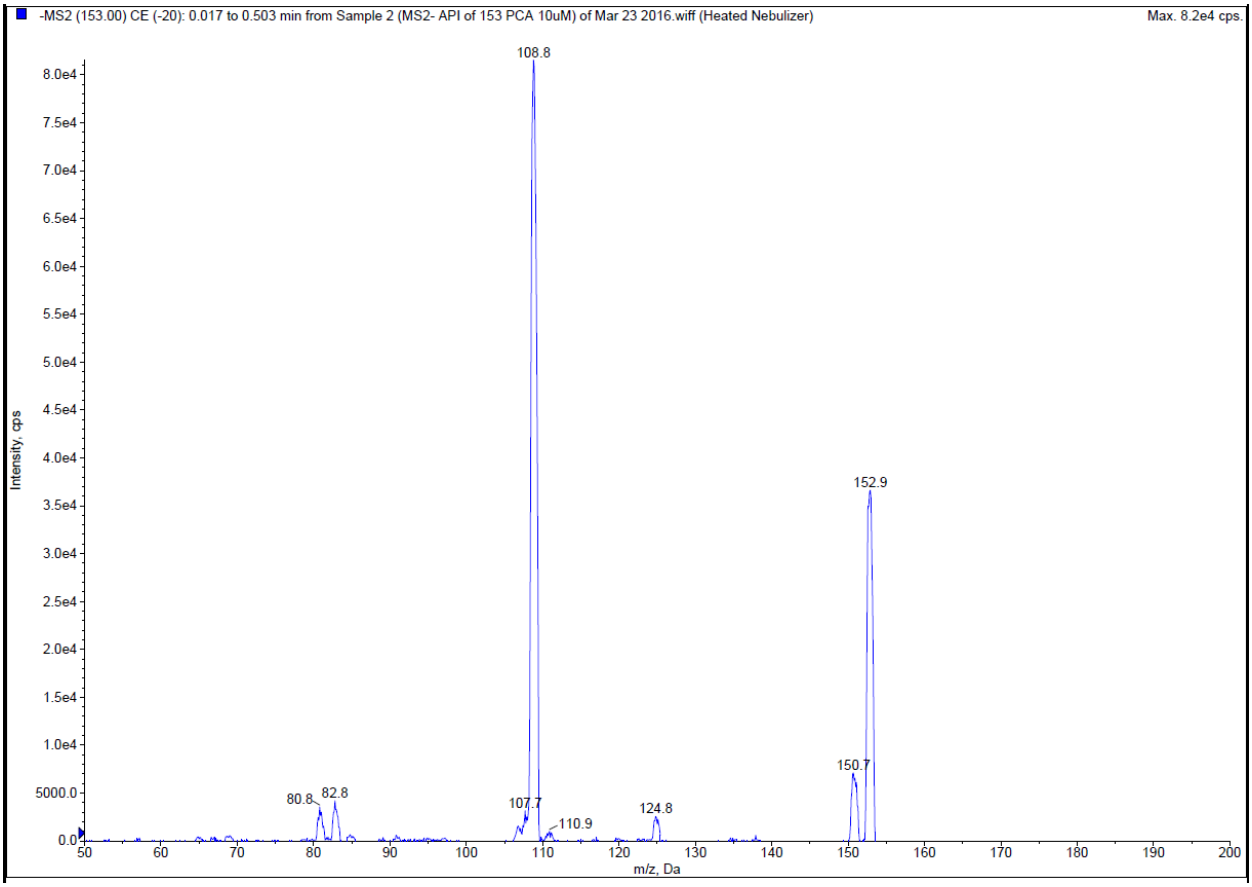

Appendix E: Mass spectrogram for protocatechuic acid (PCA) standard (10 µM) when dissolved in 10% methanol/water (v/v). Results show the daughter ions produced from PCA in MS/MS for peak 153.0 Da. .

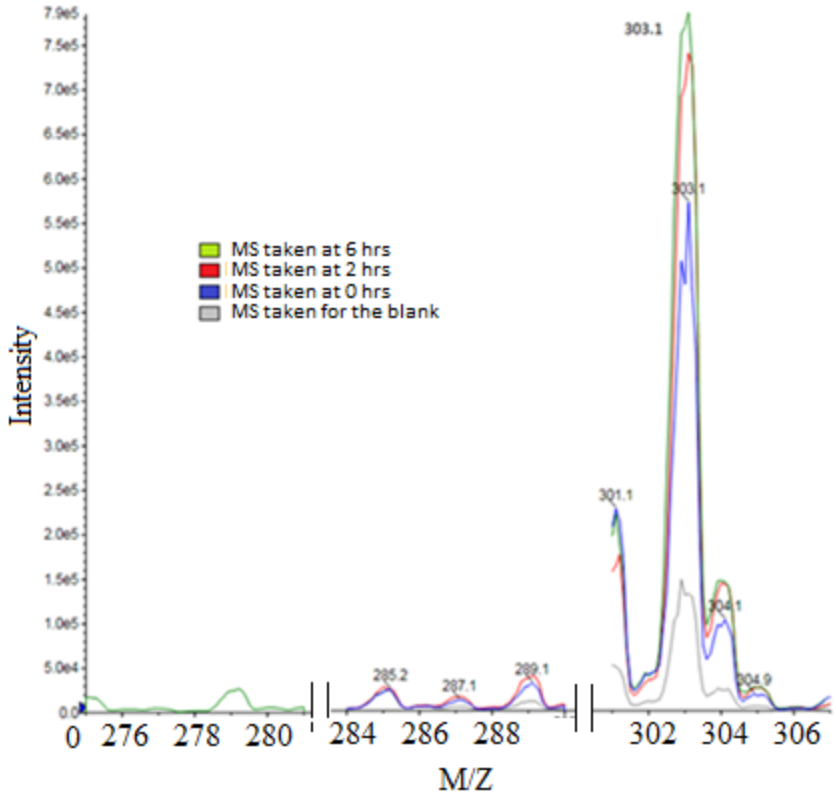

Appendix F: **MS/MS of a solution of cyanidin in 10% methanol in water at different times.** Stock samples were diluted in a mixture of 90% water and 10% methanol (pH 7.3) to a final concentration of 10µM. Immediately after the preparation, samples were directly injected in Applied biosystems MDS SCIEX 4000 Q TRAP mass spectrometer . Results show the detection of a peak at 303 m/z corresponding to 304 Da and a small peak at 285 m/z corresponding to 286 Da at time zero until at least 6 h after adding cyaniding to (pH 7.4). Both chalcone and hemiketal have a molecular weight of 304 Da. A very small peak at 285 corresponds to 286 Da which equals the molecular weight of the quinoidal compound.

a.

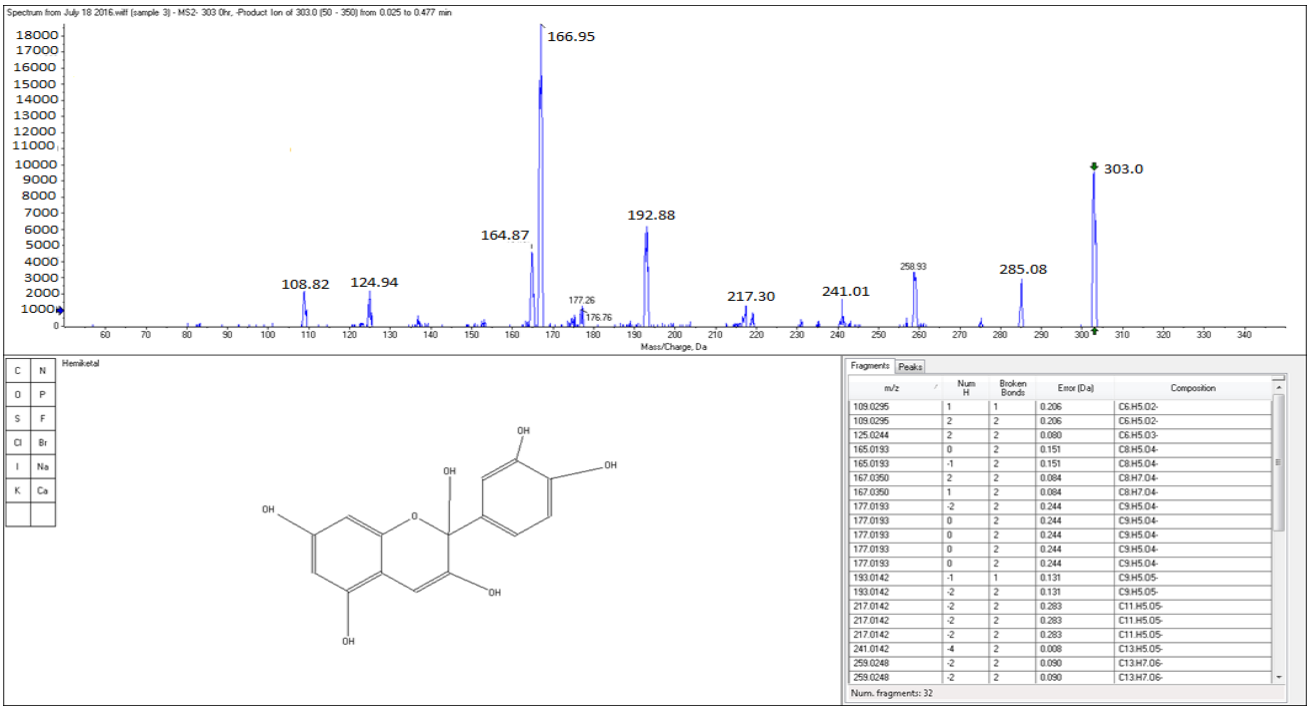

b.

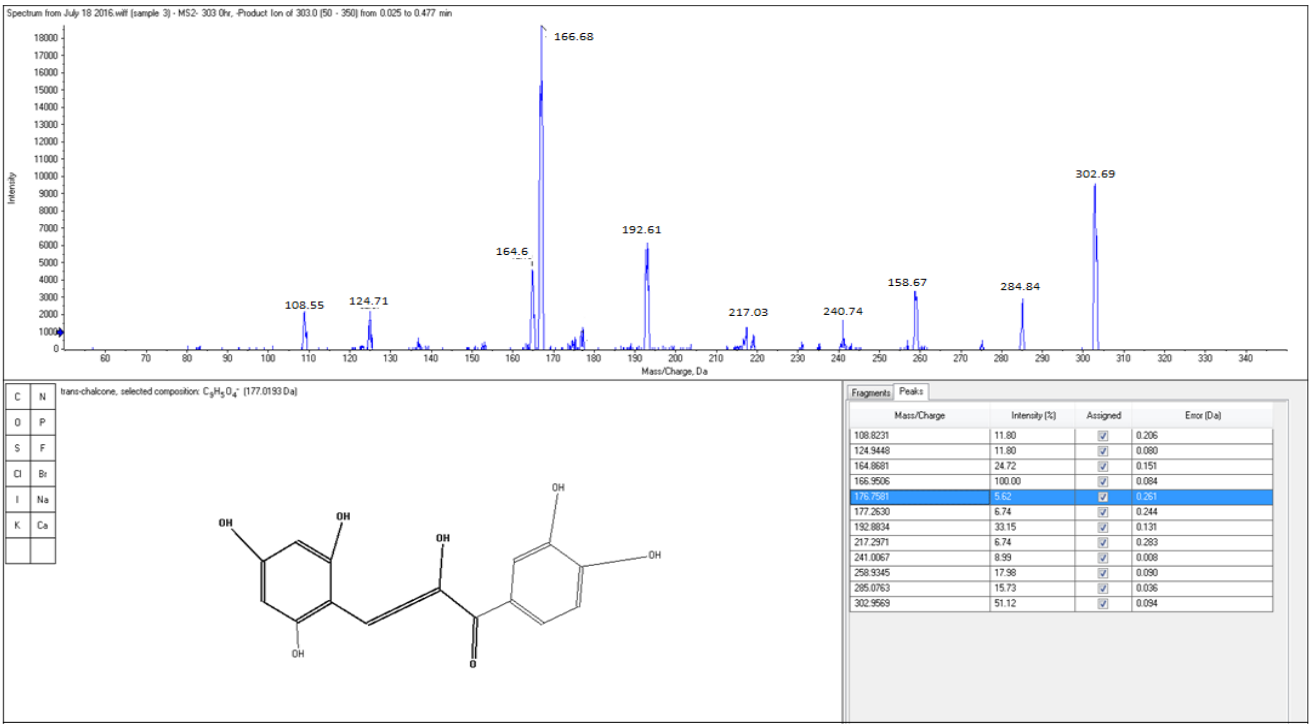

Appendix G.a and G.b: Image taken from Peakview software showing the matching peaks produced by MS/MS (negative mode) for peak 303 with the predicted product ions produced by allowing the breakage of 1 or 2 bonds in the structure of the a) hemiketal b) chalcone structures.

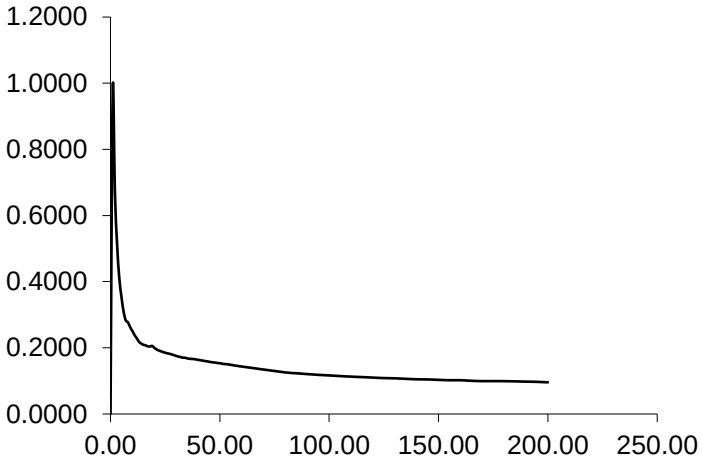

Appendix H: Degradation of cyanidin in LC-grade water with 10% methanol. The degradation of cyanidin was measured using UV-vis absorbance at λ_{max} of 600nm. A rapid degradation of cyanidin